FLUME EXPLORATION OF ENTRAINMENT, TRANSPORT, AND DEPOSITION OF CASSITERITE AND MAGNETITE IN A GRAVEL BED

By

HAMISH WEATHERLY

B.Sc., University of Waterloo, 1993

A THESIS SUBMITTED IN PARTIAL FULFILLMENT OF THE
REQUIREMENTS FOR THE DEGREE OF
MASTER OF SCIENCE

in

THE FACULTY OF GRADUATE STUDIES

Department of Geological Sciences

We accept this thesis as conforming to
the required standard

THE UNIVERSITY OF BRITISH COLUMBIA

April, 1996

In presenting this thesis in partial fulfilment of the requirements for an advanced degree at the University of British Columbia, I agree that the Library shall make it freely available for reference and study. I further agree that permission for extensive copying of this thesis for scholarly purposes may be granted by the head of my department or by his or her representatives. It is understood that copying or publication of this thesis for financial gain shall not be allowed without my written permission.

Department of GEOLOGICAL SCIENCES

The University of British Columbia
Vancouver, Canada

Date APRIL 12TH -1996

ABSTRACT

The economic importance of placer deposits has prompted both field and experimental research into the processes controlling their formation. Flume studies have advanced the understanding of placer formation but most have failed to adequately replicate the natural conditions under which most form. A uniform sand-sized bed has been commonly used to investigate the transport behaviour of heavy minerals with densities less than 5.2 g/cm^3. Fluvial placers, however, generally occur in gravel-bed steams and it is unresolved whether the transport behaviour of low density heavy minerals approximates higher density minerals such as cassiterite ($\rho \sim 7.0$ g/cm^3) or gold ($\rho \sim 17.0$ g/cm^3). This study addressed these limitations by using a gravel-sand bed mixture with cassiterite and magnetite ($\rho \sim 4.9$ g/cm^3) as the heavy fraction to simulate conditions characteristic of Harris Creek, a placer-bearing gravel-bed stream in the interior of British Columbia. Field observations at this site showed that pavement break-up during spring flooding was necessary to mobilize gold and magnetite deposited within the sandier substrate. In this study, a coarse surface pavement was developed over four days and then broken up by a high-energy flood for fifteen to sixty minutes. Six experimental runs were conducted under slightly different hydraulic and sedimentological conditions.

During pavement development flow competence was insufficient to mobilize cassiterite. Selective entrainment of the lighter sand-sized fractions led to the concentration of cassiterite in the immediate subsurface as a lag deposit. A 6.0 cm board placed beneath the flume tailgate reduced downstream erosion rates and subsequent cassiterite concentrations were lower downstream. Magnetite, due to its lower density, was transported during pavement development but its transport rates were disproportionately less than its presence in the bed. Subsurface enrichment of magnetite

occurred only in the lower reach. Frequent entrapment of mobilized magnetite grains in close contact with the bed and low downstream erosion rates were responsible for this pattern of enrichment.

High-energy flooding broke up the developed pavement and mobilized the heavy fractions. Cassiterite, however, was at no time transported out of the flume and transport distances were apparently small based on results in Run 5. This was a result of its high density and fine grain size relative to the bed which created numerous opportunities for entrapment. The mobility of magnetite did not increase significantly during flooding with transport rates remaining disproportionately less than its presence in the bed. Low density fractions finer than 0.354 mm were also transported at disproportionately lower rates. These results are consistent with a process of vertical fractionation which concentrates fine sediment at the base of the mobile bed and makes the grains more prone to entrapment. This study demonstrates the importance of density, grain size, and bed roughness as factors controlling the transport behaviour and deposition of heavy minerals in gravel-bed streams.

TABLE OF CONTENTS

Abstract ii
Table of Contents iv
List of Tables vi
List of Figures viii
Acknowledgments xi

1.0 INTRODUCTION 1
 1.1 Flume modelling 5

2.0 LITERATURE REVIEW 7
 2.1 Settling equivalence 7
 2.2 Differential entrainment 8
 2.3 Shear sorting 12
 2.4 Transport sorting and equivalence 13
 2.5 Gravel entrainment 16

3.0 EXPERIMENTAL ARRANGEMENTS 18
 3.1 Settling velocities 23
 3.2 Experimental procedure 25

4.0 OBSERVATIONS 31
 4.1 Summary of observations 31
 4.2 Run results 41
  4.2.1 Run #1 41
  4.2.2 Run #2 46
  4.2.3 Run #3 51
  4.2.4 Run #4 53
  4.2.5 Run #5 57
  4.2.6 Run #6 64
 4.3 Magnetite transport 67

5.0 DISCUSSION 74

5.1 Cassiterite transport behaviour during pavement development 74

5.2 Cassiterite transport behaviour during flooding 80

5.3 Magnetite transport behaviour during pavement development 88

5.4 Magnetite transport behaviour during flooding 90

5.5 Overview of enrichment and transport processes 93

6.0 CONCLUSIONS 101

7.0 REFERENCES 104

APPENDIX A - Summary of sediment transport rates for Runs 1 - 6 108

APPENDIX B - Velocity profile data for Runs 2 - 6 115

APPENDIX C - Size distribution of light fractions as a percentage of total sediment transported for Runs 1 - 6 131

APPENDIX D - Fractional proportions of transported sediment relative to presence in bed (p_i / f_i) 140

APPENDIX E - Water surface slope and average depth for Runs 2 - 6 147

LIST OF TABLES

Table 3-1 Grain size distribution of sediment used in experimental runs 21

Table 3-2 Grain size distribution of heavy minerals used in experimental runs. Cassiterite was present in all runs while magnetite was added to Runs 4 - 6 21

Table 3-3 Median settling velocities (w_s) of cassiterite, magnetite, and light fractions. Observed fall velocities are compared to values determined by formulae of Gibbs et al. (1971) and Dietrich (1982) 24

Table 4-1 Measured and calculated hydraulic parameters for each experimental run 32

Table 4-2 Total sediment transport rates for Run 1, stage 1 ($Q = 0.016\ m^3/s$) 42

Table 4-3 Comparison of transport rates for Runs 2 and 3 52

Table 4-4 Weight percentage of cassiterite in subsurface samples during pavement development and after flooding in Run 3. Subsurface was sampled between 2 and 4 m 52

Table 4-5 Vertical sampling of cassiterite at 7.5 and 9.5 m at the close of Run 3 Sediment height was 3.75 cm at 7.5 m and 5.0 cm at 9.5 m 54

Table 4-6 Weight percentage of cassiterite and magnetite in subsurface samples during pavement development of Run 4. Subsurface sampled between 2 and 4 m 54

Table 4-7. Weight percentage and grain size distribution of cassiterite in vertical samples of Run 4. Sample intervals refer to height above flume bottom 59

Table 4-8. Weight percentage and grain size distribution of magnetite in vertical bed samples of Run 4. Sample intervals refer to height above flume bottom 60

Table 4-9. Weight percentage of cassiterite and magnetite in subsurface samples (Run 5). Subsurface sampled between 2 and 4 m 62

Table 4-10. Weight percentage and grain size distribution of magnetite and cassiterite in vertical bed samples of Run 5. Sample intervals refer to height above flume bottom 65

Table 4-11 Size distribution of transported magnetite as a percentage of total sediment transported for Runs 4, 5, and 6 68

Table 5-1 Expected cassiterite concentrations in subsurface samples taken to a depth of 1.25 cm based on varying amounts of degradation. Values were calculated based on the assumption that cassiterite was immobile 79

Table 5-2 Fractional percentage of transported sediment relative to fractional percentage in bed during flooding of Runs 3 - 6 85

Table 5-3 Coefficients of variation (CV) for relative concentrations of magnetite (Mag). For Runs 4 - 6, n = 3, 6, and 4 respectively. CV_{min} is in bold and underlined. Similar fractions for light and heavy grains are italicized and underlined 92

Table 5-4 Estimated critical shear stresses for entrainment of sediment from developed pavements of Runs 2 - 4. Shear stresses were determined using the equation of Andrews (1983) 97

LIST OF FIGURES

Figure 2-1	Shields' curve of the dimensionless critical shear stress (θ_t) versus Reynolds grain number (Re_*) (after Shields, 1936)	10
Figure 2-2	Critical shear stress versus grain diameter for spherical grains of quartz, monazite, and gold in water at 20°C. Shear stresses determined from Shields' dimensionless relation	11
Figure 3-1	Schematic diagram of flume. Flume length is 9.7 m	19
Figure 3-2	Grain size distribution of flume sediment	22
Figure 3-3	Sediment transport rate of Run 3 as a function of time. Total elapsed time was 96 hours	28
Figure 4-1	Friction factor as a function of Re / f for smooth boundary channels (after Vanoni, 1975)	36
Figure 4-2	Depth versus discharge for Harris Creek, British Columbia	38
Figure 4-3	Velocity versus discharge for Harris Creek, British Columbia	39
Figure 4-4	Pavement development after 96 hours for the second stage of Run 1. The photograph was taken at 5.5 m in the middle of the channel with flow from left to right. The brass disk is 3.0 cm in diameter	44
Figure 4-5	Grain size distribution of surface material after 2 and 96 hours in Run 1 ($Q = 0.043\ m^3/s$) and original flume mixture	45
Figure 4-6	Change in fractional proportions of transported sediment, 2.0 - 11.0 mm, during pavement development (Run 2, $Q = 0.037\ m^3/s$)	48
Figure 4-7	Change in fractional proportions of transported sediment, 0.354 - 2.0 mm, during pavement development (Run 2, $Q = 0.037\ m^3/s$)	49
Figure 4-8	Change in fractional proportions of transported sediment, 0.090 - 0.354 mm, during pavement development (Run 2, $Q = 0.037\ m^3/s$)	50

Figure 4-9	Patches of surface cassiterite (brown, fine granular material) after a one hour simulated flood for Run 3. The above photograph was taken at 5.9 m while the lower one was taken at 6.2 m. Flow is from left to right. The coloured gravel provide a scale (i.e. yellow = 8 - 11 mm, green = 11 - 16 mm)	55
Figure 4-10	View from 6.5 m looking upstream after the fifteen minute simulated flood of Run 4. All sediment up to 4.5 m was removed as a result of transport rates up to 800 kg/hr	56
Figure 4-11	a) Photograph of parabolic cassiterite dunes at the close of Run 4. View is from 5.0 m looking downstream. b) Vertical slice (~ 3.0 cm) of cassiterite dune sampled at 5.4 m	58
Figure 4-12	Run 5 concentrations of cassiterite after 10 min of flooding. Photo taken at 3.7 m with flow from left to right. Scale is given by the brass disk, 3.0 cm in diameter	63
Figure 4-13	Run 5 surface concentrations of cassiterite after 40 min of flooding. Photo taken at 3.5 m with flow from left to right. Scale is given by the brass disk, 3.0 cm in diameter	63
Figure 4-14	Fractional weight of magnetite as a percentage of total magnetite, transported during pavement development (Run 4, Q = 0.016 m^3/s)	70
Figure 4-15	Fractional weight of magnetite as a percentage of total magnetite, transported during pavement development (Run 5, Q = 0.040 m^3/s)	71
Figure 4-16	Fractional weight of magnetite as a percentage of total magnetite, transported during pavement development (Run 6, Q = 0.025 m^3/s)	72
Figure 5-1	Fractional percentage of transported sediment relative to fractional percentage in bed versus time during pavement development of Run 4 (fractions from 0.5 to 2.0 mm)	76
Figure 5-2	Fractional percentage of transported sediment relative to fractional percentage in bed versus time during pavement development of Run 4 (fractions from 0.090 to 0.50 mm)	77
Figure 5-3	Schematic diagram of sedimentological conditions in flume at close of pavement development in Runs 2 - 6	81

Figure 5-4 Fractional percentage of transported sediment relative to fractional percentage in bed versus time during flooding of Run 5 (fractions from 0.5 to 2.0 mm) 86

Figure 5-5 Fractional percentage of transported sediment relative to fractional percentage in bed versus time during flooding of Run 5 (fractions from 0.125 to 0.50 mm) 87

Figure 5-6 Schematic representation of vertical fractionation of the mobile bed during flooding. Finer grains are transported in frequent contact with the bed resulting in preferential entrapment. Magnetite is represented by the darker grains 94

ACKNOWLEDGMENTS

As usual in this section there are a number of people to thank, all who have contributed in some manner to the completion of this thesis. Ignoring the obvious candidates for the time being [i.e. my advisor and committee member(s)?], I would like to thank Laura Rempel who had the unenviable task/pleasure of being the first to proof-read all sections. Her insightful comments and continual support helped me through periods of discontent. That isn't to say I haven't enjoyed my experience as a master's student. The last two and a half years have been one of the more pleasurable periods in my life. My parents must also be thanked as they have gently steered me through university without imposing in any way. My advisor, K Fletcher, and committee member, Michael Church, receive my gratitude at this point. K was never to busy to take time out of his schedule to help me, while Mike's suggestions led me to develop a greater interest in fluvial geomorphology. The same can be said of Marwan Hassan who taught me everything I wanted to know (and more) about flume experiments. Support staff have also been instrumental during my studies. Bryan Cranston and Ray Rodway provided invaluable technical advice and help in the construction of flume accessories. I would also like to thank Sandy Lapsky whose generosity enabled me to write the majority of my thesis in the Geography Department. To finish I would like to thank all my friends who provided me with an escape from school, Carlo Giovanella who never failed to make me laugh, and NSERC who provided the funding for this project.

1.0 INTRODUCTION

Placers are defined as mineral deposits that form by mechanical concentration of heavy mineral grains. Grains with a density exceeding 3.5 g/cm^3 are defined herein as "heavy minerals". Such deposits are usually fluvial, with water acting as the concentrating agent, but beach and eolian concentrates are not uncommon. Fluvial placers have received attention from exploration companies due to their economic importance and are the focus of this study. Well known fluvial placers of economic value include the Witswatersrand gold paleoplacers of South Africa (Minter and Toens, 1970), Klondike gold placers, and cassiterite placers in southeast Asia which are the world's largest source of tin (Toh, 1978). Despite their economic importance, the sedimentological processes that control placer formation are still poorly understood due to the complex nature of sediment transport in water. A greater understanding of the entrainment and transport behaviour of heavy minerals would improve the ability of exploration geochemists to interpret geochemical patterns and locate the source area of placers. This study uses an experimental flume environment to examine the behaviour of magnetite and cassiterite under specific hydraulic and sedimentological conditions.

Much of our understanding of placers comes from field studies that have attempted to infer the various conditions under which heavy minerals concentrate and the processes involved in their formation (Rittenhouse, 1943; Hand, 1967; Slingerland, 1977; Komar and Wang, 1984; Fletcher et al., 1992). These studies have identified local river hydraulics, densities of the light and heavy fractions, river morphology, and bed roughness as critical factors governing heavy mineral transport and deposition. Results are difficult to interpret though due to a complex interaction of these variables at the fluid-sediment interface. Furthermore, replication of results is practically impossible as field conditions are continually varied.

Flume experiments complement field studies by reducing the natural variability of streams, in an environment where hydraulic and sedimentological variables can be controlled. Specific aspects of heavy mineral transport and deposition have been successfully modelled by Minter and Toens (1970), Brady and Jobson (1973), Steidmann (1980), Best and Brayshaw (1985), and Kuhnle (1986). Several advantages of flume experiments over field studies include: i) hydraulic variables such as slope and water depth are controlled, ii) experimental conditions can be duplicated to confirm results, iii) steady, uniform conditions can be maintained, iv) flow can be stopped at any time to permit sampling and observation of the bed, v) all sediment leaving the channel is retrieved for analysis, and vi) the surface of the bed during flooding can be readily observed.

Flumes, however, are limited in several respects. The primary drawback is that most flumes appropriately model only two dimensions of three-dimensional streams. Channel width and depth can be scaled to represent a stream's cross-sectional area. Variability in channel geometry and morphology along its length, however, lead to a complex distribution of flow across the channel which is not in general, replicated within a flume. For instance, the preferential accumulation of heavy minerals along the inside curve of a meander (Hattingh and Rust, 1993) is impossible to simulate in a standard flume. Secondly, even using a two-dimensional model problems arise in maintaining scaling relations (i.e. ensuring the model is representative of the prototype). If a model is not representative of field conditions then the similarity is brought into question. The history of the stream must also be considered because long-term interactions between hydraulic variables and sediment are responsible for placer formation. A flume cannot adequately represent the time scale under which placers form. These limitations do not invalidate flume models as an experimental tool, but care must be taken in applying results to natural systems.

Previous flume studies involving heavy mineral transport have used grains with densities less than 5.2 g/cm^3 as the heavy fraction, and most have used uniform sand-sized sediment as the low density fraction. Kuhnle's (1986) investigation on heavy mineral transport in a gravel-sand mixture is a notable exception in that it addressed the limitations of previous studies: i) the transport behaviour of "low density" heavies (i.e. magnetite and ilmenite) cannot necessarily be extrapolated to higher density minerals such as cassiterite and gold, and ii) fluvial placers generally occur in mixed size deposits, particularly in gravel-bed streams where high slopes and high magnitude floods are capable of transporting particles of high density (Slingerland and Smith, 1986). Kuhnle (1986) used a poorly sorted gravel to investigate the concentrating processes of three minerals of varying density under a range of imposed flows and sediment feed rates. The heavy fraction consisted of 3 % by weight of tungsten (ρ = 19.3 g/cm^3), lead (ρ = 11.4 g/cm^3), and magnetite (ρ = 5.2 g/cm^3). Under nondegrading conditions the heavy minerals became concentrated in a thin layer (heavy infralayer) beneath a mixed surficial layer of lighter sediment. Heavy minerals were not transported past a given location in the flume until this heavy infralayer layer had formed. Transport of heavy minerals occurred along the upper surface of the heavy infralayer when the light surficial layer was temporarily removed. Initial development of a heavy infralayer was also noted under conditions of overall bed degradation in the absence of sediment feed, but the run was stopped before the infralayer had fully developed. Conditions of steady flow and transport (i.e. nondegrading conditions) are not typical of fluvial channels though, and Kuhnle and Southard (1990) questioned the direct relevance of Kuhnle's results to stream channels.

With these factors in consideration, this flume study was conducted to model sediment transport behaviour characteristic of gravel-bed streams. The low density sediment used was a gravel-sand mixture, while cassiterite (ρ = 6.85 g/cm^3) and magnetite (ρ = 4.85 g/cm^3) composed the heavy fractions. In contrast to Kuhnle (1986), an attempt was made to model a gravel-bed stream using appropriate scaling factors. Harris Creek, a placer-bearing gravel-bed stream located in the interior of British Columbia, was selected as the prototype. Fletcher and Wolcott (1991) have investigated the transport behaviour of naturally occurring magnetite and gold in this stream. A representative sample of gravel from Harris Creek was scaled down by a factor of twenty to yield a sediment mixture ranging in size from 0.090 - 32.0 mm with a median diameter of 1.4 mm. A similar scaling factor could not be applied to the heavy fraction (0.090 - 0.354 mm), because heavies occupy the fine sand range of gravel-bed streams and scaling would result in impracticable grain sizes of less than 18 microns. The heavy fraction is expected to retain transport characteristics similar to those observed in nature, however, as the grain size is still fine relative to the low-density sediment.

Sediment transport in gravel-bed streams of British Columbia is minimal through most of a stream's annual hydrograph due to low discharge rates and the development of a coarse surface layer (pavement). High sediment transport rates and heavy mineral mobilization occur when the flow is of sufficient competence to break the surface pavement, releasing the finer underlying sediment. Discharges of sufficient magnitude generally occur in late spring when the influx of snowmelt augmented by precipitation result in flooding. Re-development of the pavement provides a trap for the finer sediment as the flood recedes. This sequence of events was noted by Fletcher and Wolcott (1991) in Harris Creek and provided the motivation for flume experiments conducted in this study. A coarse surface pavement was allowed to develop over a four day period and then discharge was increased to simulate a spring flood and pavement break-up. Of interest were transport rates and redistribution within the bed of the low and high density sediment and the vertical and longitudinal distribution of the heavy fraction along the bed.

1.1 Flume modelling

To ensure that a model is representative of the prototype three types of similarity must be maintained; geometric, kinematic, and dynamic similarity (Sharp, 1981). Geometric similarity requires the shape of the model to be the same as that of the prototype. It is attained by reducing each length of the prototype by a constant scaling factor. In this study a scaling factor of twenty was used, therefore channel cross-sectional area and grain size distribution were reduced twenty times. Kinematic similarity refers to water flow direction and magnitude which must be the same for both the model and prototype. Dynamic similarity requires the ratio of corresponding forces to be the same and is the primary focus of many scale models, because models which maintain geometric and dynamic similarity are also kinematically similar.

For models of open channel flow, the primary forces acting on a fluid are gravity, viscosity, and inertia. These forces can be expressed as dimensionless ratios: Reynolds number, Re (ratio of inertial to viscous forces), and Froude number, Fr (ratio of inertial to gravitational forces).

$$Re = V\,L / \nu \tag{1.1}$$

$$Fr = V / (L\,g)^{1/2} \tag{1.2}$$

where V is flow velocity, L is a length scale (for rivers the hydraulic radius, R, or water depth is normally used), ν is the kinematic viscosity, and g is the acceleration due to gravity. Dynamic similarity can be attained by ensuring that Reynolds and Froude numbers are the same in model and prototype.

Difficulties arise in maintaining both Reynolds and Froude scaling, however, because changes in the length scale (in this case a factor of 20) require a reduction in water velocity and viscosity. Water velocity can be decreased to satisfy Froude scaling, but a reduction in viscosity requires either an increase in temperature or the use of a different fluid to maintain Reynolds similarity. An increase in water temperature from 20°C to 55°C reduces viscosity only by half, while the costs and technical difficulties of using a different fluid are beyond the scope of most laboratories. Thus, there is a contradiction between the Reynolds and Froude scaling requirements.

As a compromise, models of sediment transport in gravel-bed rivers strive for geometric and Froude similarity while relaxing the constraints for Reynolds similarity. The basis for a relaxation in Reynolds scaling is discussed in detail by Parent (1988). He noted that under a hydraulically rough flow regime the dominant forces are the gravitational acceleration of water and channel friction. Viscous forces are not relevant for macroscale phenomena and therefore the Reynolds number is not critical. The upper boundary of this flow regime is approximated by the following formula (Rouse, 1959) :

$$4\,Re\,(f)^{0.5}\,k_s\,/\,4\,R\;>\;200 \tag{1.3}$$

where f is the friction factor and k_s is the relative bed roughness (generally taken as the D_{50} or D_{90} of the bed). Because $f = 8\,g\,R\,S\,/\,V^2$ and $Re = R\,V\,/\,\nu$, equation 1.3 can also be expressed as

$$(8\,g\,R\,S)^{0.5}\,k_s\,/\,\nu\;>\;200 \tag{1.4}$$

Since g, S, and k_s are fixed for a given experiment, there is a minimum R for a given ν under which the flow is hydraulically rough. Reynolds scaling can, therefore, be relaxed so long as the flow remains hydraulically rough as defined by equation 1.4.

2.0 LITERATURE REVIEW

Before the experimental design and procedures of the flume experiments are considered in greater detail, the present body of research concerning placer formation will be more thoroughly reviewed. As noted previously there is a complex interaction of hydraulic and sedimentological variables that govern the transport and deposition of heavy minerals. These interactions are still poorly understood, but a useful approach to the problem was developed by Slingerland (1984) who examined enrichment processes at the grain scale. The processes considered were settling, differential entrainment, shear sorting, and transport sorting. This chapter examines these processes and addresses their role in placer formation. Also considered is the critical shear stress required for general mobilization of the pavement.

2.1 Settling equivalence

Grains that have the same settling or fall velocities are said to exhibit settling equivalence. A relation between size distribution of heavy mineral accumulations and settling velocities was first suggested by Rubey (1933). Using magnetite as an example he stated that "... whatever the conditions may have been which permitted the deposition of quartz grains of a certain size, these conditions would also permit the deposition of magnetite grains that had the same settling velocity.". Thus, Rubey believed that transported grains of equal settling velocity would settle out of suspension together and come to rest at the same horizon. Rittenhouse (1943) termed this sorting process hydraulic equivalence, although he was more vague in its definition stating "... whatever the hydraulic conditions may be that permit the deposition of a grain of particular physical properties, these conditions will also permit the deposition of other grains of equivalent hydraulic value." Rubey and Rittenhouse recognized that settling velocity was not the only factor controlling the occurrence of heavy minerals in placer deposits, but the term hydraulic equivalence became synonymous with settling equivalence (i.e. grains of equal settling velocity are of equal hydraulic value).

The role of settling equivalence as a primary sorting mechanism was questioned as subsequent studies demonstrated that, generally, light and heavy minerals deposited together in a fluvial environment do not have the same settling velocities (Hand, 1967; Lowright et al., 1972; Slingerland, 1977; Komar and Wang, 1984). Attempts to quantify settling equivalence are complicated by water turbulence, suspended sediment concentrations, and grain shape, all of which affect settling rates (Slingerland and Smith, 1986).

2.2 Differential entrainment

Recognizing the lack of settling equivalence in the majority of heavy mineral accumulations, research began to focus on the differential entrainment of grains off a bed to resolve the primary controlling forces of heavy mineral concentrates. Each grain has an associated threshold entrainment stress that is defined as the minimum stress necessary for transport. In an uniform deposit it is intuitively obvious that the greater density of the heavy fraction will require higher shear stresses for entrainment than does the light fraction. A lag deposit forms when shear stresses are sufficient to entrain only the light fraction. Shields' (1936) dimensionless relation for grain entrainment threshold permits a quantitative analysis of this statement. Shields developed the functional relation, which is a ratio of entraining versus resisting forces, using the following fluid and grain variables: grain diameter D, grain density ρ_s, fluid density ρ, acceleration due to gravity g, kinematic fluid viscosity ν, and the shear stress of the fluid flow τ ($\tau = \rho\, g\, R\, S$ where R is the hydraulic radius and S is the water surface slope). These parameters were combined into the dimensionless relation

$$\theta = \tau \ / \ [\rho_s - \rho] \, [g \, D] = f \, (Re_*) \qquad (2\text{-}1)$$

$$Re_* = U_* \, D / \nu \qquad (2\text{-}2)$$

where θ is referred to as Shields entrainment number or dimensionless shear stress, Re_* is the grain Reynolds number, and U_* (the shear velocity) is equal to $(\tau / \rho)^{1/2}$.

The relation between the dimensionless shear stress and the grain Reynolds number is presented in Figure 2-1. The data plot as a narrow band, which encompasses the threshold level for grain entrainment. Shields' entrainment function remains relatively constant when Re_* exceeds 100, indicating that critical shear stress is primarily a function of particle weight (size and density). This illustrates that larger and more dense grains require greater shear stresses for entrainment (Figure 2-2). Ljunggren and Sundborg (1968), Grigg and Rathbun (1969), and Brady and Jobson (1973) have all used Shields' criterion in their examination of heavy mineral entrainment. It must be noted, however, that Shields' functional relation was developed from experimental studies using compact, uniform sands and does not accurately predict critical shear stresses for mixed size deposits.

In the case of poorly sorted deposits, Einstein (1950) and Egiazaroff (1965) identified the shielding effect of larger grains as an important factor inhibiting the entrainment of the smaller fraction. Hand (1967) was the first to extend this concept to entrainment of heavy grains. Grains close to the median diameter of the bed are more easily entrained than finer sediment because they protrude higher into the flow and have smaller reactive angles (Slingerland, 1977, 1984; Komar

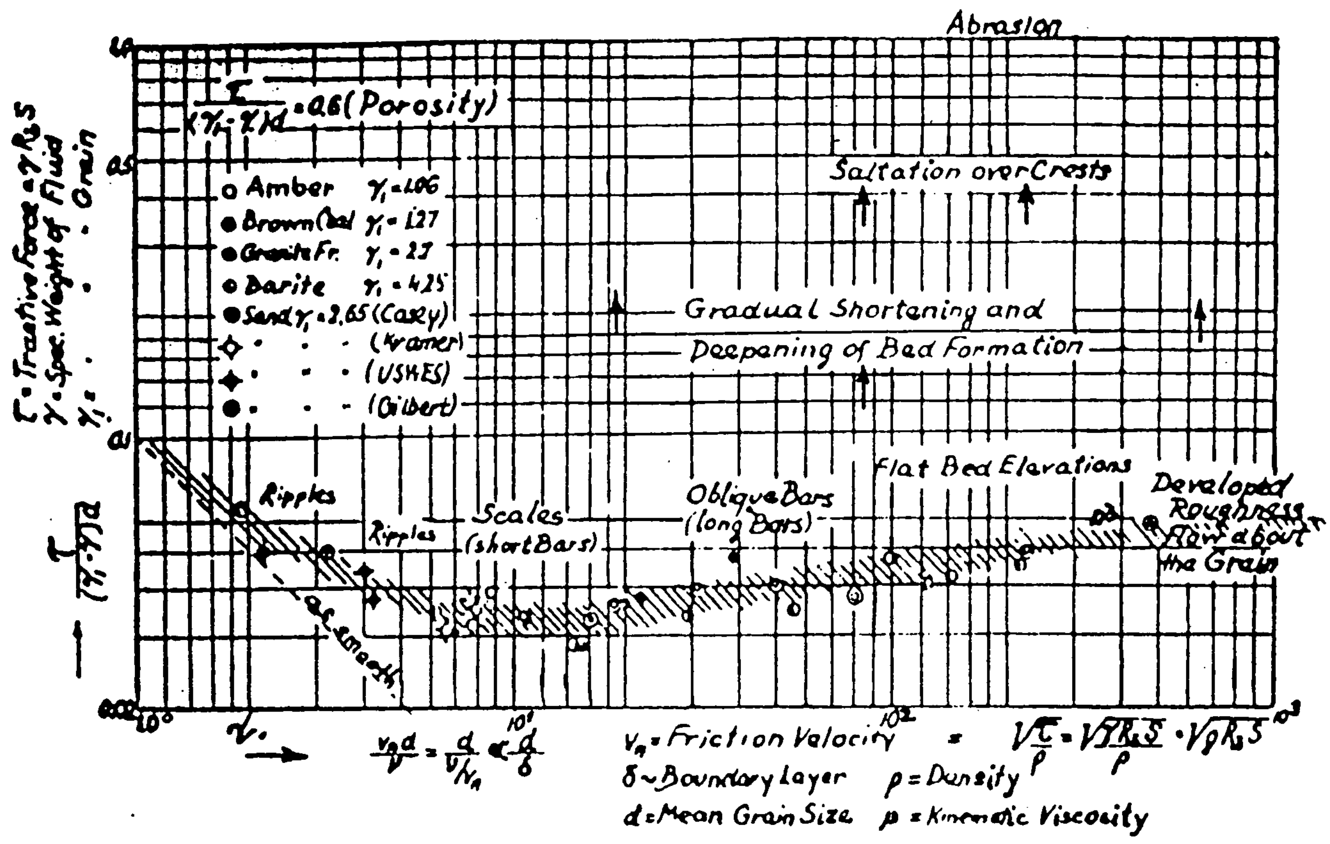

Figure 2-1. Shields' curve of the dimensionless critical shear stress (θ_t) versus Reynolds grain number (Re_*) (after Shields, 1936).

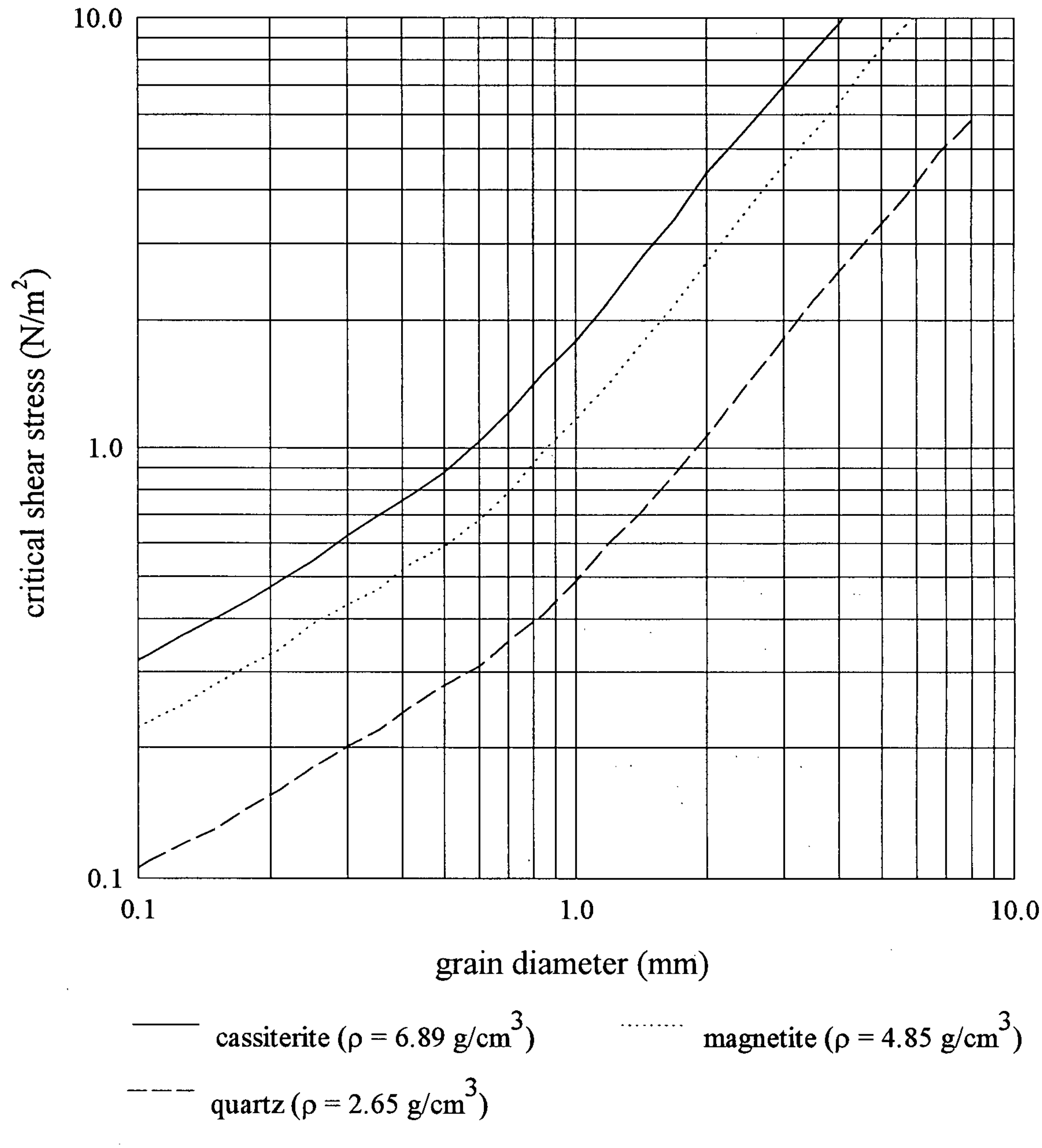

Figure 2-2. Critical shear stress versus grain diameter for spherical grains of quartz, magnetite, and cassiterite in water at 20°C. Shear stresses determined from Shields' dimensionless relation.

and Wang, 1984). Grains much smaller than the median diameter, irregardless of density, are less easily entrained due to the "shielding" effect from larger grains. Because heavy minerals tend to dominate the finer fractions, they often concentrate as a lag deposit while mode-sized and less dense grains are preferentially transported away (Komar and Wang, 1984). Slingerland and Smith (1986) and Komar and Wang (1984) have developed entrainment functions that consider the shielding effect of large grains.

2.3 Shear sorting

Shear sorting refers to the vertical fractionation of grains due to dispersive pressures within a moving bed layer (Inman et al., 1966). Bagnold (1954) argued that when a sediment deposit is sheared by fluid forces, the grains interact to produce a dispersive pressure at right angles to the shearing force (i.e. perpendicular to the bed). He demonstrated that the dispersive force was proportional to the product of the grain diameter squared and grain density. Accordingly, within a horizon larger and denser grains are subjected to greater dispersive pressures than smaller or less dense grains. This results in larger grains being pushed upward in a moving layer to produce an inversely graded bed. Kinetic sieving, introduced by Middleton (1970) is a process similar to shear sorting in that it refers to the downward movement of fine grains between the interstices of coarser sediment. Sallenger (1979) invoked shear sorting to explain heavy mineral laminations in beach sands, where the heavies were concentrated at the base of an inversely graded bed. More substantial concentrations may form when a beach face is progressively cut back and the repeated shearing concentrates and drives the fine heavy minerals downward while the larger quartz grains are exposed in the swash zone and entrained (Komar and Wang, 1984). While the process of shear sorting has been applied to beach placers, its potential role as a concentrating process in fluvial placers has yet to be investigated.

2.4 Transport sorting and equivalence

Transport sorting results when grains of varying size and density are transported at a different rate from one another and are deposited in separate locations. Since variable transport rates are a function of the probability of entrainment and average velocity while in transport, transport sorting incorporates the principles of differential entrainment. Transport sorting has proven difficult to model as fractional transport rates cannot be accurately predicted by existing sediment transport formulae (Gomez and Church, 1989). Slingerland (1984) and Day and Fletcher (1991) have addressed the problem by utilizing Einstein's bedload equation (1950), which allows for grain shielding effects by incorporating a "hiding" factor into the equation. Einstein's equation did not enable the authors to quantitatively predict the formation of placer deposits, but it did provide a useful framework to evaluate the probable effect of changing hydraulic and sedimentological conditions on heavy mineral accumulations (Day and Fletcher, 1991).

Slingerland (1984) used Einstein's equation to theoretically predict what hydraulic and sedimentological conditions were favourable to placer development. Employing an idealized settling-equivalent distribution of medium sand-size quartz and 10% fine-size magnetite, he found that placer formation was dependent on shear stress and the size of the heavy fraction with respect to bed roughness. He predicted that heavy mineral enrichment of the bed was maximized when the median diameters of the light fractions approached the bed roughness and shear stress was such that the finer heavy grains traveled with more bed contact than the light grains.

Einstein's bedload equation was used by Day and Fletcher (1991) to model observed accumulations of heavy minerals in Harris Creek by Fletcher and Wolcott (1991). Field observations indicated that gold and magnetite preferentially accumulated in the voids of bar-head gravels rather than in bar-tail sands. Emphasizing depositional controls, Day and Fletcher proposed the following conceptual model to explain the observed distribution of heavy mineral accumulations.

During snowmelt floods, peak discharges are often sufficient to break-up pavement gravels and cobbles and entrain the sandier substrate (fully competent floods are much less frequent than annual floods). After discharge has peaked the cobbles and gravels are the first fractions to stabilize, reforming a surface framework. Sand-size heavy grains traveling in intermittent contact with the bed are first entrapped in the interstitial voids while light minerals of the same size remain in transport. Heavy minerals in the silt-sized range do not concentrate in this environment as they are transported in suspension and test the bed infrequently. As discharge continues to decline, bedload transport rates decrease and the remaining void space is quickly filled by sand-sized light sediment. A simulation of these seasonal events using Einstein's bedload equation yielded similar results, with heavy mineral enrichment of the gravel voids.

Harris Creek is not a unique case for demonstrating the importance of interstitial voids in controlling placer development. A well known example that demonstrates this process is the Witwatersrand paleoplacers where conglomerate units have placer gold concentrations ten times those of associated sands (Smith and Minter, 1980). Rudimentary flume experiments by Minter and Toens (1970) had previously modeled the entrapment process thought to account for these deposits.

A recent approach by Fletcher et al. (1992) to address the transport of heavy minerals considered the relative transport rates of the light and heavy fractions. They defined transport equivalent particles as ones that have the same average net transport rate, which is a function of entrainment frequency, average velocity while in motion, and settling rate. Transport equivalent particles are therefore transported at proportionally similar rates in all flow conditions despite differences in their physical properties. Estimates of transport equivalent sizes were determined by calculating the relative transported weights of the magnetic fractions versus the light fractions

$$100\ (Mag_i\ /\ Sed_j) \qquad (2.3)$$

where Mag_i and Sed_j are the weights of the magnetic and light sediment in size fractions i and j. Fractions displaying the least variation in relative transport rates over a range of discharge conditions were said to approach transport equivalence. Field observations from Harris Creek indicated that each magnetite size fraction was transported at a rate similar to a larger, settling equivalent fraction. The authors were not able to distinguish the relative importance of settling versus entrainment sorting to the relative transport rates of the light and heavy fractions. However, the close association between settling and estimated transport equivalent sizes suggested that particle settling was an important factor.

While the processes herein have been considered separately they are strongly interdependent. The nature of sediment transport is cyclic with entrainment of an individual grain leading to transport within the flow, and eventual deposition. Therefore, while the primary objective of this study is to examine the transport behaviour of magnetite and cassiterite in a gravel-bed stream during flooding, the interdependence of the processes requires that entrainment and deposition also be examined.

2.5 Gravel entrainment

As noted in the introduction and previous section, heavy mineral transport in Harris Creek occurs when the pavement is broken, releasing the finer substrate. It would, therefore, be of interest to estimate the critical shear stress required for pavement break-up. Parker et al. (1982), reanalyzing data gathered by Milhous (1973) from a gravel-bed stream in Oregon, noted that bedload and subpavement size distributions were similar during flooding. That is, all grain sizes demonstrated equal mobility above critical shear stress values that initiated pavement break-up. This led to the development of an empirical relation between Shields' entrainment number, θ_t (equation 2.1), and the median grain diameter of the subsurface that allowed estimates of critical shear stress for individual grain sizes. The value of θ_t for each grain size was calculated by correlating the transport rate of the size fraction with the given shear stress. Critical values of θ_t (θ_c) were then computed for each size fraction by setting the transport rate to a small value. The relation was of the form

$$\theta_c = a\,(D_i / D_{50})^{b} \qquad (2.4)$$

where a and b were 0.0876 and -0.982 respectively. Equation 6.1 was developed for bed particles between 0.045 to 4.2 times the median diameter and the approximate inverse relation (b ~ -1) implied a common threshold of entrainment for these grain sizes (i.e. no selective entrainment).

Andrews (1983) developed a similar relation based on a large range of discharges from gravel-bed streams in Idaho and Wyoming. For bed particles between 0.3 and 4.2 times the median grain diameter of the subsurface bed, a and b values were 0.0834 and -0.872 respectively.

The lower value of b indicated that fine particles were entrained at a slightly lower shear stress than coarser particles, but the difference was not large. For particles 4.2 times the median diameter, θ_c approached a constant value of 0.020 and a common threshold for sediment entrainment no longer applied. Komar et al. (1987) reanalyzed data from Parker et al. (1982) and suggested that a common threshold entrainment for the majority of grain sizes did not exist. They argued that Parker et al. had restricted their analysis to observations in which all the sediment was in motion and that selective entrainment did occur at lower stresses. Andrews equation, however, satisfies this argument and will provide a basis for future discussion in this thesis.

3.0 EXPERIMENTAL ARRANGEMENTS

All the experiments were conducted in a water recirculating, tilting flume, located in the Geography Department of the University of British Columbia (Figure 3-1). The flume measured 9.7 m in length with a width of 0.80 m. The first 1.5 m were covered by angular to sub-angular gravel (11 to 32 mm) to facilitate mixing and dispersion of eddies from the headbox (Wolcott, 1990). The turbulent nature of the recirculated water was further dissipated by a 0.02 m thick wooden float within the headbox and a honeycomb of cylindrical tubing (0.03 m diameter and length) placed over the channel entrance The sidewalls consisted of clear plexiglass, 0.02 m thick and 0.40 m high.

The water was recirculated using a variable speed electric motor and an axial pump. These were connected to a digital operator station that allowed precise control of motor speed, measured as number of revolutions per minute (RPM). Discharge was calculated from depth measurements and velocity profiles which were obtained with a hot film probe. Two additional water reservoirs connected to the tailbox maintained near uniform water temperatures throughout a run. Water temperatures would typically rise 2°C during a run (96 hours) with temperatures varying from 13 to 21°C over the course of the experimental study.

All sediment transported out of the channel was collected in a wire mesh (0.100 mm sieve size) covered box placed beneath the water overfall in the tailbox. A 0.06 m high board placed across the width of the flume and beneath the tailgate prevented the bed from eroding below 0.06 m at the tail end of the flume. Without the addition of sediment during a run and with the lack of bed

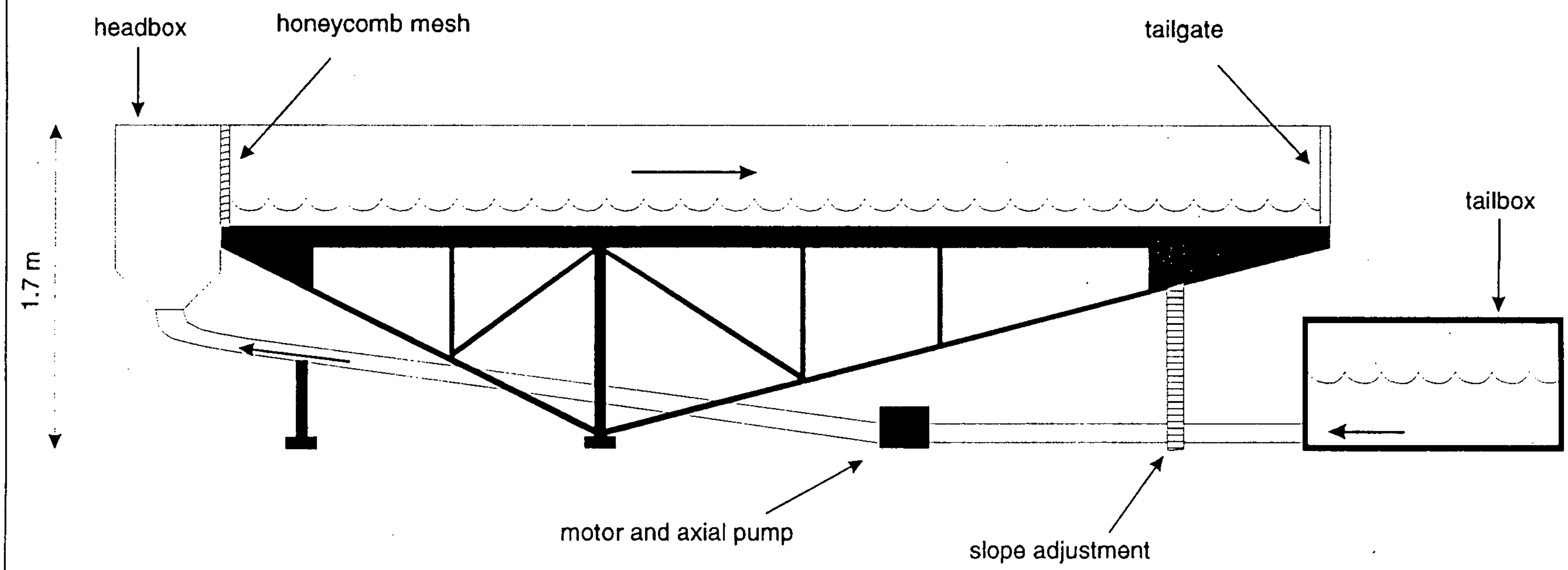

Figure 3-1. Schematic diagram of flume. Flume length is 9.7 m.

degradation at the tail end of the flume, the surface could develop a pavement in a relatively short period of time (ninety-six hours).

The sediment contained in the flume was acquired from local sand and gravel companies whose products are outwash sands and gravels with low heavy mineral concentrations (< 0.02 % of the sand fraction consisted of heavies in this study). This eliminated concern for contamination of the heavy fraction by magnetite, which is common in streams throughout British Columbia. The sediment ranged in size from 0.090 mm to 32 mm for experiments 1 - 4 with a D_{50} of 1.40 mm (Table 3-1, Figure 3-2). Removal of the three coarsest fractions provided a finer sediment mix for experiments 5 and 6 (D_{50} = 1.33 mm) . As noted in section 1-1, this grain-size distribution characterizes Harris Creek scaled down by a factor of twenty.

The gravels were sub-rounded to well-rounded with a Corey shape factor (CSF) of approximately 0.70.

$$CSF = c / (a\ b)^{1/2} \qquad (2.1)$$

where a, b, and c are the long, intermediate, and short axes of the particle. The sand fraction was more angular with a similar CSF. The four coarsest fractions, which formed the bulk of the surface framework, were coated with marine paint to facilitate the monitoring of pavement development. In order from coarsest (22.6 - 32.0 mm) to finest fraction (8.0 - 11.0 mm) the colours used were blue, orange, green, and yellow.

The heavy fraction of the sediment consisted of 1.09 % cassiterite (density = 6.89 g/cm^3) and 1.00 % magnetite (density = 4.85 g/cm^3) by weight. Random sampling of the mixture (n = 10) resulted in standard deviations of $\pm$ 0.10 % and $\pm$ 0.11 % by weight for cassiterite and magnetite

Table 3-1. Grain size distribution of sediment used in experimental runs.

Grain size (mm)	fractional % Runs 1 - 4	% finer than	fractional % Runs 5 - 6	% finer than
> 32.0	0.0	100.0	0.0	
22.6 - 32.0	1.1	98.9	0.0	
16.0 - 22.6	1.1	97.8	0.0	
11.3 - 16.0	2.1	95.7	0.0	100.0
8.0 - 11.3	3.2	92.5	3.3	96.7
5.66 - 8.0	4.6	87.9	4.8	91.9
4.0 - 5.66	9.3	78.6	9.7	82.2
2.83 - 4.0	8.9	69.7	9.3	72.9
2.0 - 2.83	7.9	61.8	8.3	64.6
1.41 - 2.0	11.4	50.4	11.9	52.7
1.0 - 1.41	14.0	36.4	14.6	38.1
0.71 - 1.0	8.1	28.3	8.5	29.6
0.50 - 0.71	6.8	21.5	7.1	22.5
0.354 - 0.50	7.4	14.1	7.7	14.8
0.250 - 0.354	5.9	8.2	6.2	8.6
0.177 - 0.250	3.8	4.4	4.0	4.6
0.125 - 0.177	3.2	1.2	3.3	1.3
0.090 - 0.125	1.2	0.0	1.3	0.0

Table 3-2. Grain size distributions of heavy minerals used in experimental runs. Cassiterite was present in all runs while magnetite was added to runs 4 - 6.

Grain size (mm)	Cassiterite % of heavy fraction	Magnetite % of heavy fraction
0.250 - 0.354	8.2	38.2
0.177 - 0.250	42.8	34.6
0.125 - 0.177	42.2	27.1
0.090 - 0.125	6.9	-

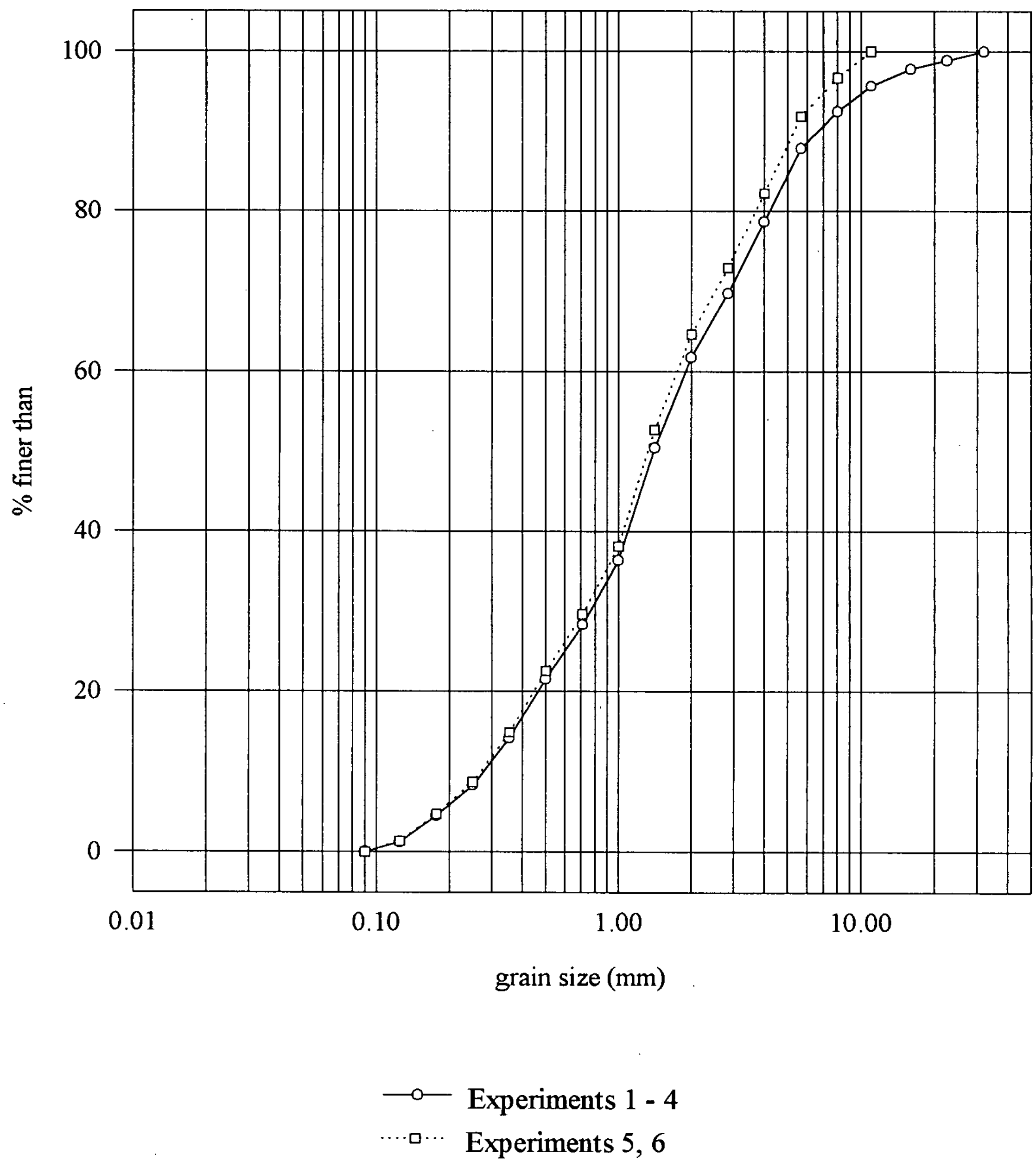

Figure 3-2. Grain size distribution of flume sediment.

respectively. The cassiterite ranged in size from 0.354 to 0.090 mm (Table 3-2) and was obtained from a tin placer in Malaysia. The magnetite was sieved from a crushed product and ranged in size from 0.354 to 0.125 mm. The weight percentages of cassiterite and magnetite in the sand fraction greatly exceeded those found naturally; however, this facilitated the accurate determination of heavy mineral percentages. Kuhnle (1986) found that higher percentages of heavy minerals had little effect on transport processes of either the light or heavy fractions.

3.1 Settling velocities

Settling velocities of the cassiterite and light sand fractions (Table 3-3) were determined by the visual-accumulation-tube method as described by the United States Inter-Agency Committee on Water Resources (1958). The sedimentation tube was 1.2 m long, with a diameter of 25 mm in the main sedimentation section (first 0.8 m) and a diameter of 7.0 mm in the accumulation section (last 0.2 m). A correction factor was applied to the initial fall distance of 1.2 m due to sediment (1 to 2.5 g) accumulating at the base of the sedimentation tube. Listed settling velocities are median values as each size fraction represents a range of sediment diameters. Determination of settling equivalence for cassiterite and quartz illustrated that a cassiterite grain had a fall velocity equivalent to a quartz grain 2.3 times greater in diameter.

The visual-accumulation-tube was unsuitable for the magnetite fractions due to the mutual attraction of grains, instead settling velocities were determined by dropping individual grains into a tube 15 cm in diameter and 1.15 m in length. Placement of a white board behind the tube facilitated observation of the settling grains, which were allowed to attain terminal fall velocity before timing commenced. Listed magnetite fall velocities are an average of ten

Table 3-3. Median settling velocities (w_s) of cassiterite, magnetite, and light fractions. Observed fall velocities are compared to values determined by formulae of Gibbs et al. (1971) and Dietrich (1982).

size fraction (mm)	geometric mean (mm)	viscosity (cm^2/s)	w_s observed (cm/s)	w_s Dietrich (cm/s)	w_s Gibbs et al. (cm/s)
Quartz					
1.41 - 2.00	1.68	0.00873	15.0	17.6	25.1
1.00 - 1.41	1.19	0.00873	13.3	14.1	19.3
0.71 - 1.00	0.84	0.00854	11.2	11.1	14.7
0.50 - 0.71	0.60	0.00854	9.2	8.1	11.0
0.354 - 0.50	0.421	0.00914	7.5	5.5	8.2
0.250 - 0.354	0.297	0.00836	5.5	3.7	6.1
0.177 - 0.250	0.210	0.00854	3.5	2.3	4.6
0.125 - 0.177	0.149	0.00873	2.2	1.4	3.7
0.090 - 0.125	0.106	0.00914	1.0	0.8	3.1
Cassiterite					
0.250 - 0.354	0.297	0.00873	10.2	9.3	11.2
0.177 - 0.250	0.210	0.00873	8.2	6.1	8.2
0.125 - 0.177	0.149	0.00873	6.0	3.9	6.1
0.090 - 0.125	0.106	0.00873	4.1	2.4	4.7
Magnetite					
0.250 - 0.354	0.297	0.00914	8.1	7.7	9.2
0.177 - 0.250	0.210	0.00914	5.7	5.0	6.8
0.125 - 0.177	0.149	0.00914	3.6	3.1	5.1

measurements over a fall distance of 0.7 m. Magnetite grains had fall velocities equivalent to quartz grains 1.5 times larger.

Settling velocity of each size fraction was also determined using the empirically derived equations of Gibbs et al. (1971) and Dietrich (1982) (Table 3-3). The equation of Gibbs et al. (1971) overestimated the fall velocities of the light and magnetite fractions, which is expected as the equation was derived using *spherical particles* and does not consider particle shape. One would expect the same outcome for the cassiterite fraction due to its irregular shape (CSF = 0.7), but the calculated settling rates were very similar to those observed. Dietrich (1982) developed a more complex equation that accounted for the effects of shape (Corey Shape Factor) and roundness (scale between 0, perfectly angular, and 6, perfectly round). The use of appropriate shape (0.7) and roundness factors (3.5), however, failed to approximate the observed settling velocities of the light and cassiterite fractions, with the majority of calculated values underestimating the observed settling velocities. Dietrich's equation had more success in approximating the fall velocities of the magnetite fractions. The overall performance of these equations, however, illustrates the need for direct determination of settling velocities for varying natural material if the results are to be used in a quantitative analysis.

3.2 Experimental procedure

Prior to the first run, the flume sediment was prepared according to Table 3-1 and thoroughly mixed to ensure an even distribution of cassiterite throughout the flume (magnetite was not added to the sediment until Run 4). This was accomplished by grouping the sediment into several size classes and preparing the mixture in 10 kg portions. The cassiterite and finest sediment class were first combined and thoroughly homogenized by hand mixing before coarser fractions were progressively added. In total, 950 kg of prepared sediment were placed in the flume. The sediment was then leveled with the aid of a channel-wide scraper which rides along the top of the flume side-walls, to create a uniform sediment depth of 7.0 cm.

Because all the sediment could not be removed and dried prior to the addition of magnetite in Run 4, the mixing process for magnetite occurred by hand within the flume. While this procedure was hampered by damp sediment, a desired precision of ± 0.11 % (8 random samples of the mixture) was achieved after several thorough mixings.

Following each run sediment transported out of the channel was redistributed evenly over the channel and remixed. Five random grab samples were taken to ensure an even distribution of cassiterite and magnetite throughout the channel sediments. If the weight percentages were not within the standard deviation of the average (± 0.10 % for cassiterite, ± 0.11 % for magnetite) then the sediment was remixed and sampled until a desired homogeneity was achieved.

After leveling of the bed, a minimal discharge was applied to allow settlement of the sediment without transporting any fine material. This discharge was initially allowed to infiltrate slowly into the sediment to avoid trapped air pockets. Within twenty-four hours the sediment settled approximately 1 cm leaving a sediment column of 6 cm. The motor was then set to a desired RPM value and a pavement was allowed to develop over a period of 96 hours. A higher discharge was then applied for up to one hour to "simulate" a flood. An exception to this procedure occurred in Run 1 when three progressively higher discharges were employed for 96 hours each.

During pavement development, the following sedimentological and hydrologic measurements were established:

i) The amount of sediment transported was sampled at 0.5, 1, 2, 4, 8, 16, 32, 48, 72, and 96 hours. Ninety-six hours was considered a cutoff point for pavement development because sediment transport rates are very close to zero after this period of time, irregardless of discharge. This is reflected in Figure 3-3 where the sediment transport rate for Run 3 is seen to decrease exponentially with time. The transported sediment which collected in the sediment trap was dried, weighed, and sieved at 1/2 ϕ intervals to determine the grain size distribution. Due to large samples (up to 80 kg), material less than 5.66 mm was split into a sample weight of 400 - 700 g.

ii) Velocity measurements were taken at 4, 8, 32, 48, 72, and 96 hours. Measurements were not made within the first four hours when high sediment transport rates could damage the submerged probe. Velocity readings were taken at six to seven water depths to construct a vertical velocity profile at 5.2, 5.6, and 6.0 m along the length of the flume. Profiles were taken in the middle of the channel at all three locations and at 5.6 m, additional velocity profiles were taken 15.0 cm on either side of the centerline.

iii) Measures of water depth and slope were taken at 8, 32, 72, and 96 hours. Water depths were measured along a transect at 6.0 m with measurements 5.0 cm apart. Average depth was calculated as the mean of the fifteen readings. Water surface slope was determined from a least-squares fit through water surface elevations measured along the centerline at five stations, each one meter apart starting three meters downstream of the channel entrance.

iv) To monitor development of the pavement, surface samples were taken at 2, 8, 32, and 96 hours. A piston sampler (14 cm diameter) covered with a stiff clay-water mixture was pushed

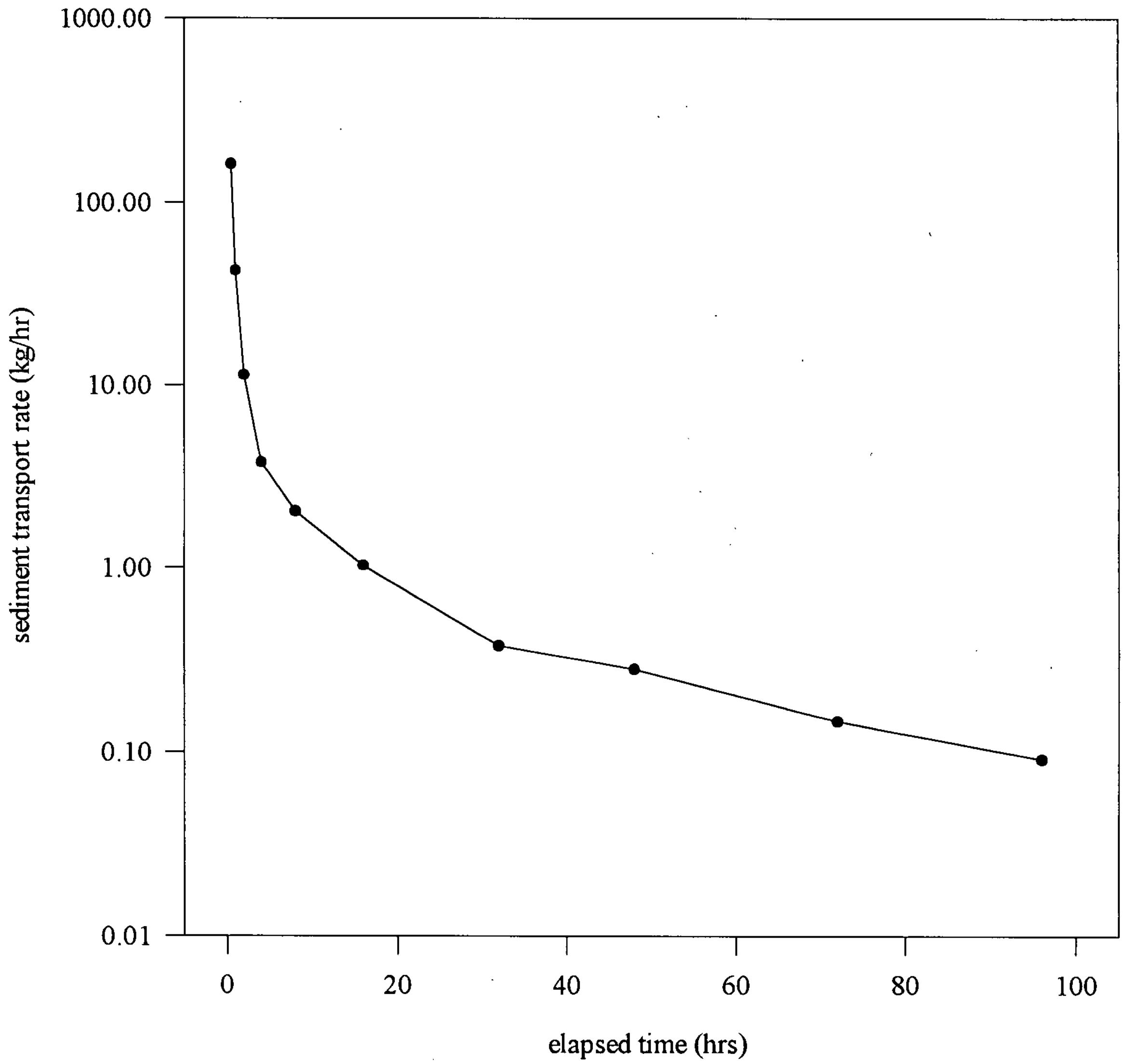

Figure 3-3. Sediment transport rate of Run 3 as a function of time. Total elapsed time was 96 hours.

gently into the surface, effectively sampling the surface grain layer. This procedure was repeated five times across the width of the channel to produce a surface sample of 700 to 900 g. To remove the clay fraction the clay-sediment mixture was placed in a 0.125 mm sieve and rinsed with warm water (finer sediment, 0.090 to 0.125 mm, was present within the bed, but concentrations were insignificant on the bed surface). Surface samples were taken 2 to 4 m downstream of the channel entrance. An unfortunate consequence of sampling the surface during experiments is that the subpavement is subjected to renewed degradation at the point of sampling. While this leads to an increase in sediment transport, the pavement quickly redevelops, thus minimizing the disturbance.

Starting with Run 3, the subsurface was sampled at the same frequency and location as the surface samples to assess the preferential accumulation of heavy minerals beneath the pavement. The subsurface was sampled using a jar lid (5 cm in diameter and depth of 1.25 cm) which was pushed into the sediment until flush with the surface. A rectangular sheet of metal was then placed beneath the lid and the sample lifted out.

v) Vertical samples of the substrate were collected along the length of the flume at the end of Runs 3, 4, and 5 to assess the vertical and longitudinal distribution of the heavy fraction following the simulated flood. Samples were obtained by digging a small trench and sliding a thin metal plate, 8.0 cm by 12.0 cm, into the sediment. Resulting samples varied in thickness from 1 to 3 cm and weighed 250 to 550 g.

High rates of sediment transport and frequent sampling during simulated floods limited hydraulic measurements. Determination of water depth was restricted to an average of six or seven measurements along a transect at 6.0 m (one to two sets) and water surface slopes were assumed to remain constant following pavement development. While the slope may have changed during a simulated flood (see section 4.2.1), the time required for accurate slope measurements precluded its determination. Velocity profiles could not be constructed due to high sediment transport rates and, as a consequence, velocity readings were taken only at 0.4 x water depth. Velocity measurements were further restricted to the centerline at 5.2, 5.6, and 6.0 m and, depending on the duration of the flood, one or two sets of velocity readings were taken.

To determine the heavy mineral concentrations in the analyzed samples, the sediment was sieved down to 0.50 mm and the magnetite was removed with a hand magnet. The remaining sediment was analyzed for cassiterite by standard heavy liquid separation using bromoform (2.9 g/cm^3 density) as the separating agent.

4.0 OBSERVATIONS

This chapter focuses on experimental observations and is subdivided into three sections. In order these sub-sections deal with: i) a summary of measured and calculated hydraulic parameters for all runs, ii) detailed descriptions of individual runs, iii) transport behaviour of magnetite in Runs 4 through 6.

4.1 Summary of observations

Table 4-1 summarizes measured and calculated hydraulic parameters for Runs 1 through 6. Each run is divided into two components (except for the first run which was structured as three consecutive discharges of increasing magnitude), pavement development and simulated "flood". To maintain consistency all listed values for pavement development refer to measurements taken at 96 hours. This is especially important for velocity and depth readings which changed reciprocally during pavement development in response to increasing bed roughness. The increase in bed roughness led to decreased flow velocities, which was countered by an increase in flow depth to maintain constant discharge. Slope values generally decreased during pavement development, but this was not a consistent trend.

Initial conditions varied during pavement development with slopes ranging from 0.006 to 0.014 (values typical of gravel-bed streams) and water depths ranging from 2.7 to 5.3 cm. Despite varying hydraulic conditions the shear stress applied to the bed was similar in some instances. Before considering this statement further the concept of *corrected* shear stress must be addressed.

Table 4-1. Measured and calculated hydraulic parameters for each experimental run.

RUN #	Run time (hrs)	Depth ($\times 10^{-2}$ m)	Slope	Velocity (m/s)	Discharge (m^3/s)	Surface D_{50} (mm)	Temp. (°C)
1	96	2.7	0.0106	0.75	0.016	4.8	17.5
	96	4.8	0.0079	1.11	0.043	7.5	18.5
	96	6.6	0.0057	1.36	0.072	8.1	20.5
2	96	4.6	0.0081	1.00	0.037	8.0	17.0
	30 min	8.5		1.83	0.124		17.0
3	96	4.6	0.0078	0.92	0.034	8.5	16.5
	1	8.0		1.54	0.099		13.5
4	96	2.8	0.0143	0.72	0.016	8.2	16.0
	15 min	6.2		1.97	0.098		16.0
5	96	5.3	0.0060	0.95	0.040	5.0	16.5
	15 min	5.7		1.25	0.057		16.5
	1	6.5		1.37	0.071		16.5
6	163	3.0	0.0089	1.04	0.025	5.1	16.5
	18 min	4.5		1.39	0.052		17.0
	80 min	5.0		1.45	0.058		17.0

Discharge = velocity x depth x width (0.80 m)
Temp. = water temperature
D_{50} = median diameter of developed surface

Table 4-1 (cont.)

RUN #	Run time (hrs)	ν ($x10^{-6}$ m^2/s)	Fr	Re	R ($x\ 10^{-2}$ m)	R_b ($x\ 10^{-2}$ m)	τ (N/m^2)	τ_{corr} (N/m^2)
1	96	1.07	1.55	17,730	2.5	2.6	2.63	2.67
	96	1.04	1.65	45,742	4.3	4.4	3.32	3.41
	96	0.99	1.89	77,825	5.7	5.7	3.17	3.18
2	96	1.08	1.49	38,200	4.1	4.3	3.28	3.39
	30 min	1.08	2.21	118,790	7.0	7.0	5.57	5.58
3	96	1.10	1.36	34,505	4.1	4.3	3.16	3.31
	1	1.18	1.87	87,010	6.7	6.9	5.23	5.42
4	96	1.11	1.50	16,974	2.6	2.7	3.67	3.80
	15 min	1.11	2.68	95,270	5.4	5.5	7.64	7.77
5	96	1.10	1.43	40,417	4.7	4.9	2.75	2.87
	15 min	1.10	1.78	56,690	5.0	5.0	2.94	2.94
	1	1.10	1.85	69,640	5.6	5.6	3.29	3.28
6	163	1.10	1.87	26,385	2.8	2.8	2.44	2.45
	18 min	1.08	2.16	54,130	4.2	4.4	3.96	4.12
	80 min	1.08	2.14	59,670	4.4	4.7	4.19	4.39

ν = kinematic viscosity of water
Fr = Froude number equal to $V / (R_b\ g)^{1/2}$ where g is the acceleration due to gravity taken as 9.81 m^2/s
Re = Reynolds number equal to R V / ν
R = hydraulic radius, calculated as the area divided by the wetted perimeter
R_b = corrected hydraulic radius
τ = calculated shear stress prior to side-wall correction
τ_{corr} = corrected shear stress

In flume experiments the substrate is generally much rougher than the side-walls, leading to a greater applied stress to the bed. Consequently, a correction procedure must be applied to the average shear stress which is defined as

$$\tau = \rho g R S \tag{4.1}$$

where ρ is the fluid density, g is the acceleration due to gravity, R is the hydraulic radius, and S is the water surface slope.

The corrected shear stresses of Table 4-1 were calculated using the side-wall correction procedure of Vanoni and Brooks (1957). The principal argument, first proposed by Einstein (1942), is that the shear force can be separated into two components, one acting on the bed (cross-sectional area A_b) and the other acting on the lateral boundaries (cross-sectional area A_w). It is also assumed that the Darcy-Weisbach relation (equation 4.2) can be applied to each part of the cross section as well as to the whole (Vanoni, 1975).

$$V^2 / S = 8g R / f = 8g R_b / f_b = 8g R_w / f_w \tag{4.2}$$

where $R = A / P$ (P is the wetted perimeter), V = average velocity, f = Darcy-Weisbach friction factor, and the subscripts b and w refer to the bed and wall sections, respectively.

Equation 2 can be re-arranged utilizing the following geometrical relationships: $A = A_w + A_b$ and $P = P_w + P_b = 2d + b$, where d equals depth and b equals channel width

$$f_b = f + (2 d / b)(f - f_w) \tag{4.3}$$

The remaining unknown variable, f_w, can be determined by considering Figure 5.1, where the friction factor is plotted as a function of Re / f (where Re is the Reynolds number) for smooth boundary channels. As it can be proven that

$$Re_b / f_b = Re_w / f_w = Re / f \qquad (4.4)$$

the ratio Re / f (both variables are known quantities from experimental data) can be calculated and thus also Re_w / f_w. Then f_w can be read directly off Figure 4.1 and the corrected hydraulic radius can be expressed as

$$R_b = V^2 f_b / 8g S \qquad (4.5)$$

The corrected bed shear stress is then given by

$$\tau_{corr} = \rho g R_b S \qquad (4.6)$$

As mentioned some of the runs had similar shear stresses despite varying slopes and water depths. Comparable experiments are Runs 2 and 4 (Run 3 was a replicate of Run 2) and Runs 5 and 6 where a finer sediment mix was employed. Because the shear stresses were similar for these two sets of runs (Table 4-1), one would expect similar pavements to develop. This was reflected in the median diameters of the developed surface with D_{50} values of 8.0 and 8.2 mm for Runs 2 and 4 respectively and D_{50} values of 5.0 and 5.1 mm for Runs 5 and 6 respectively.

An alternative procedure for determining the shear stress is to use the velocity profile method, which yields a shear stress for a particular point on the bed. This study, however, is interested in the areal average bed behaviour and a number of velocity profiles would be required

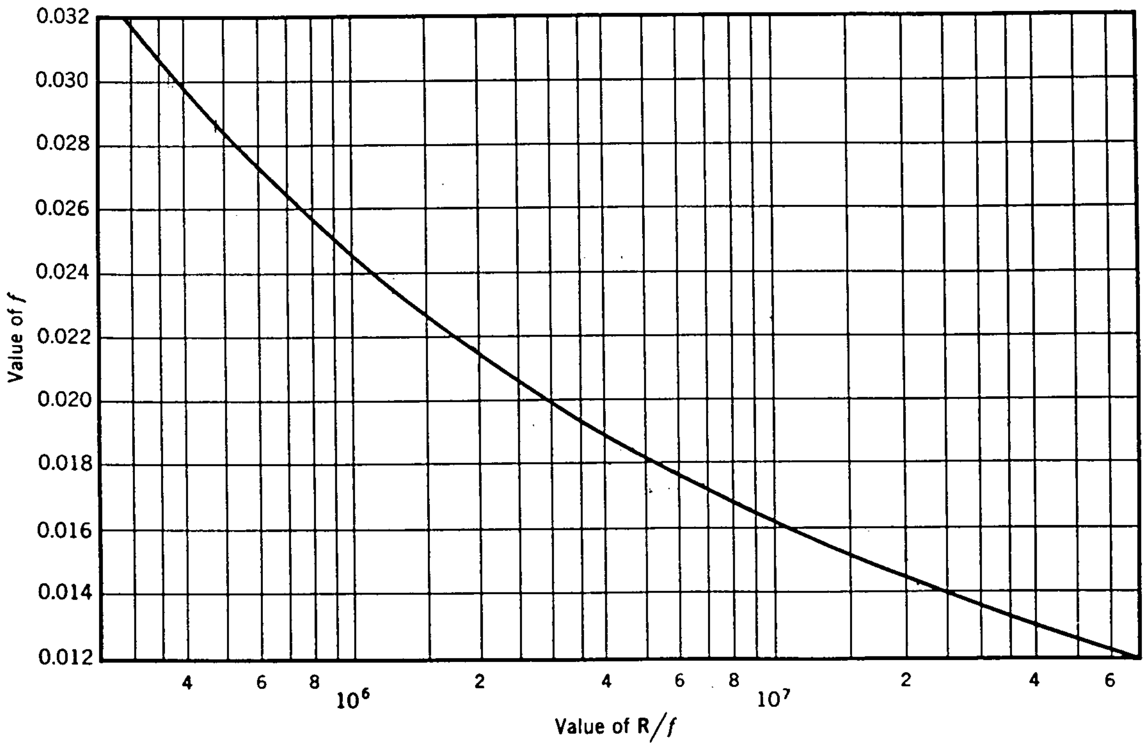

Figure 4-1. Friction factor as a function of Re / f for smooth boundary channels (after Vanoni, 1975)

to obtain a representative value. The approach used (i.e. $\tau = \rho g R S$) is an average measure of shear stress over the bed and is valid so long as flow is uniform, a condition which was satisfied.

For the runs to be representative of Harris Creek, the flow regime had to be hydraulically rough and Froude similarity had to be preserved. Reynolds numbers were below values characteristic of Harris Creek during flooding. Equation 1.4 was satisfied for all flood events, however, indicating that the flow regime was hydraulically rough and Reynolds scaling could be relaxed. Froude numbers typical of Harris Creek were determined from hydraulic measurements taken from 1988 to 1993. The highest flow during this period was 13.5 m^3/s, but it has been estimated that floods up to 25 m^3/s have occurred in the recent past (M. Church, pers. comm.). To estimate the Froude number at this discharge, the hydraulic geometry at Harris Creek was determined. Figures 4-2 and 4-3 plot depth and velocity, respectively, versus discharge on a log-log scale. Depth and velocity are average values based on the width of the channel at low flow. Therefore, during high flow frictional bank effects are negated and estimated Froude numbers are more realistic of flume conditions where the side-walls are practically frictionless. A least-squares fit through the data results in the following relations

$$d = 0.19\, Q^{0.46} \tag{4.7}$$

$$V = 0.42\, Q^{0.44} \tag{4.8}$$

Taking 10 m^3/s as the lower limit for pavement break-up (Day and Fletcher, 1991) and 25 m^3/s as the upper flood limit, Froude numbers of 0.50 and 0.60 can be determined based on equations 4.7 and 4.8. These values are well below the Froude numbers generated in the flume, which ranged from 1.36 to 2.68. The implication is that inertial forces dominated over

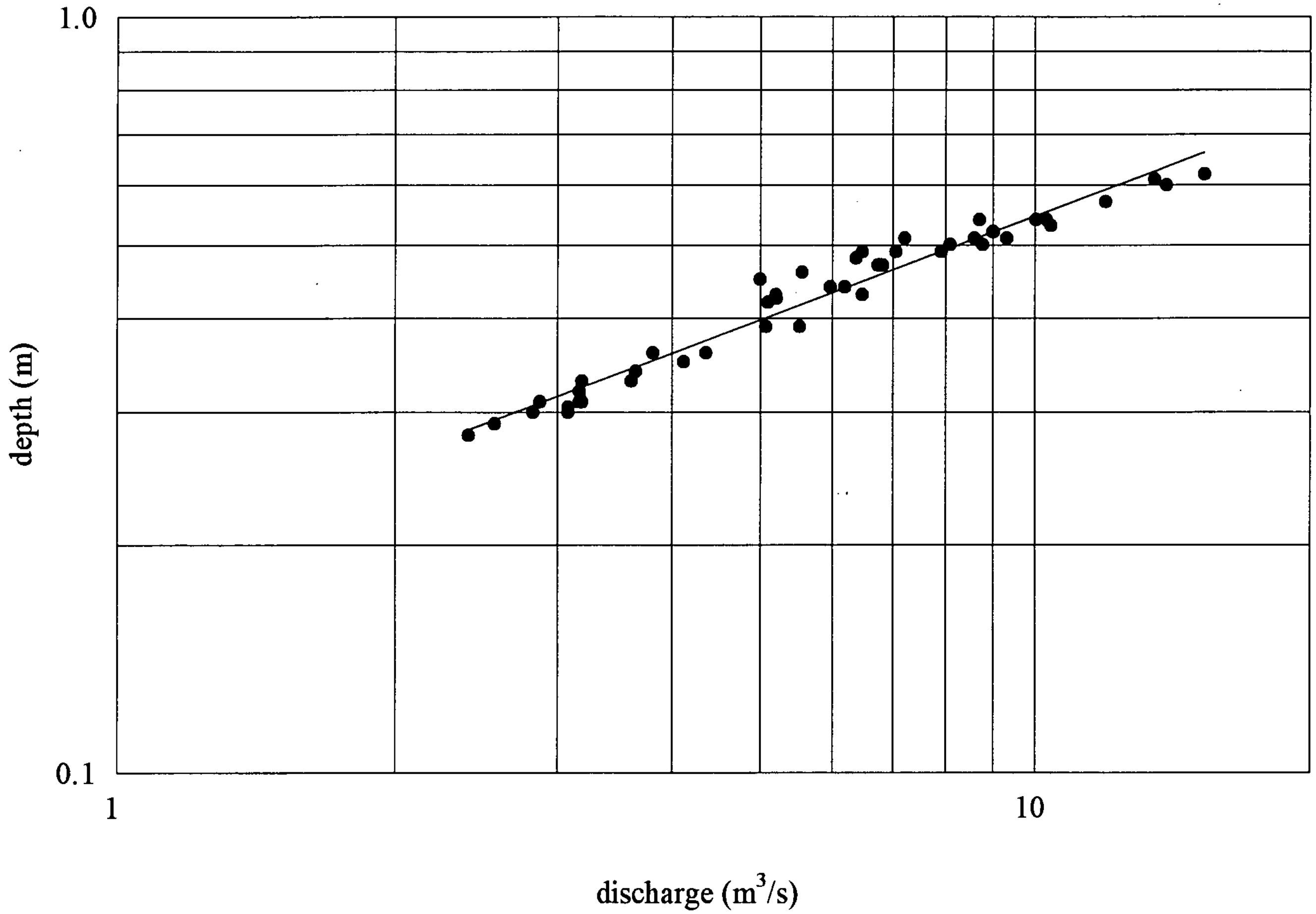

Figure 4-2. Depth versus discharge for Harris Creek, British Columbia.

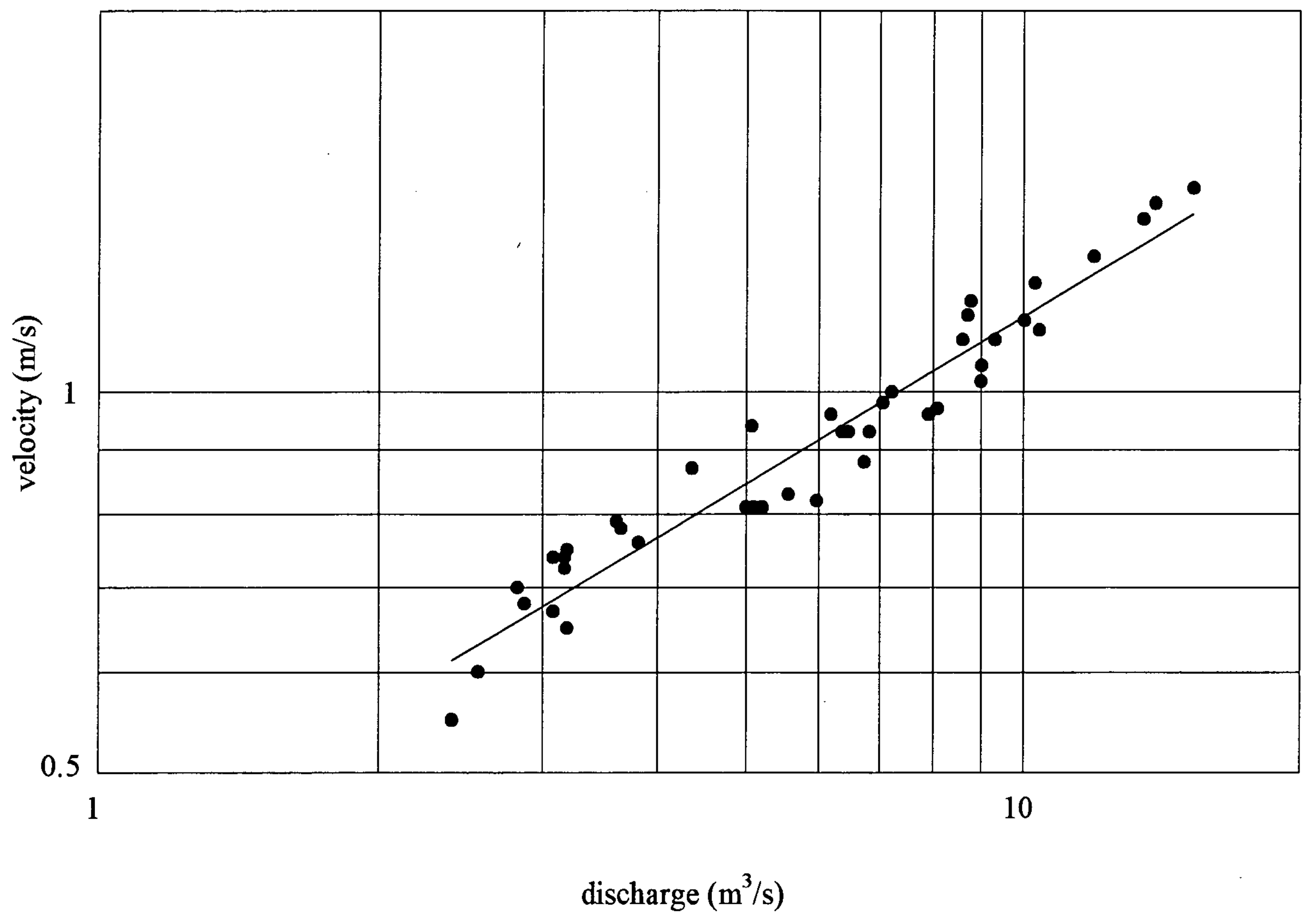

Figure 4-3. Velocity versus discharge for Harris Creek, British Columbia.

gravitational forces in the flume and as a consequence, full similitude between Harris Creek and the flume was not achieved. A portion of this disparity can be attributed to the absences of major form resistance elements in the flume. The presence of bar structures and bank irregularities in nature reduce Froude numbers by increasing flow resistance. It should also be noted that the variable slope (0.060 to 0.014) experienced in the flume deviates from the slope at Harris Creek, $S_{hc} \sim 0.013$. High Froude numbers and variable slope are important factors to consider when assessing the degree of similitude between Harris Creek and the flume model.

4.2 Run results

The following sections highlight experimental results and procedures for Runs 1 through 6. The reader is asked to refer to Appendices A through E for a complete reference of experimental results. This includes total sediment transport rates, velocity profile data, fractional percentages of transported, surface, and subsurface sediment samples, and slope data.

4.2.1 Run #1

Previous flume experiments at the University of British Columbia revealed that a relatively low flow would result in pavement development, but the hydraulic conditions necessary to mobilize cassiterite were unclear. Consequently, Run 1 evaluated the transport behaviour of cassiterite to provide a framework for subsequent runs.

The run began with the development of a pavement under low flow conditions ($Q = 0.016$ m^3/s). Initial sediment transport rates were high, with the majority of sediment transport occurring in the first hour as the bed degraded to a stable configuration (Table 4-2). Sediment transport was minimal after ninety-six hours, $Q_b = 0.058$ kg/hr, indicating that maximum pavement development had effectively occurred under the imposed conditions. The developed pavement was appreciably coarser than the original surface conditions ($D_{50} = 4.80$ mm as compared to $D_{50} = 1.40$ mm), however, the abundance of fines upon the surface indicated poor pavement development overall.

Water depth was then increased by 2.1 cm, yielding a discharge of 0.043 m^3/s. This flow was sufficient to break up the pavement and transport sediment up to 11.3 mm in diameter out of

Table 4-2. Total sediment transport rates for Run 1, stage 1 (Q = 0.016 m^3/s).

Elapsed time (hrs)	Sediment transport rate (kg/hr)
0.5	46.15
1	22.02
2	6.271
4	2.180
8	1.044
16	0.383
32	0.228
48	0.123
72	0.067
96	0.058

the channel. Cassiterite, however, was not transported out of the channel. This flow was continued for ninety-six hours to assess the development of the surface under increased hydraulic stress. At the end of the second stage, the surface material had a median diameter of 7.52 mm and the majority of the fines had been winnowed away from the surface to yield a well-developed coarse surface. Subsequent experiments consequently employed a similar shear stress (3.4 N/m^2) for initial pavement development. Figure 4-4 presents the developed pavement of the second stage of Run 1, typical of Runs 2 - 4.

The pavement was broken up again by an increased discharge in a final effort to mobilize cassiterite. Water depth was increased by an additional 1.8 cm which doubled the discharge to 0.072 m^3/s. Although cassiterite was not transported beyond the tailgate by the increased flow, it was observed on the surface in the lea of coarser sediment after the initial hour of pavement break-up.

Though the pavement was allowed to develop over four days during each stage of Run 1, its coarse nature was evident after two hours. Figure 4-5 compares the grain size distributions of the pavement after 2 and 96 hours during stage 2. The distributions are notably similar, with a minor coarsening evident. This similarity is expected due to the exponential nature of the sediment transport with the majority of transportation occurring in the first two hours. After two hours the coarse framework is stable and protruding into the flow; this shields finer sediment from entrainment.

Referring to Table 4-1, one will note that the water surface slope decreased from 0.0106 in stage 1 to 0.0057 in stage 3 despite no adjustment in slope. Because the flume tailgate prevents bed erosion at the downstream end of the channel,sediment at the channel entrance is preferentially

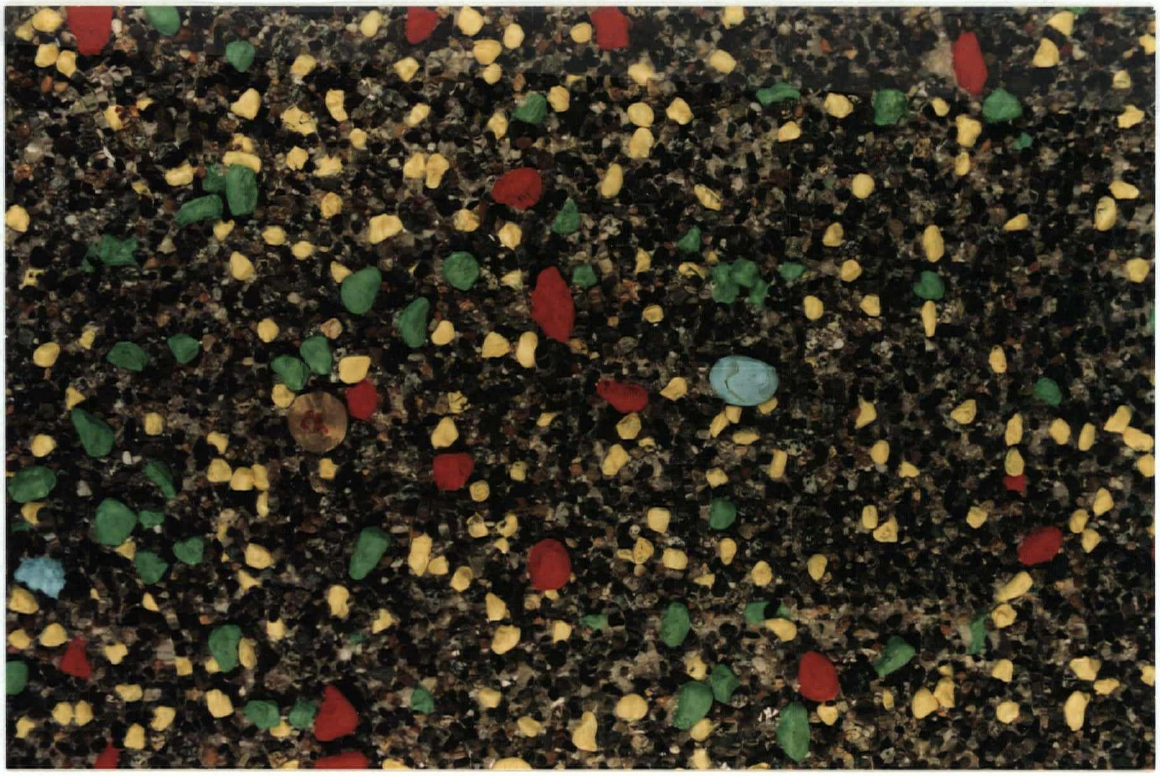

Figure 4-4. Pavement development after 96 hours for the second stage of Run 1. The photograph was taken at 5.5 m in the middle of the channel with flow from left to right. The brass disk is 3.0 cm in diameter.

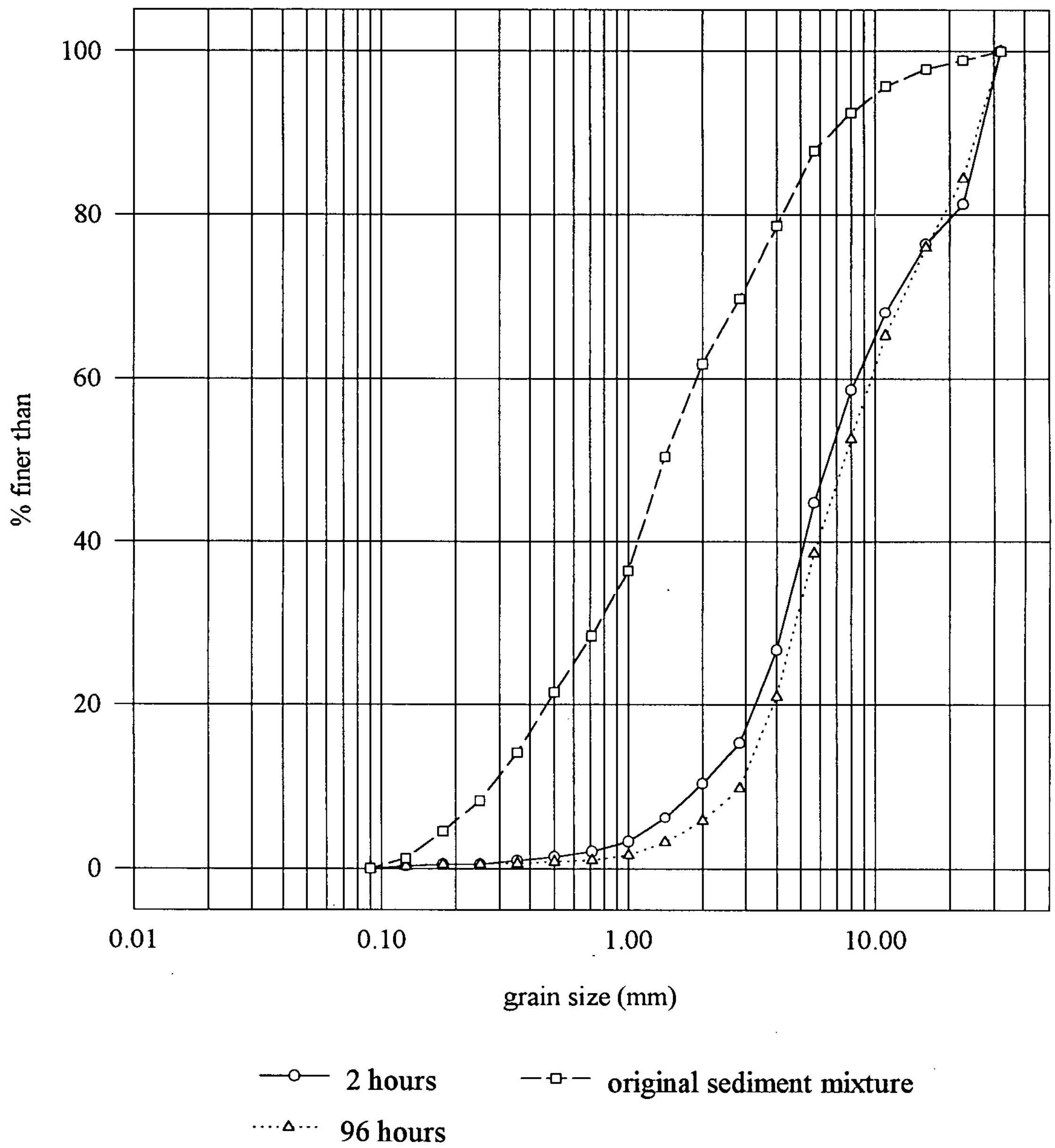

Figure 4-5. Grain size distribution of surface material after 2 and 96 hours in Run 1 ($Q = 0.043\ m^3/s$) and original flume mixture.

eroded away. This results in a wedge-shaped longitudinal profile of the bed material (i.e. a sediment depth of 6 cm at the tailgate and depths of 2 to 4 cm at the channel entrance). Higher shear stresses transport greater amounts of sediment and produce a steeper sediment wedge which leads to lower water surface slopes, as reflected in the slope data. This differential erosion is of little concern as long as uniform flow is maintained. A useful check is to ensure that the ratio of the block height at the exit to flume length is less than 0.06 (M. Church, pers. comm.). For this experimental study the calculated value of 0.006 was well within the limits of uniform flow.

The calculated slopes can result in misleading estimates of shear stress. For example, the calculated shear stress of stage 3 was reduced from stage 2 (Table 4-1) although the actual shear stress was evidently higher as it disrupted the pavement developed in stage 2. When flow is initially increased, the water surface slope decreases in response to the steeper wedge profile developed, but the calculated shear stress reflects conditions after the initial high sediment transport rates when the slope has stabilized. For instance, the initial slope of stage 3 was 0.0078 until two hours of high sediment transport reduced the slope to 0.0060. As a result, the initial stress applied to the bed is calculated at 5.33 N/m^2 before decreasing to 3.18 N/m^2 in response to slope adjustment. Applying the same reasoning the initial shear stress of stage 2 was 4.74 N/m^2.

4.2.2 Run #2

Cassiterite observed on the bed surface during the third stage of Run 1 suggested that "flooding" a developed surface would be sufficient to mobilize the cassiterite. This was the premise for Run 2: develop the surface for 96 hours under conditions similar to the second stage of Run 1, before increasing the discharge to break the pavement.

An initial water depth of 0.046 m and a slope of 0.0081 were established. After the pavement had fully developed over ninety-six hours, the water depth was increased to 0.085 m yielding velocities of 1.83 m/s and a discharge of 0.124 m^3/s. These simulated flood conditions were sustained for thirty minutes until the first half-meter of sediment had been washed away leaving the plexi-glass bottom exposed. Although sediment transport rates peaked at 175 kg/hr and sediment up to 16.0 mm was transported, the high discharge was insufficient to move the cassiterite out of the channel. As in Run 1, cassiterite was noted on the bed surface occupying scour zones and in the lee of coarse sediment. Whether the surface concentrations were lag deposits, preferential accumulations of cassiterite due to minor transport, or a combination of these two processes, was unclear.

The proportional transport rates of the light fractions exhibited a characteristic pattern during pavement development. Figures 4-6, 4-7, and 4-8 plot the change in proportional transport with time for the various size fractions of Run 2. The coarser fractions, 2.83 to 11.0 mm, are transported at proportionally high rates during the first hour before leveling off to constant values (Figure 4-6). The fractions from 0.71 to 2.83 mm display little variation with time while the amount of transported fine sand increases proportionally over the initial hour before leveling off (Figures 4-7 and 4-8). A similar pattern was exhibited during pavement development of Runs 3 through 6.

High proportions of coarse sediment initially being transported result from the lack of surface texture at the start of the run. When a flow is imposed the finer sediment acts as a conveyor belt upon which coarser sediment can roll. This phenomenon, however, is rapidly destroyed as the surface develops. The initial transport rates of the fine sand are low due to the large amounts of coarser sediment being transported, which reduces the proportional concentration

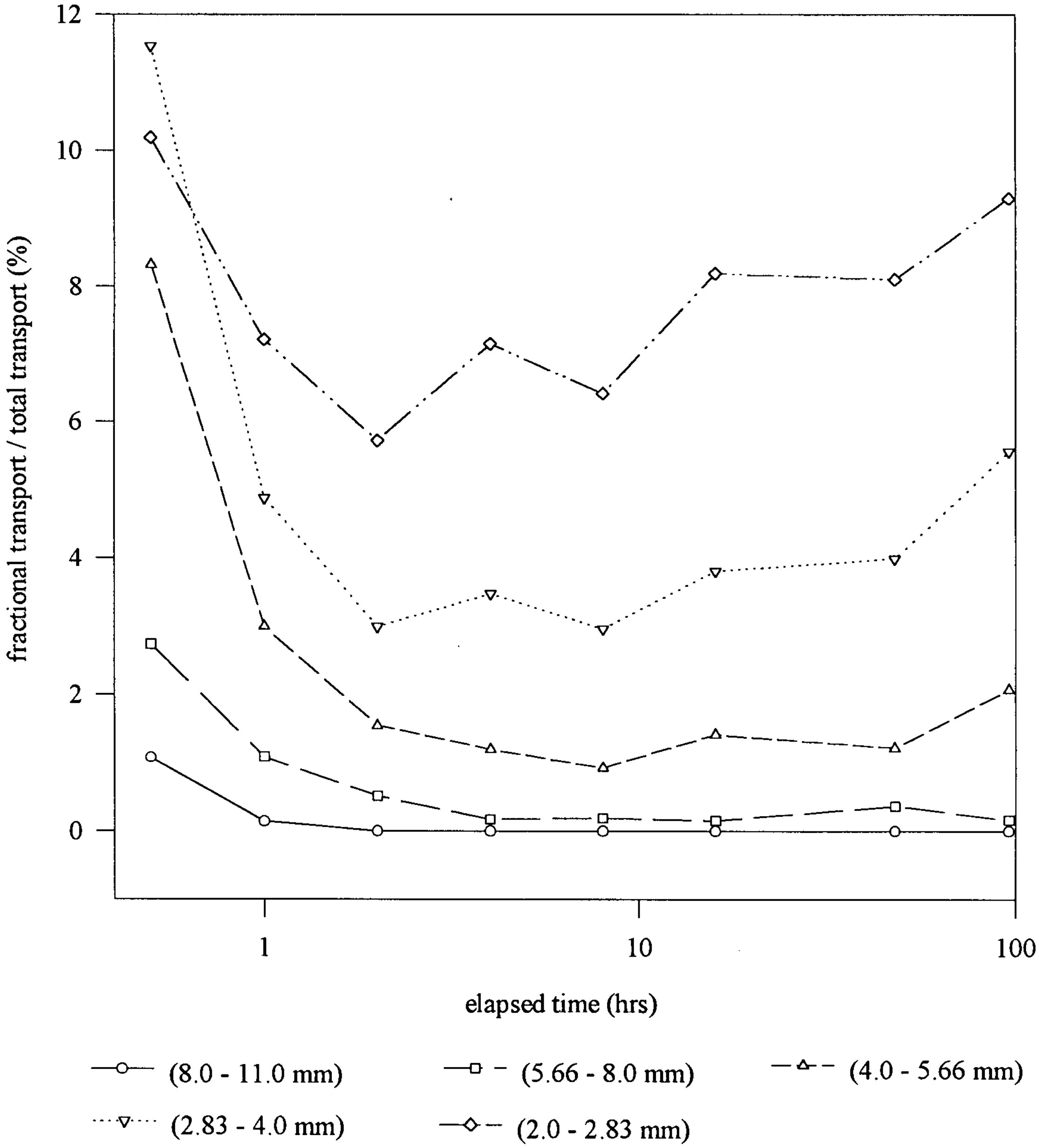

Figure 4-6. Change in fractional proportions of transported sediment, 2.0 - 11.0 mm, during pavement development (Run 2, Q = 0.037 m^3/s).

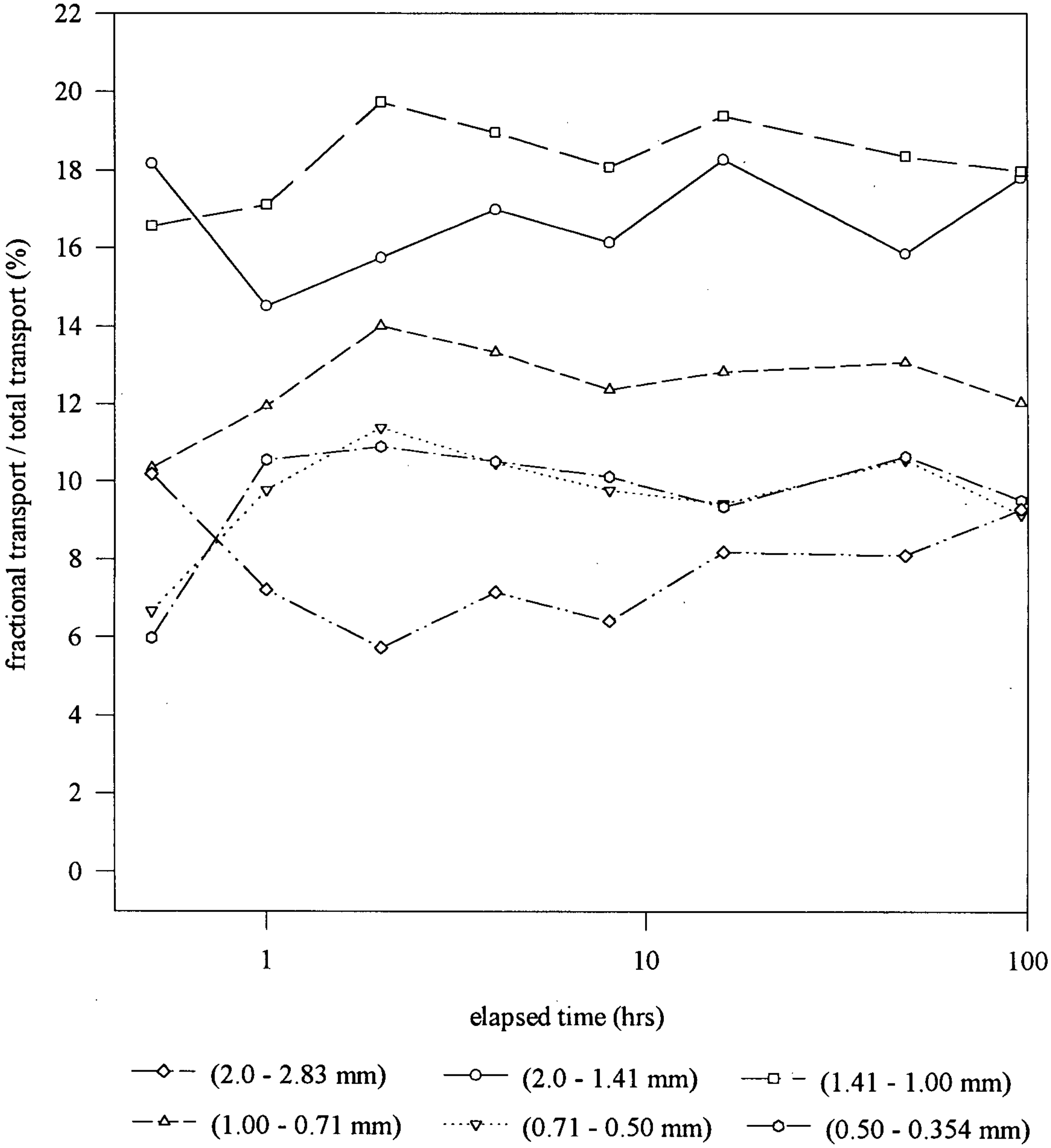

Figure 4-7. Change in fractional proportions of transported sediment, 0.354 - 2.0 mm, during pavement development (Run 2, Q = 0.037 m^3/s).

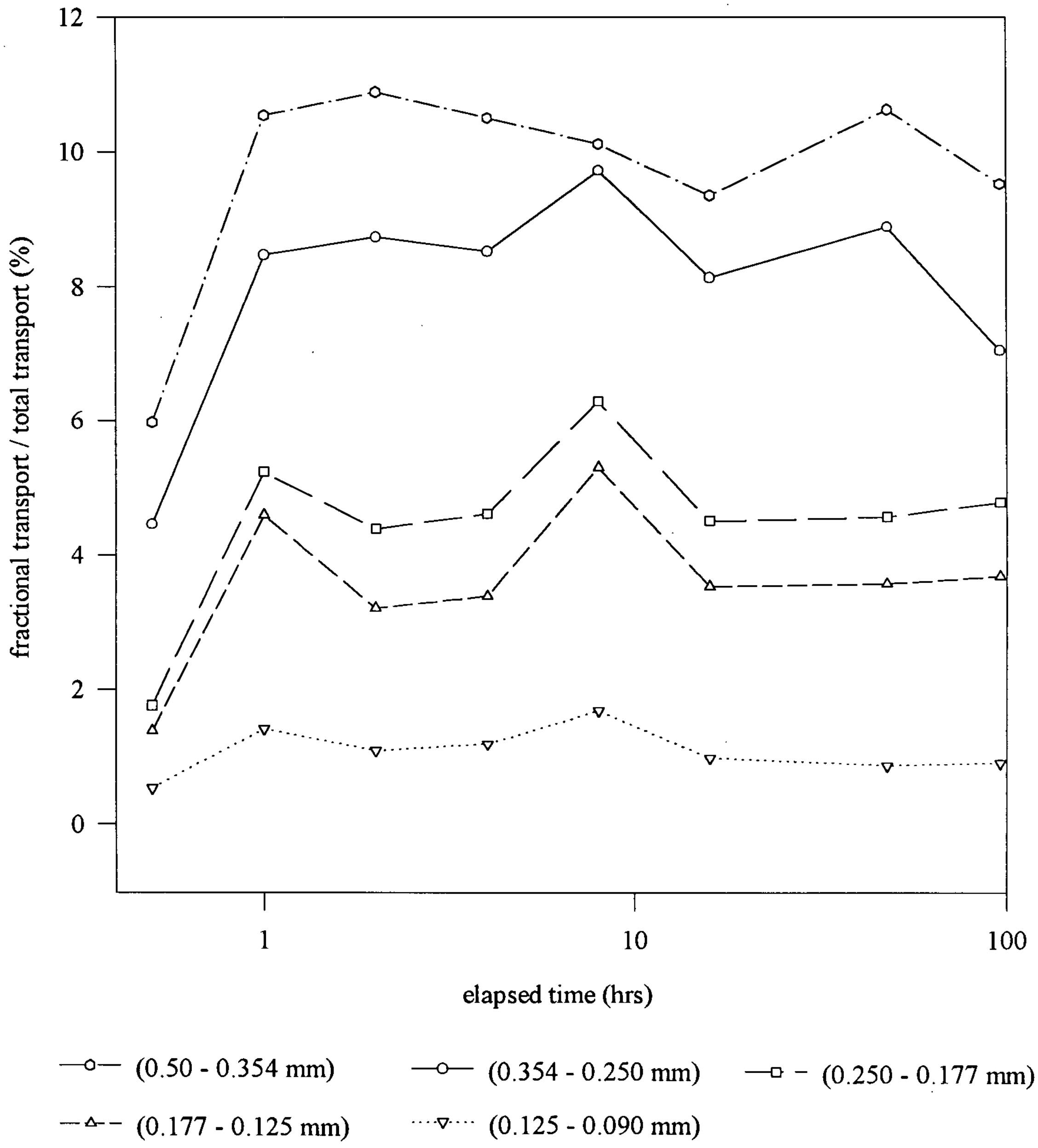

Figure 4-8. Change in fractional proportions of transported sediment, 0.090 - 0.354 mm, during pavement development (Run 2, Q = 0.037 m^3/s).

of the finer material in the total load. Quantities of the intermediate fractions are sufficiently large that the quantitative perturbation introduced by the coarsest fractions is not noticed materially.

4.2.3 Run #3

The conditions of Run 2 were replicated to assess the reproducibility of the results and to investigate the cassiterite distribution more thoroughly. The former condition was satisfied as the total sediment transport rates of Runs 2 and 3 were very similar (Table 4-3), although there was some discrepancy in the measured velocities at the close of pavement development (i.e. 1.00 vs 0.92 m/s for Runs 2 and 3 respectively).

During Runs 1 and 2 it was expected that cassiterite would be mobilized by the imposed flow conditions yielding data on fractional transport rates. As a consequence, a thorough description of the subsurface cassiterite distribution was disregarded. To more accurately describe the cassiterite distribution in Run 3 three additional measurements were made; i) the immediate subsurface was sampled during pavement development, ii) photos were taken of the surface cassiterite concentrations at the end of the simulated flood, and iii) vertical samples of the subpavement were taken at the end of the flood.

During pavement development the subsurface samples demonstrated an enrichment of cassiterite in the upper 1.25 cm (Table 4-4). It seems reasonable to conclude that the high density cassiterite grains are not easily entrained by the relatively low flow and consequently, infiltrate into the underlying sediment as light sediment surrounding them becomes entrained. The cassiterite is therefore concentrated as a lag deposit with greater rates of degradation producing higher subsurface concentrations.

Table 4-3. Comparison of transport rates for Runs 2 and 3.

Elapsed time (hrs)	Run #2 transport rate (kg/hr)	Run #3 transport rate (kg/hr)
0.5	165.47	162.33
1	44.81	43.31
2	11.61	11.36
4	5.40	3.77
8	2.28	2.02
16	1.04	1.03
32	0.37	0.38
48	0.28	0.28
72	0.16	0.15
96	0.10	0.09
10 min	65.85	80.56
20 min	176.17	151.93
30 min	135.13	175.04
40 min	-	75.83
50 min	-	80.35
60 min	-	49.89

Table 4-4. Weight percentage of cassiterite in subsurface samples during pavement development and after flooding in Run 3. Subsurface was sampled between 2 and 4 m.

Elapsed time (hrs)	Flow (m^3/s)	Cassiterite %
Pavement development		
2	0.032	1.46
8	0.032	1.80
32	0.032	1.85
96	0.032	1.95
Flooding		
1	0.099	2.75

The flood was run for one hour with samples of transported sediment taken at ten minute intervals. Cassiterite patches were first observed on the surface after thirty minutes up to 4.8 m along the channel. The number of heavy mineral patches increased with time and after fifty minutes were visible up to 7.0 m from the channel entrance. After one hour the sediment had been completely scoured from the first 0.70 m and the cassiterite patches had not progressed beyond 7.0 m. Photographs after the flood show typical patches of cassiterite which tended to develop in the lee of coarser sediment and within areas of more concentrated occurrence of coarse grains (Figure 4-9). Two random vertical sections sampled at 7.5 and 9.5 m after the flood indicated that the subsurface enrichment of cassiterite was restricted to the top centimeter (Table 4-5).

4.2.4 Run #4

The slope was increased to 0.0143 and the depth decreased to 0.028 m yielding a lower discharge than the two previous experiments (Q = 0.016 m^3/s). The shear stress, however, remained comparable. Magnetite was added prior to this experiment to evaluate the transport behaviour of a heavy mineral with a density lower than cassiterite. The specific transport behaviour of magnetite is detailed in section 4.3 as it shares patterns common to subsequent runs. The cassiterite subsurface samples during pavement development demonstrated the same pattern of enrichment as in Run 3 while the magnetite displayed minimal enrichment (Table 4-6).

The bed was flooded at 0.098 m^3/s for fifteen minutes after pavement development. An increased slope resulted in the highest calculated shear stress, 7.77 N/m^2, of all six experiments. Sediment transport rates peaked at 800 kg/hr during this period and all size fractions were in transport. All the sediment up to 4.5 m from the channel entrance was washed away due to the intense transport rates (Figure 4-10). Although cassiterite was not transported into the tailbox it

Table 4-5. Vertical sampling of cassiterite at 7.5 and 9.5 m at the close of Run 3. Sediment height was 3.75 cm at 7.5 m and 5.0 cm at 9.5 m.

Height above flume bottom (cm)	7.5 m cassiterite %	9.5 m cassiterite %
5.00 - 3.75		1.57
3.75 - 2.50	2.33	1.13
2.50 - 1.25	1.05	1.13
1.25 - 0.00	1.07	1.10

Table 4-6. Weight percentage of cassiterite and magnetite in subsurface samples during pavement development of Run 4. Subsurface sampled between 2 and 4 m.

Elapsed time (hrs)	Cassiterite %	Magnetite %
2	1.84	1.01
8	2.25	1.19
32	2.45	1.18
96	-	1.52

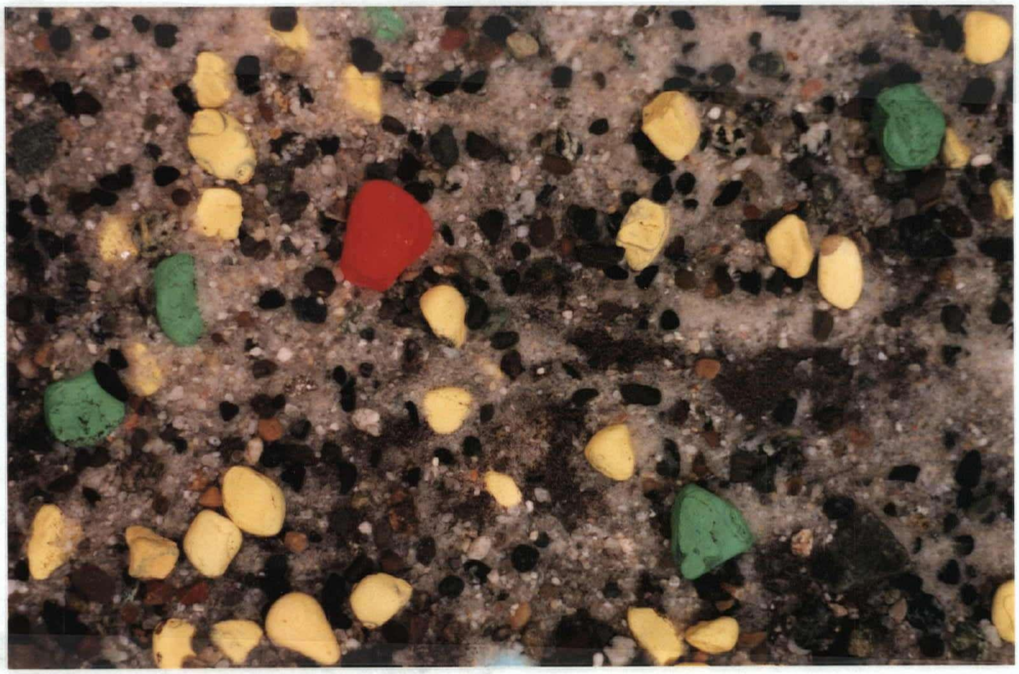

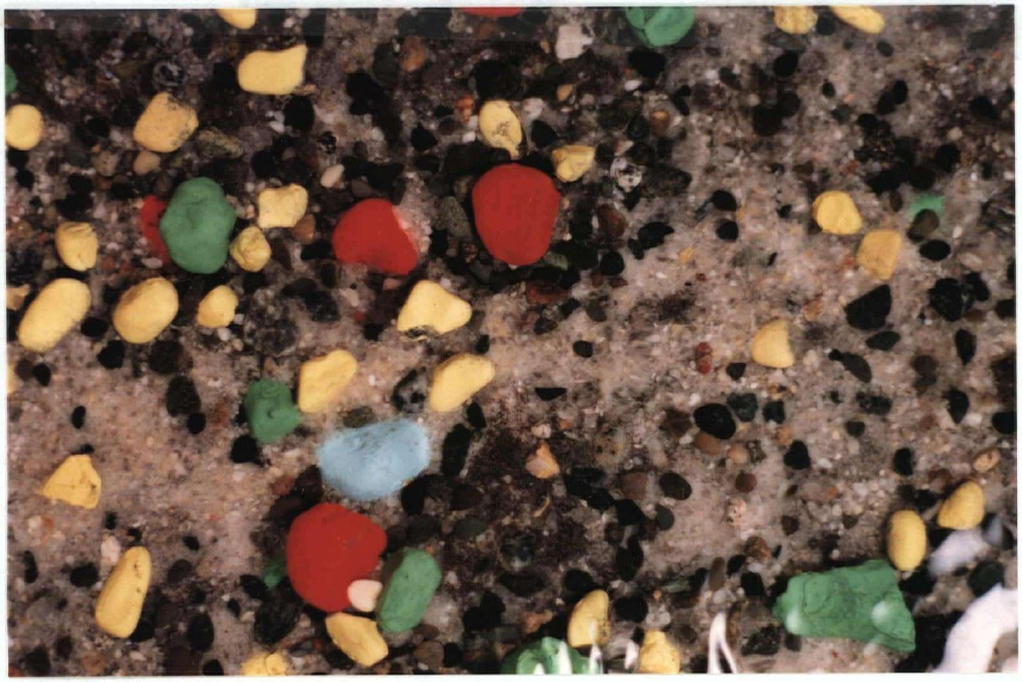

Figure 4-9. Patches of surface cassiterite (brown, fine granular material) after a one hour simulated flood for Run 3. The upper photograph was taken at 5.9 m while the lower one was taken at 6.2 m. Flow is from left to right. The coloured gravel provide a scale (i.e. yellow = 8 - 11 mm, green = 11 - 16 mm).

Figure 4-10. View from 6.5 m looking upstream after the fifteen minute simulated flood of Run 4. All sediment up to 4.5 m was removed as a result of transport rates up to 800 kg/hr.

was present on the surface up to 6.5 m, forming small scale, parabolic dunes up to 0.5 cm in thickness (Figure 4-11).

The bed was sampled at seven locations (downstream of the cassiterite surface concentrations) subsequent to the flood to observe the vertical distribution of the cassiterite and magnetite. The sediment was depleted in cassiterite in the top centimeter of the subpavement in some samples, with the greatest concentrations found at depths between 1 and 2 centimeters (Table 4-7). This trend is a result of high transport rates which formed sand waves up to 0.5 cm thick. Cassiterite was unlikely present in significant quantities in the sand waves due to its high density, resulting in depleted cassiterite values in the top centimeter sampled. Where the sand waves were thin or absent, cassiterite concentrations were high in the uppermost layer (e.g. at 7.0 and 8.5 m). Magnetite was enriched heavily in the upper layer and to a lesser extent at a depth of one to two centimeters (Table 4-8). There appeared to be no preferential accumulation of a particular size fraction of either cassiterite or magnetite.

4.2.5 Run #5

The slope in Run 5 was decreased to 0.0060 because high transport rates in Run 4 removed the sediment at the channel entrance. A decrease in slope was also required since the three coarsest fractions were removed prior to the start of the experiment which reduced the median grain size and the stability of the resulting pavement. It was predicted that the finer substrate would facilitate the transport of cassiterite by reducing the shielding effect of coarse sediment. To determine if the cassiterite was being mobilized for short distances, a portion of the flume from 5.1 to 5.3 m was dug out and the heavy fraction was removed.

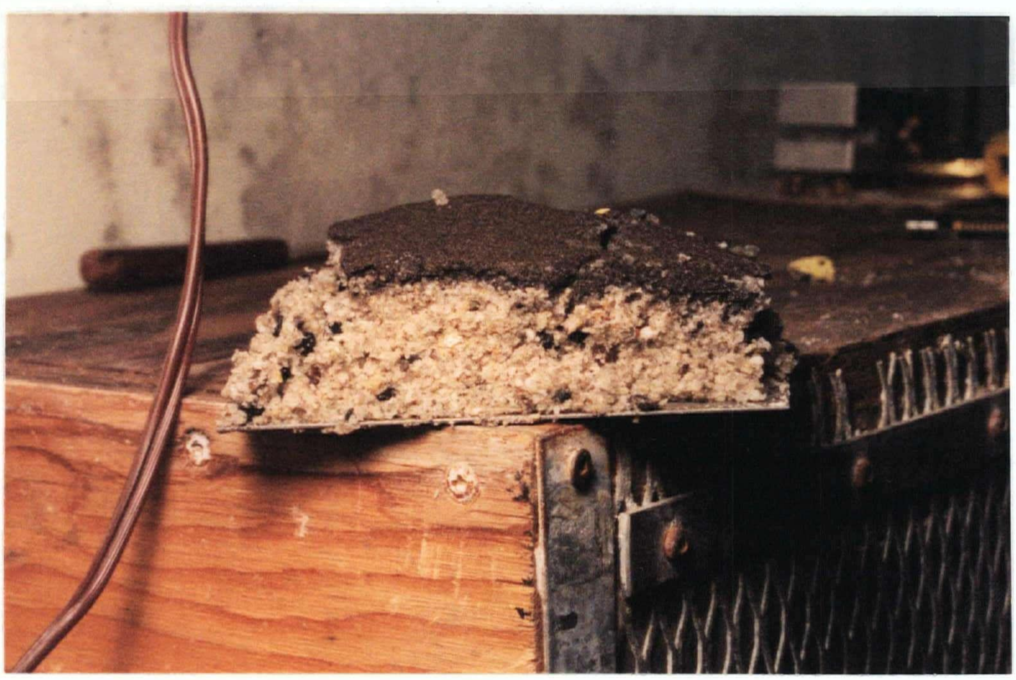

Figure 4-11. a) Photograph of parabolic cassiterite dunes at the close of Run 4. View is from 5.0 m looking downstream. b) Vertical slice (~ 3.0 cm) of cassiterite dune sampled at 5.4 m.

Table 4-7. Weight percentage and grain size distribution of cassiterite in vertical samples of Run 4. Sample intervals refer to height above flume bottom.

		Size fraction (mm)			
Sample	*Cassiterite weight %*	0.250 - 0.354 fractional %	0.177 - 0.250 fractional %	0.125 - 0.177 fractional %	0.090 - 0.125 fractional %
VERT 1 @ 6.8 m					
5 - 4 cm	*1.41*				
4 - 3 cm	*3.09*				
3 - 0 cm	*1.17*				
VERT 2 @ 7.0 m					
5 - 4 cm	*2.13*	7.3	36.7	49.5	6.6
4 - 3 cm	*2.13*				
3 - 0 cm	*1.57*	6.9	41.7	44.4	7.0
VERT 3 @ 8.0 m					
5 - 4 cm	*1.16*	6.1	47.5	37.8	8.6
4 - 3 cm	*1.71*	8.4	41.7	41.6	8.3
3 - 0 cm	*1.42*	8.8	42.5	42.0	6.7
VERT 4 @ 8.2 m					
6 - 5 cm	*0.65*				
5 - 4 cm	*1.69*				
4 - 2 cm	*1.18*				
2 - 0 cm	*1.08*				
VERT 5 @ 8.5 m					
5 - 4 cm	*2.32*				
4 - 3 cm	*1.62*				
3 - 0 cm	*1.33*				
VERT 6 @ 8.8 m					
6 - 5 cm	*0.16*				
5 - 4 cm	*1.63*	9.9	41.7	41.2	7.1
4 - 2 cm	*1.02*	6.2	42.1	43.7	8.0
2 - 0 cm	*1.19*	7.8	42.2	43.1	6.9
VERT 7 @ 9.5 m					
6 - 5 cm	*0.71*	9.6	43.6	40.4	6.4
5 - 4 cm	*1.05*	9.1	42.8	41.3	6.7
4 - 2 cm	*0.91*				
2 - 0 cm	*1.09*	8.8	41.3	43.3	6.5

Table 4-8. Weight percentage and grain size distribution of magnetite in vertical bed samples of Run 4. Sample intervals refer to height above flume bottom.

			Size fraction (mm)	
Sample	*Magnetite weight %*	0.250 - 0.354 fractional %	0.177 - 0.250 fractional %	0.125 - 0.177 fractional %
VERT 1 @ 6.8 m				
5 - 4 cm	*3.26*	50.7	26.9	22.4
4 - 3 cm	*1.84*	39.2	34.8	26.0
3 - 0 cm	*1.07*	45.8	28.1	26.1
VERT 2 @ 7.0 m				
5 - 4 cm	*3.08*	51.3	30.2	18.4
4 - 3 cm	*1.63*	36.8	36.7	26.5
3 - 0 cm	*1.44*	44.7	31.9	23.3
VERT 3 @ 8.0 m				
5 - 4 cm	*4.31*	33.9	37.8	28.3
4 - 3 cm	*2.22*	45.6	32.3	22.1
3 - 0 cm	*1.40*	36.4	33.9	29.6
VERT 4 @ 8.2 m				
6 - 5 cm	*3.03*	47.9	28.5	23.5
5 - 4 cm	*1.87*	36.5	32.6	30.9
4 - 2 cm	*1.25*	46.0	29.8	24.2
2 - 0 cm	*1.19*	38.6	34.0	27.3
VERT 5 @ 8.5 m				
5 - 4 cm	*5.24*	38.9	35.9	25.2
4 - 3 cm	*1.46*	45.9	28.4	25.7
3 - 0 cm	*1.28*	37.0	25.5	37.5
VERT 6 @ 8.8 m				
6 - 5 cm	*2.91*	39.1	33.0	28.0
5 - 4 cm	*1.92*	45.0	31.6	23.4
4 - 2 cm	*1.13*	42.3	36.7	21.0
2 - 0 cm	*1.24*	43.7	31.5	24.8
VERT 7 @ 9.5 m				
6 - 5 cm	*2.76*	48.4	29.4	22.2
5 - 4 cm	*1.11*	37.7	28.3	34.0
4 - 2 cm	*1.03*	44.5	31.3	24.1
2 - 0 cm	*1.13*	35.9	34.1	30.0

Due to the initial low slope the calculated shear stress was only 2.87 N/m^2. The pavement that formed, however, was well developed as the removal of the coarsest fractions reduced the shielding effect that had protected the finer sediment in Runs 1-4. Subsurface sampling of magnetite and cassiterite during pavement development followed the pattern of Run 4, with high concentrations of cassiterite and no substantial enrichment of magnetite (Table 4-9). Sampling of the heavy mineral free zone at the end of pavement development demonstrated that cassiterite had not been transported by the initial flow.

An intermediate discharge of 0.057 m^3/s was then applied for fifteen minutes to examine the behaviour of the finer substrate under elevated discharges, the concern being that the finer pavement would break-up easily under high flow conditions, washing all the sediment away. Minimal sediment was transported (0.4 kg) during the fifteen minutes so the discharge was increased to 0.071 m^3/s to initiate pavement break-up.

The flood was run for one hour with transported sediment sampled at ten minute intervals; transport rates varied from 24.4 to 98.7 kg/hr. After ten minutes cassiterite was noted at the surface up to 4.0 m from the channel entrance, with the majority of the patches observed within scour zones between 1.5 and 3.0 m (Figure 4-12). At the twenty minute mark cassiterite was visible up to 4.4 m, with the patches more concentrated and occupying a greater surface area. After forty minutes the cassiterite had extended downstream to 5.5 m, but the frequency and magnitude of the patches had diminished substantially leaving small isolated patches (Figure 4-13). Within the area where the heavy mineral fraction had been removed, cassiterite was detected at the surface which indicated that it was transported for short distances before coming to rest on the bed. After the flood the top centimeter of this area had concentrations of 3.63 % and 0.74 % for

Table 4-9. Weight percentage of cassiterite and magnetite in subsurface samples (Run 5). Subsurface sampled between 2 and 4 m.

Elapsed time (hrs)	cassiterite %	magnetite %
2	1.77	1.01
8	2.03	1.13
32	1.87	1.25
96	2.04	1.23

Figure 4-12. Run 5 concentrations of cassiterite after 10 min of flooding. Photo taken at 3.7 m with flow from left to right. Scale is given by the brass disk, 3.0 cm in diameter.

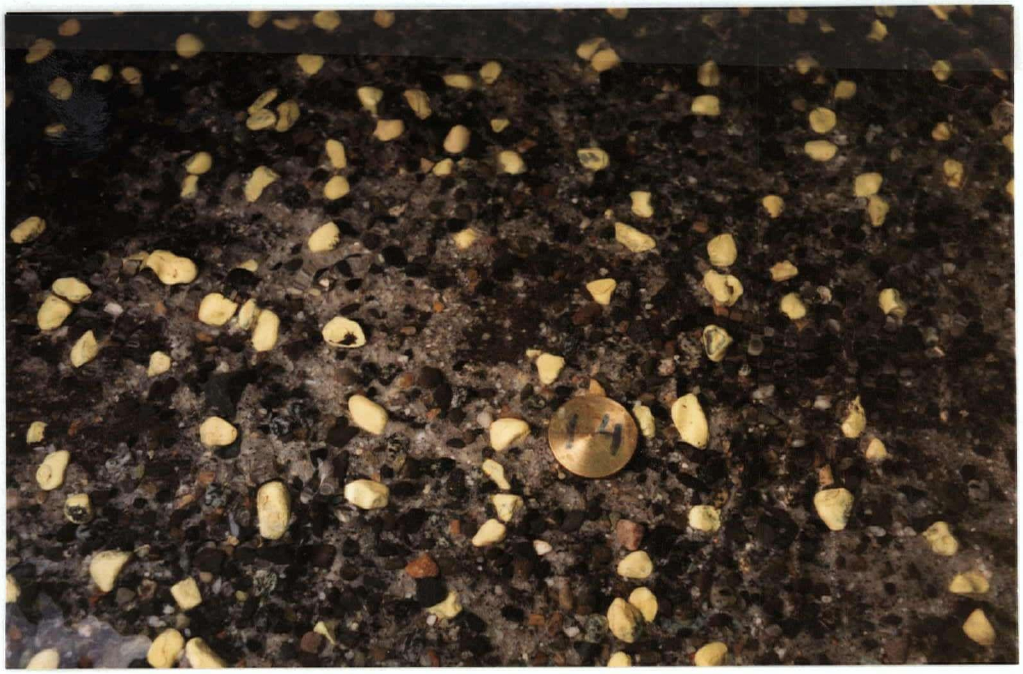

Figure 4-13. Run 5 surface concentrations of cassiterite after 40 min of flooding. Photo taken at 3.5 m with flow from left to right. Scale is given by the brass disk, 3.0 cm in diameter.

cassiterite and magnetite respectively. This implies that transport processes play a role in concentrating cassiterite within the subsurface and surface.

Vertical sampling of the post-flood substrate is summarized in Table 4-10. Two of the samples at 8.2 and 8.8 m do not display the subsurface enrichment of cassiterite observed in previous samples. As erosion in this region of the flume was minimal due to the tailgate and overall degradation rates were low, cassiterite did not concentrate as a lag deposit at these localities. A vertical sample at 9.5 m in Run 4 demonstrated a similar lack of enrichment (Table 4-7). Greater rates of degradation and minor cassiterite transport in the upper reaches resulted in high cassiterite concentrations in the subsurface at 4.4 and 6.6 m. Magnetite was also enriched within the immediate subsurface with the highest concentrations found toward the tailgate.

4.2.6 Run #6

Uniquely in this run, the pavement developed over a period of 163 hours with an increase in the sampling frequency of transported sediment. This allowed for additional magnetite transport data to be gathered. The slope was increased to 0.0089 from 0.0060 in an attempt to mobilize the cassiterite at a higher shear stress during the simulated flood. Subpavement sampling of magnetite at 2, 8, and 32 hours yielded weight percentages of 0.98, 1.81 and 2.40 respectively (there was no sampling at 96 hours). This is in contrast to the lack of enrichment noted in subsurface samples of Runs 4 and 5 (Tables 4-6 and 4-9).

After 163 hours the bed was flooded by increasing the water depth from 0.030 to 0.045 m, to yield a shear stress of 4.12 N/m^2, a 25 % increase from Run 4. After eighteen minutes the cassiterite was observed concentrating on the surface, but was not observed in sediment transport

Table 4-10. Weight percentage and grain size distribution of magnetite and cassiterite in vertical bed samples of Run 5. Sample intervals refer to height above flume bottom.

		Size fraction (mm)			
Sample	*Cassiterite weight %*	0.250 - 0.354 fractional %	0.177 - 0.250 fractional %	0.125 - 0.177 fractional %	0.090 - 0.125 fractional %
VERT 1 @ 4.4 m					
3 - 2 cm	*2.07*	8.3	44.0	41.6	6.1
2 - 1 cm	*1.35*	8.8	41.9	43.7	5.6
1 - 0 cm	*1.24*	9.1	40.9	44.7	5..3
VERT 2 @ 6.6 m					
3.5 - 2.5 cm	*1.88*	8.3	41.7	43.0	8.6
2.5 - 1.5 cm	*1.15*	8.8	43.5	41.5	8.3
1.5 - 0 cm	*1.13*	9.3	42.4	42.8	5.5
VERT 3 @ 8.2 m					
5 - 4 cm	*1.10*	8.4	44.0	40.6	7.1
4 - 2 cm	*1.00*	7.0	41.6	42.8	8.6
2 - 0 cm	*0.86*	8.5	44.1	41.5	5.9
VERT 4 @ 8.8 m					
5.5 - 4.5 cm	*0.90*	10.9	41.1	40.6	7.4
4.5 - 3.5 cm	*0.94*				
3.5 - 0 cm	*0.85*				

		Size fraction (mm)		
Sample	*Magnetite weight %*	0.250 - 0.354 fractional %	0.177 - 0.250 fractional %	0.125 - 0.177 fractional %
VERT 1 @ 4.4 m				
3 - 2 cm	*1.24*	32.2	41.4	26.3
2 - 1 cm	*0.88*	42.2	32.7	25.1
1 - 0 cm	*0.82*	36.7	34.5	28.8
VERT 2 @ 6.6 m				
3.5 - 2.5 cm	*1.45*	38.5	34.8	26.7
2.5 - 1.5 cm	*1.11*	37.1	34.5	28.4
1.5 - 0 cm	*1.14*	38.9	33.9	27.2
VERT 3 @ 8.2 m				
5 - 4 cm	*1.71*	39.5	34.4	26.1
4 - 2 cm	*1.08*	32.5	39.0	28.5
2 - 0 cm	*1.01*	36.0	36.0	28.0
VERT 4 @ 8.8 m				
5.5 - 4.5 cm	*2.55*	35.7	40.3	23.9
4.5 - 3.5 cm	*1.20*	31.1	40.4	28.5
3.5 - 0 cm	*0.97*	31.8	40.3	27.9

samples leaving the channel. Run 5 indicated that the cassiterite had been transported in the upper reaches of the channel. In an effort to capture this transport, a scaled down model of a Helley-Smith sampler with an opening of 0.05 by 0.05 m was constructed. The sampler was placed on the centerline at 5.5 m because cassiterite had been noted on the surface up to this point. The flood was then restarted at a slightly higher discharge (0.058 m^3/s) with the sampler in place. Within minutes there was significant scour around the sides and beneath the sampler, rendering the sampler useless. There was also a 22 % reduction in velocity at the mouth of the sampler due to the fine mesh size of the bag (0.10 mm), which inhibited the throughflow of water. The fine mesh size of the sampler bag does not, however, explain the development of the scour zones as they formed even when the bag was removed and the frame was placed on the surface.

To counter this scour a flat metal sheet was placed across the channel flush with the sediment and the sampler was placed with its mouth 2 to 3 cm over the edge. Although there was significant scour downstream of the sheet, the region of interest in front of the sampler was unaffected. Flood conditions were maintained for eighty minutes with the transported sediment sampled at five to fifteen minute intervals. Sample sizes ranged from 0.102 to 0.401 kg. After twenty minutes, measurable quantities of cassiterite had been transported into the sampler, but by this point the sediment up to 3.8 m had been washed away and cassiterite dunes similar to Run 4 had formed.

4.3 Magnetite transport

Magnetite was transported by all imposed flows for Runs 4, 5, and 6. The fractional percentage transported, however, was always lower than its percentage weight of 1.0 % present in the bed. This is reflected in Table 4-11 which lists the weight percentage of magnetite transported during pavement development and simulated flood for Runs 4, 5, and 6. During pavement development the percentage of transported magnetite decreased exponentially with time before levelling off around the sixteen hour mark. This behaviour is in contrast to the sand-sized light fractions which were transported at rates proportional to or greater than their presence in the bed, and maintained relatively constant transport weight percentages during pavement development (Appendices C and D).

Variations in the fractional magnetite weights as a percentage of total magnetite transported were evident during pavement development (Figures 4-14, 4-15, and 4-16). Although each run was unique, features common to the diagrams are, i) the coarsest fraction (0.250 - 0.354 mm) was transported at decreasing rates relative to the finer fractions, ii) the median fraction (0.177 - 0.250 mm) displayed no consistent trend, and iii) the finest fraction (0.125 - 0.177 mm) was transported at increasing rates relative to the coarser fractions. The runs, differed, however, in the relative quantities of each magnetite fraction in transport. Assuming equal mobility of the three magnetite fractions, one would expect relative percentage values of 38.2, 34.6, and 27.1 % (from coarsest to finest size fraction). The percentages for Runs 4 and 5 are consistent with these values although the above trends were noted. In Run 6 the median fraction was present in much greater quantities than the coarsest fraction (Figure 4-16). Almost half of the magnetite transported (~ 45 %) consisted of the median fraction. It was anticipated that the transport behaviour of magnetite in

Table 4-11. Size distribution of transported magnetite as a percentage of total sediment transported for Runs 4, 5, and 6.

Run 4

Discharge (m^3/s)	Time elapsed (hrs)	0.250 - 0.354 mm (%)	0.177 - 0.250 mm (%)	0.125 - 0.177 mm (%)	Total Mag (%)
0.017	1	0.35	0.22	0.18	0.75
0.017	2	0.21	0.15	0.13	0.49
0.017	4	0.16	0.12	0.10	0.38
0.017	8	0.13	0.10	0.09	0.32
0.017	16	0.07	0.06	0.05	0.18
0.017	32	0.07	0.07	0.06	0.20
0.017	48	0.05	0.04	0.04	0.13
0.017	72	0.05	0.04	0.04	0.13
0.017	96	0.07	0.06	0.06	0.19
0.098	5 min	0.20	0.13	0.12	0.45
0.098	10 min	0.16	0.08	0.08	0.32
0.098	15 min	0.25	0.14	0.13	0.52

Run 5

Discharge (m^3/s)	Time elapsed (hrs)	0.250 - 0.354 mm (%)	0.177 - 0.250 mm (%)	0.125 - 0.177 mm (%)	Total Mag (%)
0.037	1	0.17	0.14	0.08	0.39
0.037	2	0.20	0.22	0.11	0.53
0.037	4	0.16	0.15	0.08	0.39
0.037	8	0.09	0.07	0.05	0.21
0.037	16	0.07	0.06	0.04	0.17
0.037	32	0.04	0.03	0.03	0.10
0.037	48	0.03	0.04	0.03	0.10
0.037	72	0.02	0.04	0.02	0.08
0.037	96	0.05	0.06	0.06	0.17
0.057	15 min	0.16	0.15	0.15	0.46
0.071	10 min	0.11	0.10	0.11	0.32
0.071	20 min	0.04	0.03	0.04	0.11
0.071	30 min	0.03	0.02	0.02	0.07
0.071	40 min	0.05	0.04	0.04	0.13
0.071	50 min	0.16	0.13	0.10	0.39
0.071	60 min	0.17	0.25	0.15	0.57

Table 4-11. Cont.

Run 6

Discharge (m^3/s)	Time elapsed (hrs)	0.250 - 0.354 mm (%)	0.177 - 0.250 mm (%)	0.125 - 0.177 mm (%)	Total Mag (%)
0.025	1	0.16	0.21	0.09	0.46
0.025	2	0.14	0.16	0.09	0.39
0.025	4	0.09	0.12	0.05	0.26
0.025	8	0.06	0.09	0.06	0.21
0.025	16	0.03	0.04	0.03	0.10
0.025	24	0.03	0.05	0.04	0.12
0.025	30	0.03	0.04	0.03	0.10
0.025	36	0.03	0.04	0.03	0.10
0.025	48	0.03	0.06	0.03	0.12
0.025	54	0.02	0.03	0.03	0.08
0.025	60	0.04	0.07	0.04	0.15
0.025	66	0.04	0.07	0.04	0.15
0.025	72	0.04	0.06	0.03	0.13
0.025	78	0.03	0.06	0.03	0.12
0.025	84	0.03	0.05	0.04	0.12
0.025	90	0.04	0.06	0.04	0.14
0.025	97	0.03	0.05	0.04	0.12
0.025	101	0.03	0.05	0.03	0.11
0.025	110	0.04	0.07	0.05	0.16
0.025	116	0.05	0.09	0.06	0.20
0.025	139	0.03	0.07	0.04	0.14
0.025	163	0.01	0.02	0.03	0.06
0.052	5 min	0.17	0.26	0.17	0.60
0.052	10 min	0.16	0.20	0.14	0.50
0.052	15 min				
0.052	16 min	0.10	0.10	0.09	0.29
0.052	18 min	0.17	0.21	0.13	0.51

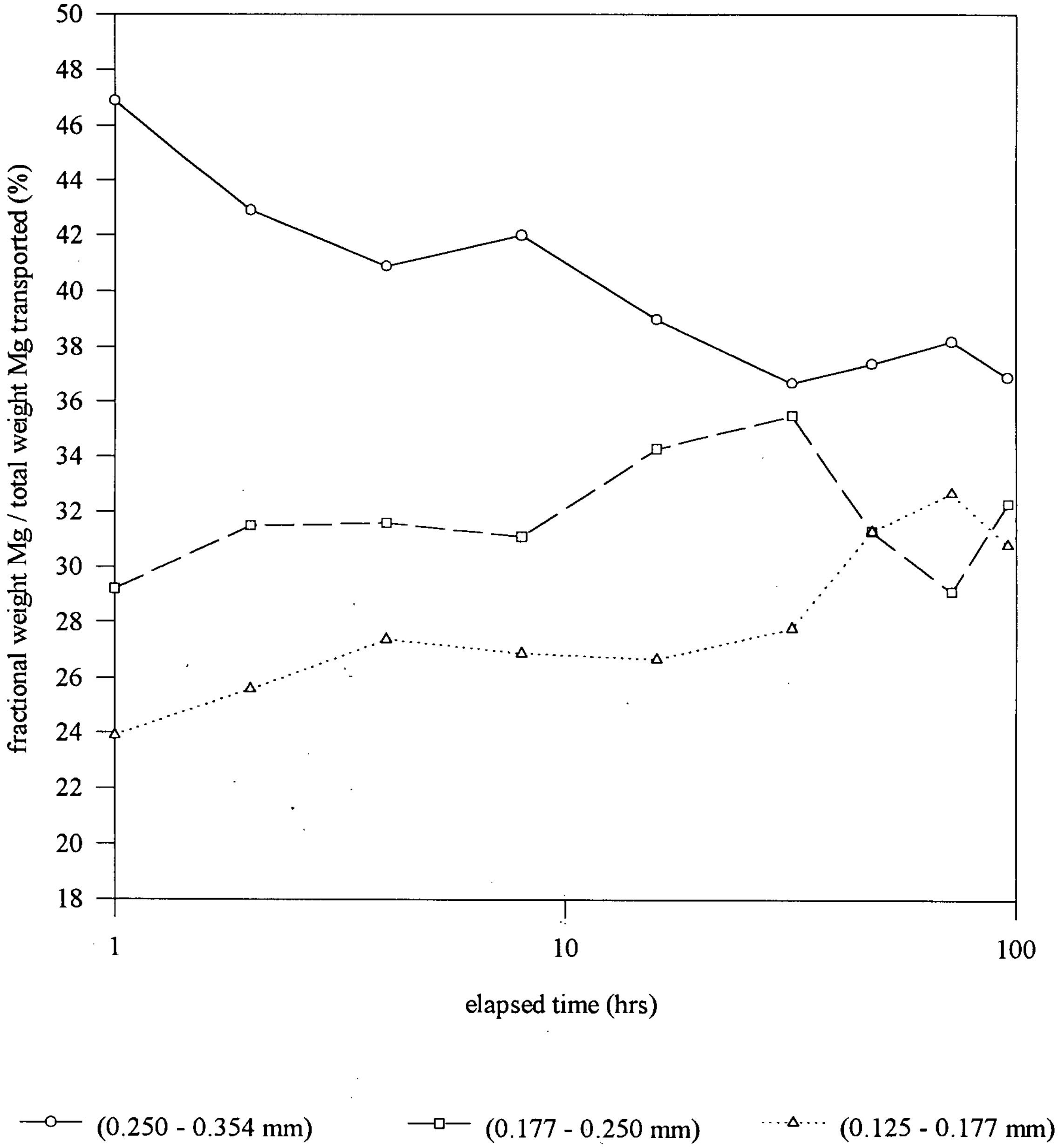

Figure 4-14. Fractional weight of magnetite as a percentage of total magnetite transported during pavement development (Run 4, Q = 0.016 m^3/s).

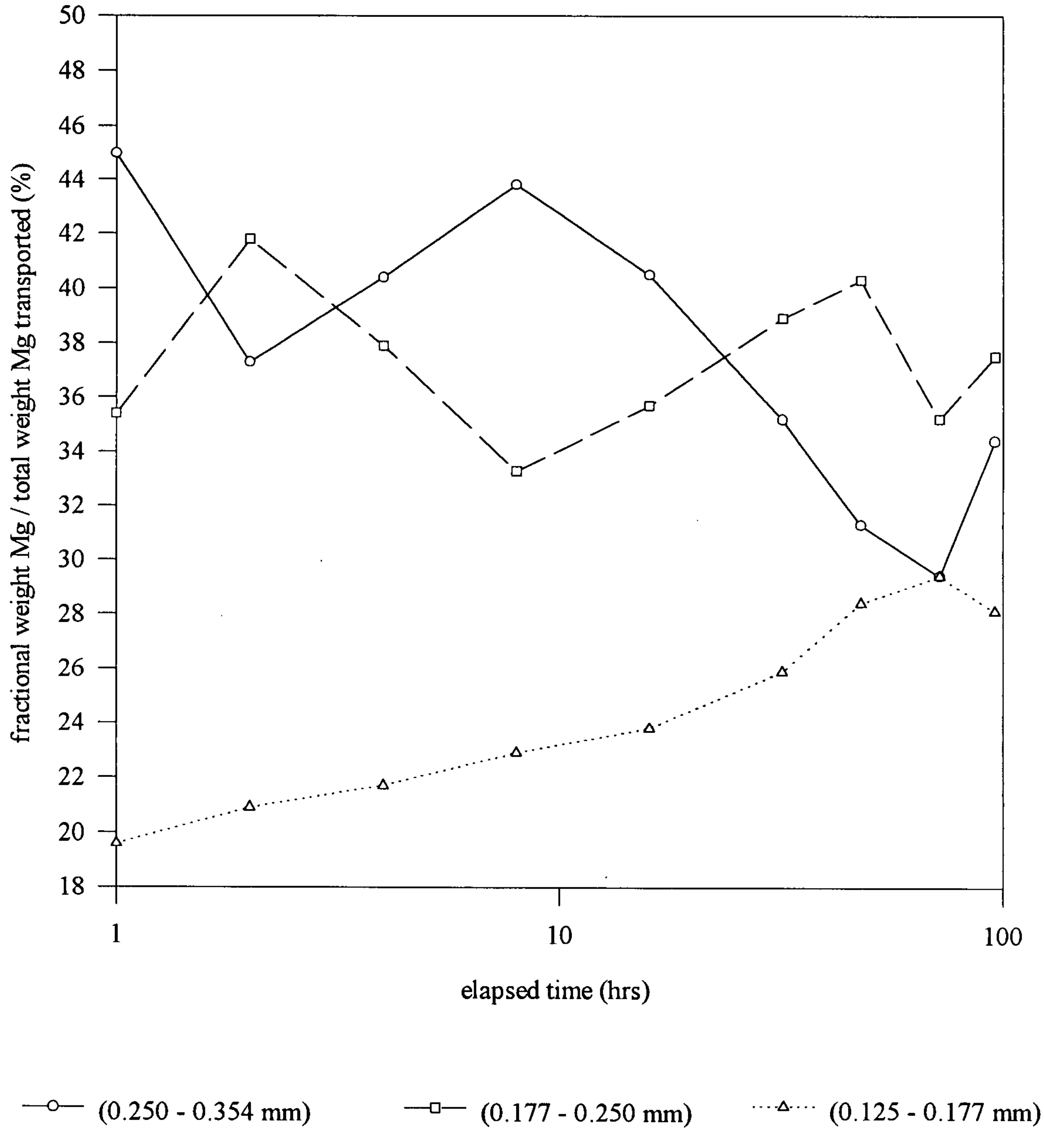

Figure 4-15. Fractional weight of magnetite as a percentage of total magnetite transported during pavement development (Run 5, Q = 0.040 m^3/s).

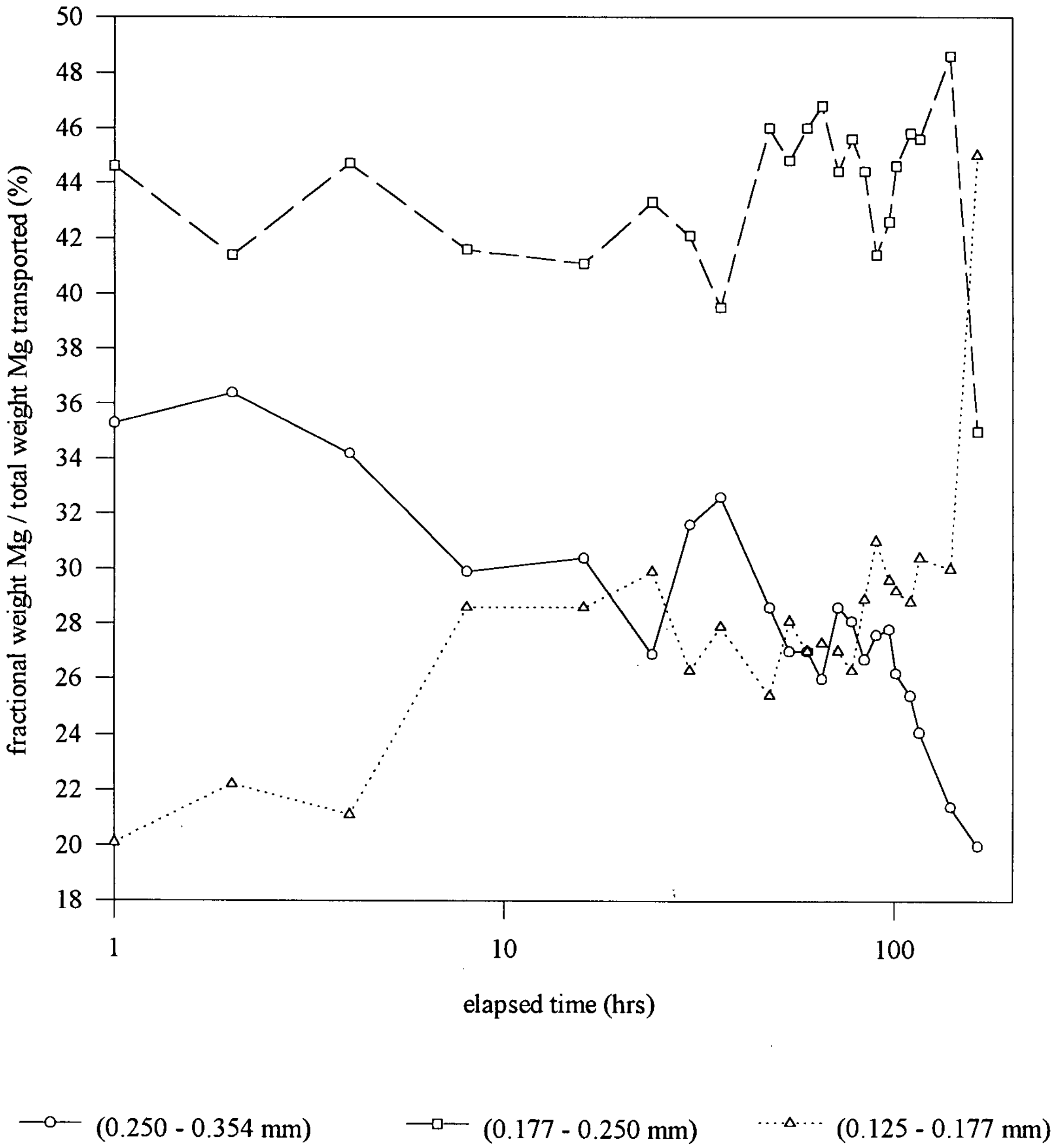

Figure 4-16. Fractional weight of magnetite as a percentage of total magnetite transported during pavement development (Run 6, Q = 0.025 m^3/s).

Run 6 would be comparable to that in Run 5 as similar shear stresses were applied to the bed (i.e. 2.45 vs 2.87 N/m^2).

Trends in the flood data are more difficult to note due to the restricted number of samples. Two observations are worth noting, i) the weight percentages of magnetite transported were less than half of the 1.0 % present in the bed, and ii) the low percentages (i.e. 0.11, 0.07, and 0.13 %) of magnetite transported during the flood of Run 5 at the 20, 30, and 40 minute mark.

5.0 DISCUSSION

5.1 Cassiterite transport behaviour during pavement development

Pavement development is a natural process whereby framework interstices are filled by sand-sized sediment and excess fines are selectively entrained from the surface. High magnitude floods break the pavement, releasing the sandier substrate within which heavy minerals reside. The primary objective of this study was to evaluate cassiterite behaviour during flooding of a pavement, but transport behaviour during pavement development was also of interest because the nature of cassiterite distribution prior to flooding determines its ultimate transport and depositional patterns within the bed.

The initial hydraulic conditions attempted to simulate sedimentological conditions observed by Fletcher and Wolcott (1991) prior to flooding of Harris Creek (i.e. coarse surface layer and high subsurface concentrations of heavy minerals). This was accomplished by maintaining uniform flow conditions for ninety-six hours, which resulted in pavement development by selective entrainment of the sand-sized sediment. During pavement development, cassiterite was detected in high concentrations in subpavement samples from Runs 3, 4, and 5 (Tables 4-4, 4-6, and 4-9). Samples taken to a depth of 1.25 cm in the upper portion of the flume (i.e. between 2 and 4 m) ranged from 1.46 to 2.45 % cassiterite by weight, while sediment leaving the channel contained no cassiterite. Similar measurements were not made for Runs 2 and 6 although the same pattern was expected. These results can be interpreted in two ways.

i) Applied shear stresses were insufficient to entrain cassiterite (for Runs 3, 4, and 5 the calculated shear stresses were 3.31, 3.80, and 2.87 N/m^2 respectively). Figure 2-2, which is based on Shields relation, suggests a shear stress less than 0.5 N/m^2 would be required to entrain all cassiterite size fractions. Shields relation, however, applies only to uniform sediment. The large differences in shear stress illustrate the effectiveness of larger grains in shielding smaller grains from entrainment in a non-uniform deposit.

Shear stresses, however, were sufficient to mobilize the sand-sized, light fractions (i.e. < 2.0 mm) which were transported out of the flume at rates proportional to and greater than their presence in the bed (Appendix D). This is reflected in Figures 5-1 and 5-2, which plot p_i / f_i versus time for Run 4 during pavement development (where p_i = fractional percentage in transport sample and f_i = fractional percentage in subsurface). The finest fraction, 0.090 - 0.125 mm, is an exception with transport rates disproportionately less than its presence in the bed. It should be noted, however, that the sediment trap at the tailbox was slightly coarser (0.100 mm) than this fraction and sediment was probably lost through the mesh. Transported sand-sized fractions in Runs 2, 3, 5, and 6 exhibited similar transport behaviour during pavement development. Because fine, low density fractions were highly mobile the implication is that the shielding effect of larger grains *and high density* of cassiterite were factors inhibiting the entrainment of cassiterite. High subsurface concentrations can then be explained as lag deposits remaining after the lighter, sand-sized fractions had been selectively entrained. Removal of these fractions created voids in the surface framework through which cassiterite infiltrated downward. Subsurface enrichment of cassiterite would have developed rapidly as the majority of sediment transport occurred in the first two hours of pavement development.

ii) Alternatively, high subsurface concentrations of cassiterite were a product of minor cassiterite transport and selective entrainment. At the start of each run sediment transport rates

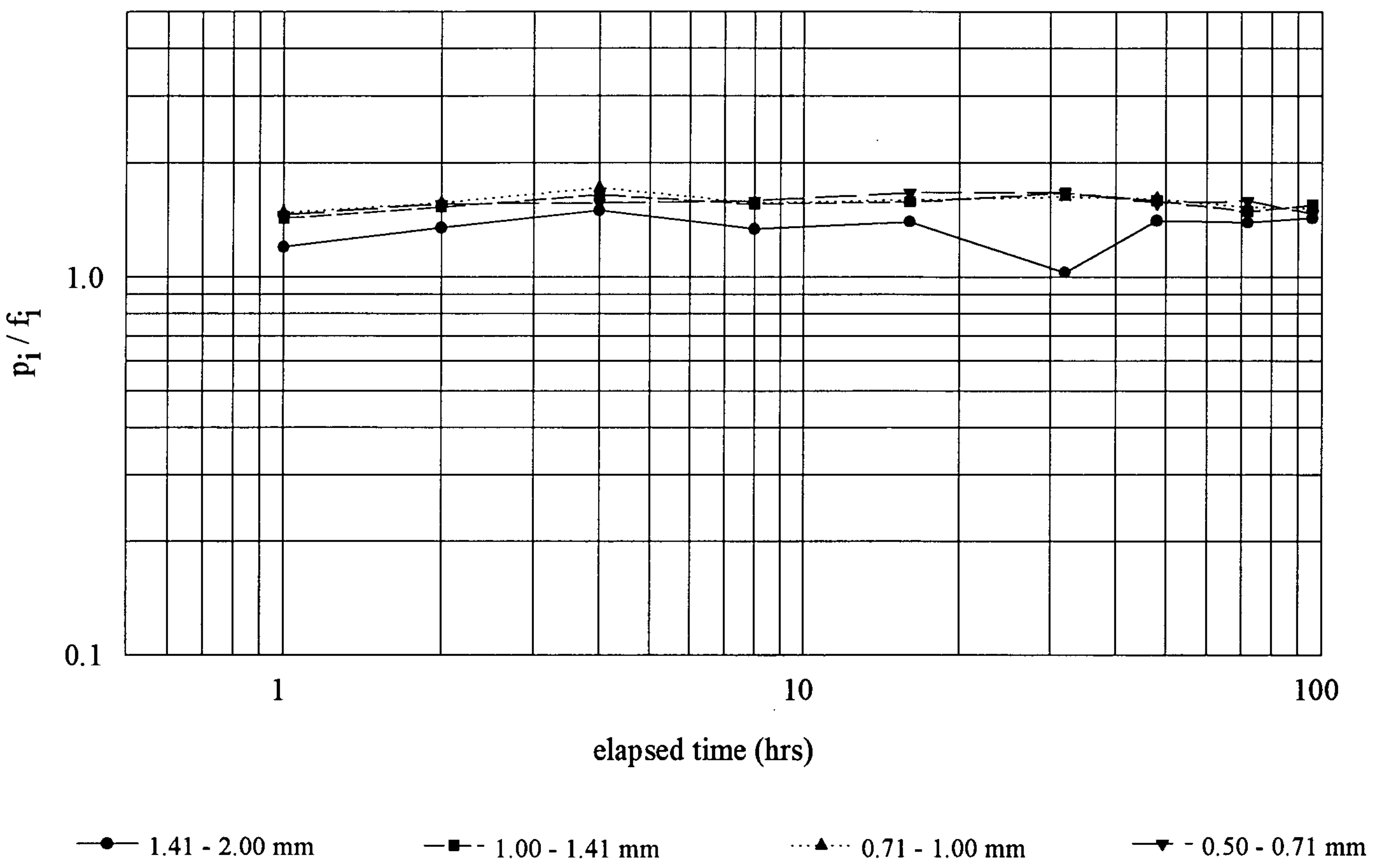

Figure 5-1. Fractional percentage of transported sediment relative to fractional percentage in bed versus time during pavement development of Run 4 (fractions from 0.5 to 2.0 mm).

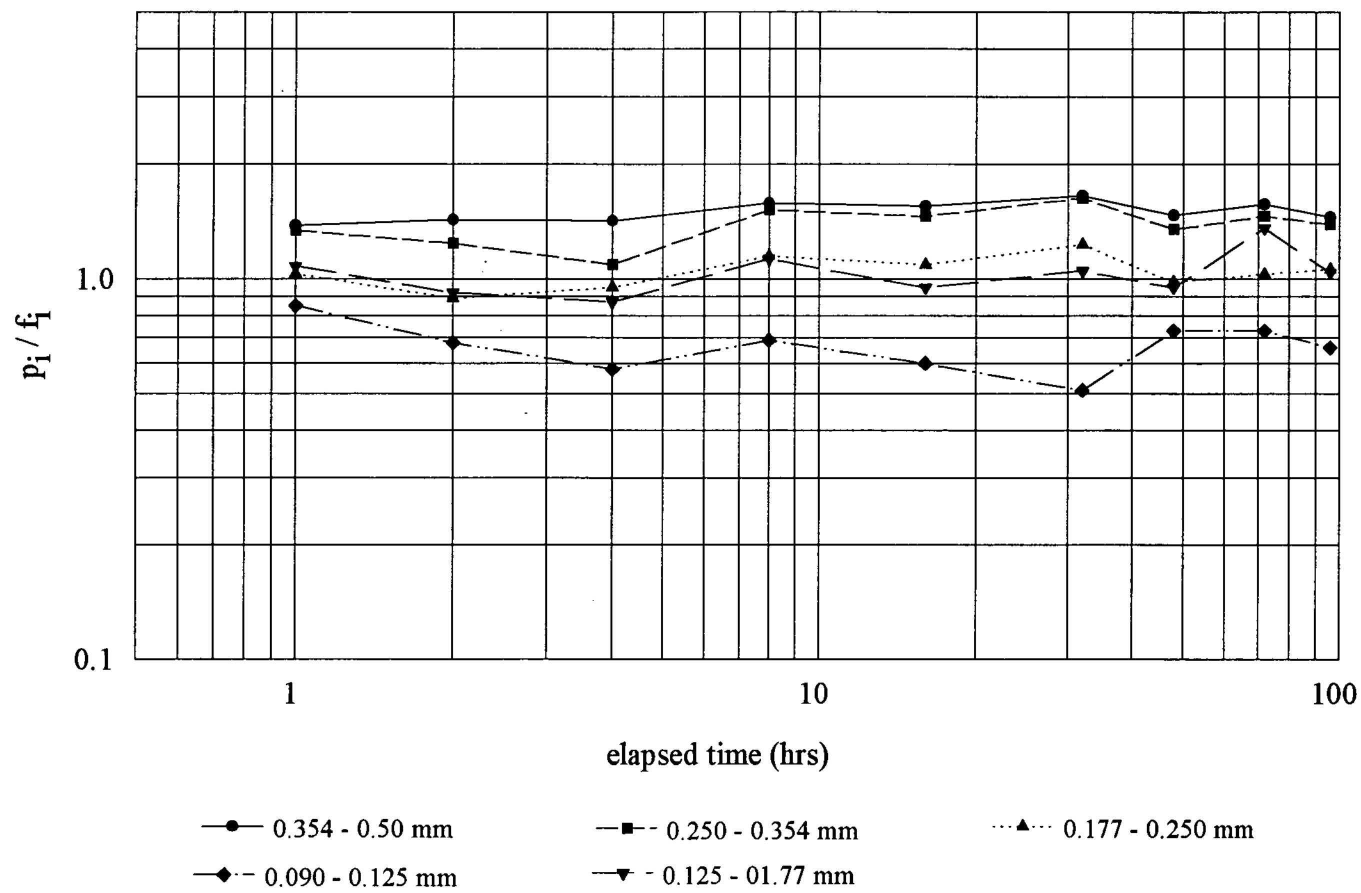

Figure 5-2. Fractional percentage of transported sediment relative to fractional percentage in bed versus time during pavement development of Run 4 (fractions from 0.090 to 0.50 mm).

were very high and an initial lack of bed structure may have allowed cassiterite transport over short distances before the heavy grains stabilized on the bed and infiltrated the subsurface.

Results from Run 5 indicated that the former hypothesis is more likely. Prior to Run 5, sediment between 5.1 and 5.3 m was extracted from the flume and the heavy fraction was removed. The low density sediment was then replaced in the flume. After 96 hours of pavement development this region of the flume was sampled to a depth of 1.25 cm. The absence of cassiterite in the sample indicated that the applied shear stresses were insufficient to mobilize the high density cassiterite grains. It is impossible to determine whether a similar lack of entrainment can be assumed for Runs 2, 3, and 4 because shear stresses applied to the bed were of greater magnitude. The coarser sediment mix utilized in these runs, however, may have enhanced the shielding effect, compensating for the increased shear stress.

If cassiterite formed as a lag deposit, high concentrations should correspond with areas of greatest erosion. Selective entrainment of the lighter fractions would concentrate cassiterite in the immediate subpavement as significant downward infiltration would be inhibited by the close packing of grains in the subsurface. Erosion of the bed during pavement development was greatest at the channel entrance and minimal at the tailgate as a result of a 6.0 cm board placed beneath the tailgate. There was generally 2 to 3 cm of erosion at the channel entrance, which progressively decreased downstream until the tailgate was reached. Had the bed therefore been sampled along the length of the flume after ninety-six hours, a progressively lower subsurface cassiterite concentration would be expected as one moved downstream. The subsurface, however, was sampled at only one location (varied between 2 and 4 m) to preserve the bed framework before flooding commenced. The expected subsurface enrichment can be approximated, however, based on the amount of degradation at a point in the flume. For example, 1 cm of erosion would result in

Table 5-1. Expected cassiterite concentrations in subsurface samples taken to a depth of 1.25 cm based on varying amounts of degradation. Values were calculated based on the assumption that cassiterite was immobile.

eroded height of sediment column (cm)	cassiterite concentration (%)
0.0	1.10
0.5	1.50
1.0	1.90
1.5	2.30
2.0	2.70
2.5	3.10
3.0	3.50
3.5	3.90
4.0	4.30

a cassiterite concentration of 1.90 % in a subsurface sample taken to a depth of 1.25 cm (the calculation is based upon knowing the initial weight and volume of sediment). Table 5-1 lists expected subsurface cassiterite concentrations based on varying amounts of degradation. Where the subsurface was sampled (i.e. between 2 and 4 m) there was generally 1.0 to 2.0 cm of erosion, therefore one would expect subsurface cassiterite concentrations of 1.90 to 2.70 %. Subsurface concentrations are in general agreement with these numbers (Tables 4-4, 4-6, and4-9) although it should be stressed that the expected values are an approximation. A schematic representation of general sedimentological conditions in the flume at the close of pavement development is shown in Figure 5-3.

5.2 Cassiterite transport behaviour during flooding

Flooding of the developed pavements of Runs 2 - 6 induced pavement break-up and intense rates of transport. The objective was to model field observations that the heavy fraction was transported only during full mobilization of the bed (i.e. pavement break-up). Although the simulated floods failed to transport cassiterite out of the channel, vertical sampling of the sediment provided direct and indirect evidence of transport during flooding. Direct evidence was provided in Run 5 wherein the heavy mineral fraction had been removed from the sediment between 5.1 and 5.3 m prior to pavement development. At the close of pavement development cassiterite was not detected in a sample taken from this area, but after sixty minutes of flooding a sample from the top centimeter of this region consisted of 3.63 % cassiterite by weight, indicating that cassiterite was mobilized by the flood. The majority of this cassiterite had infiltrated into the subsurface as it was not visible in significant concentrations on the surface.

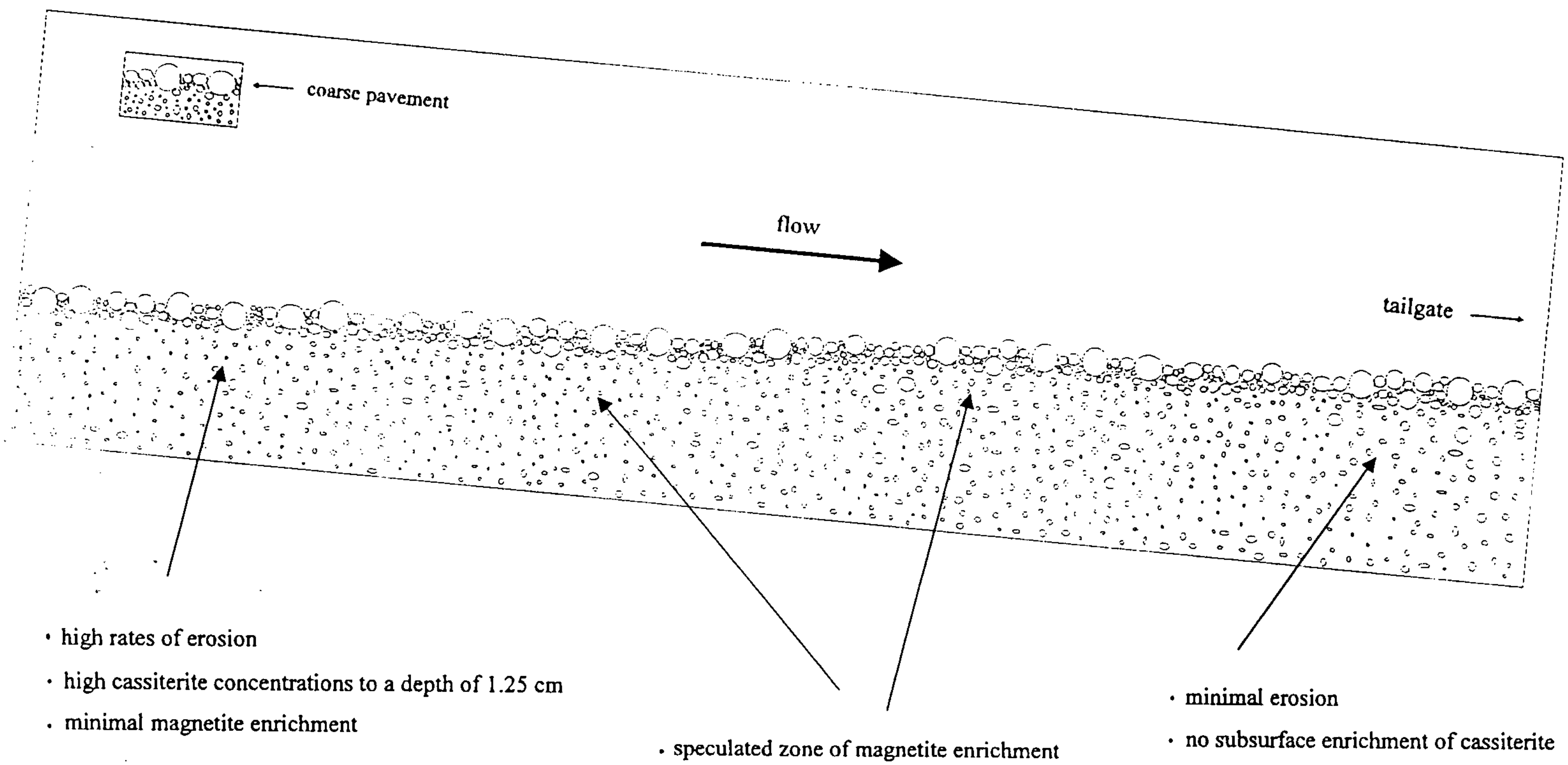

Figure 5-3. Schematic diagram of sedimentological conditions in flume at close of pavement development in Runs 2 - 6.

The origins of high subsurface cassiterite concentrations at other locations in Run 5 (Table 4-10) were unclear, because subsurface enrichment could be interpreted in two ways, i) a lag deposit of cassiterite which was not mobilized by the high energy flow, or ii) an enrichment consisting in part of a cassiterite lag and mobilized cassiterite deposited at the sample location. It could not be determined whether high concentrations noted in the uppermost centimeter at 4.4 and 6.6 m were lag deposits or a partial product of cassiterite transport. Vertical samples at 8.2 and 8.8 m were not enriched in cassiterite indicating that cassiterite transport was restricted to the upper reaches and erosional rates were insufficient to form a lag deposit. Surface patches of cassiterite (Figure 4-10) could be interpreted as exposed lag deposits, transport into low velocity zones, or a combination of the two.

Hydraulic parameters of Run 5, in which cassiterite transport was detected, provide indirect evidence of cassiterite transport in other runs. The calculated shear stress of Run 5 was 3.28 N/m^2, well below the magnitude of all other floods (Table 4-1). As shear stress is related to the near bed forces of erosion which result in sediment transport, one might assume that cassiterite was mobilized in all flood events. This is certainly true for Run 6 wherein shear stress was higher (4.12 N/m^2) and the same sediment mix was utilized. Whether the same can be said for Runs 2 - 4 in which a coarser sediment mix was employed is less clearly resolved.

Runs 2 and 3, which were replicates, were flooded at a shear stress of approximately 5.5 N/m^2 and Run 4 was flooded at a shear stress of 7.77 N/m^2. These values greatly exceeded the flood of Run 5 and most light fractions were in transport (up to 16.0 mm for Runs 2 and 3, and up to 32.0 mm for Run 4), suggesting that cassiterite transport was probable. Moreover, vertical samples of Run 4 taken at 7.0 and 8.5 m had high cassiterite concentrations to a depth of 2 cm (Table 4-7). For concentrations to be strictly lag deposits, enrichment would be restricted to the uppermost centimeter of the sample since close packing of the grains would prevent significant downward infiltration. It is postulated that high downstream concentrations at a depth of 1 - 2 cm represent lag deposits formed during pavement development, which were quickly covered by a high influx of sediment from the upper reaches once flooding commenced. Any mobilized cassiterite would have concentrated in this upper layer, thus accounting for significant concentrations in the uppermost centimeter. The short interval of flooding, 15 minutes, did not allow a sufficient period of time for all the mobilized sediment to flush through the system leaving the surface covered in well-mixed sediment. Cassiterite concentrations in the uppermost centimeter were depleted in some instances, however, indicating that its distribution throughout the mobile upper layer was variable.

The question remains why cassiterite was not transported out of the flume if flooding was sufficiently competent to entrain it. Two main factors are proposed. First, cassiterite exhibited a tendency to resist entrainment, with only a small proportion in transport. This was suggested by unusually high surface concentrations of cassiterite that formed at the close of Run 4. High shear stresses eroded all the sediment downstream to 4.5 m and at this point along the flume, parabolic cassiterite dunes formed (Figures 4-8 and 4-9). The majority of these cassiterite grains were probably mobilized once the lighter fractions were removed and the smooth substrate was exposed. Cassiterite was then re-deposited once the increased roughness of the bed was encountered below 4.5 m. The bed remained in a stable configuration beyond 4.5 m as the board beneath the tailgate prevented further erosion. A similar situation was observed at the close of Run 6. A tendency to resist entrainment, however, does not provide a complete explanation of the absence of cassiterite in transport samples. A few of those grains that were mobilized would still be expected to reach the tailgate.

The mode of cassiterite transport resulting from its high density and fine grain size is the second factor that may be cited to explain its absence in transport samples. Cassiterite was probably transported in close contact with the bed and transport out of the flume would have been unlikely as the grains continually tested the bed for a stable position. High surface roughness elements would have enhanced the entrapment process. The ability of the bed to entrap fine sediment was demonstrated by low density fractions finer than 0.50 mm, which were transported at rates disproportionately less than their presence in the bed in Runs 2 - 6 (Table 5-2). This is in contrast to low density sediment between 0.50 and 2.0 mm, which were transported at rates approximating their presence in the bed (i.e. $p_i / f_i \sim 1$). A graphical representation of these results is shown in Figures 5-4 and 5-5, which plot p_i / f_i versus time during flooding of Run 5. It should be noted, however, that the p_i / f_i ratio for sediment finer than 0.50 mm approaches one after sixty minutes of flooding in Run 5 (Figure 5-5). This would suggest that the entrapment of fine, low density sediment is most effective immediately following pavement break-up when the coarsest sediment (> 8.0 mm) is mobile.

On the basis of the foregoing discussion the following model for cassiterite transport during flooding is proposed.

i) High shear stresses associated with flooding mobilized coarser fractions and initiated pavement break-up. Cassiterite was predominantly entrained in the upper reaches where erosional rates were greatest causing high subpavement concentrations to be exposed to the flow. The 0.06 m board beneath the tailgate minimized erosion rates in the lower reaches and consequently, subpavement cassiterite was not exposed to the erosive forces of the flow. Maximum channel length beyond which cassiterite was no longer entrained depended on the applied shear stress.

Table 5-2. Fractional percentage of transported sediment relative to fractional percentage in bed during flooding of Runs 3 - 6.

Size fraction (mm)	1.41 - 2.00	1.00 - 1.41	0.71 - 1.00	0.50 - 0.71	0.354 - 0.50	0.250 - 0.354	0.177 - 0.250	0.125 - 0.177	0.090 - 0.125
Run 3									
10 min	0.91	0.72	0.77	0.60	0.47	0.55	0.53	0.69	0.90
20 min	1.22	1.05	1.14	0.81	0.49	0.31	0.11	0.08	0.10
30 min	1.34	1.15	1.17	1.21	1.06	0.83	0.48	0.34	0.46
40 min	1.28	1.04	1.18	1.07	0.84	0.61	0.43	0.42	0.49
50 min	1.13	1.11	1.19	1.27	1.26	1.23	0.97	0.84	1.12
60 min	1.19	1.25	1.27	1.35	1.26	1.21	0.99	0.82	1.11
Run 4									
5 min	0.90	0.77	0.70	0.59	0.54	0.49	0.37	0.43	0.51
10 min	1.10	1.07	1.05	1.01	0.87	0.63	0.30	0.32	0.32
15 min	1.07	1.05	0.99	1.03	0.92	0.71	0.38	0.40	0.35
Run 5									
10 min	1.09	0.88	0.75	0.47	0.33	0.37	0.51	0.56	1.03
20 min	1.26	1.17	1.07	0.75	0.47	0.35	0.26	0.41	0.53
30 min	1.23	1.21	1.12	1.09	0.80	0.56	0.32	0.29	0.38
40 min	1.34	1.18	1.24	1.06	0.63	0.91	0.56	0.38	0.68
50 min	1.06	1.16	1.20	1.20	1.21	1.11	1.02	0.75	0.60
60 min	1.22	1.09	1.20	1.23	1.32	0.91	1.28	0.74	0.80
Run 6									
5 min	0.87	0.58	0.54	0.51	0.61	0.63	1.24	1.37	1.43
10 min	0.94	0.80	0.83	0.76	0.79	0.63	0.87	0.67	0.65
16 min	0.98	0.85	0.88	0.66	0.47	0.66	0.50	0.53	0.55
18 min	1.04	0.82	0.83	0.85	0.89	0.71	0.91	0.57	0.44

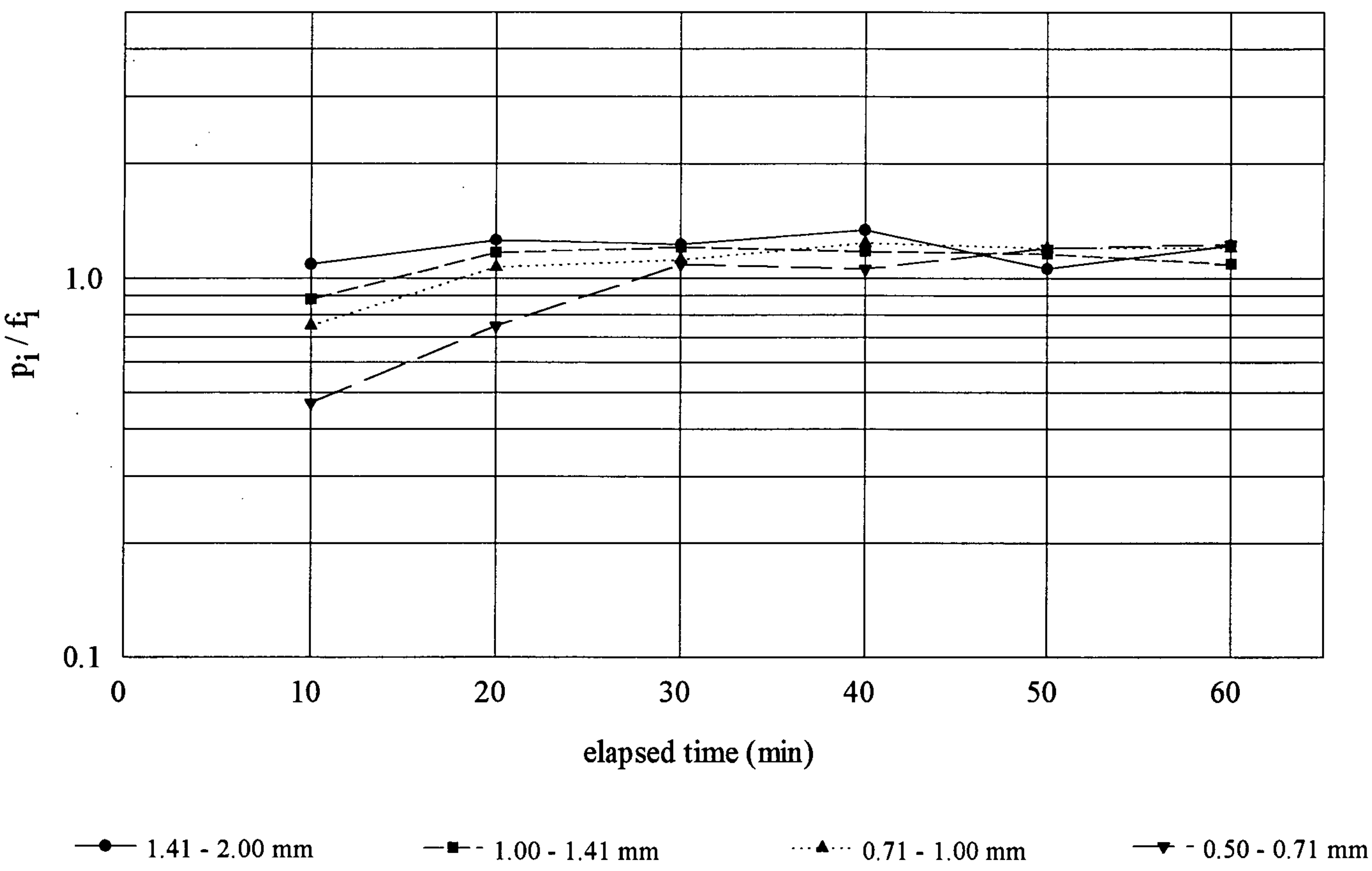

Figure 5-4. Fractional percentage of transported sediment relative to fractional percentage in bed versus time during flooding of Run 5 (fractions from 0.5 to 2.0 mm).

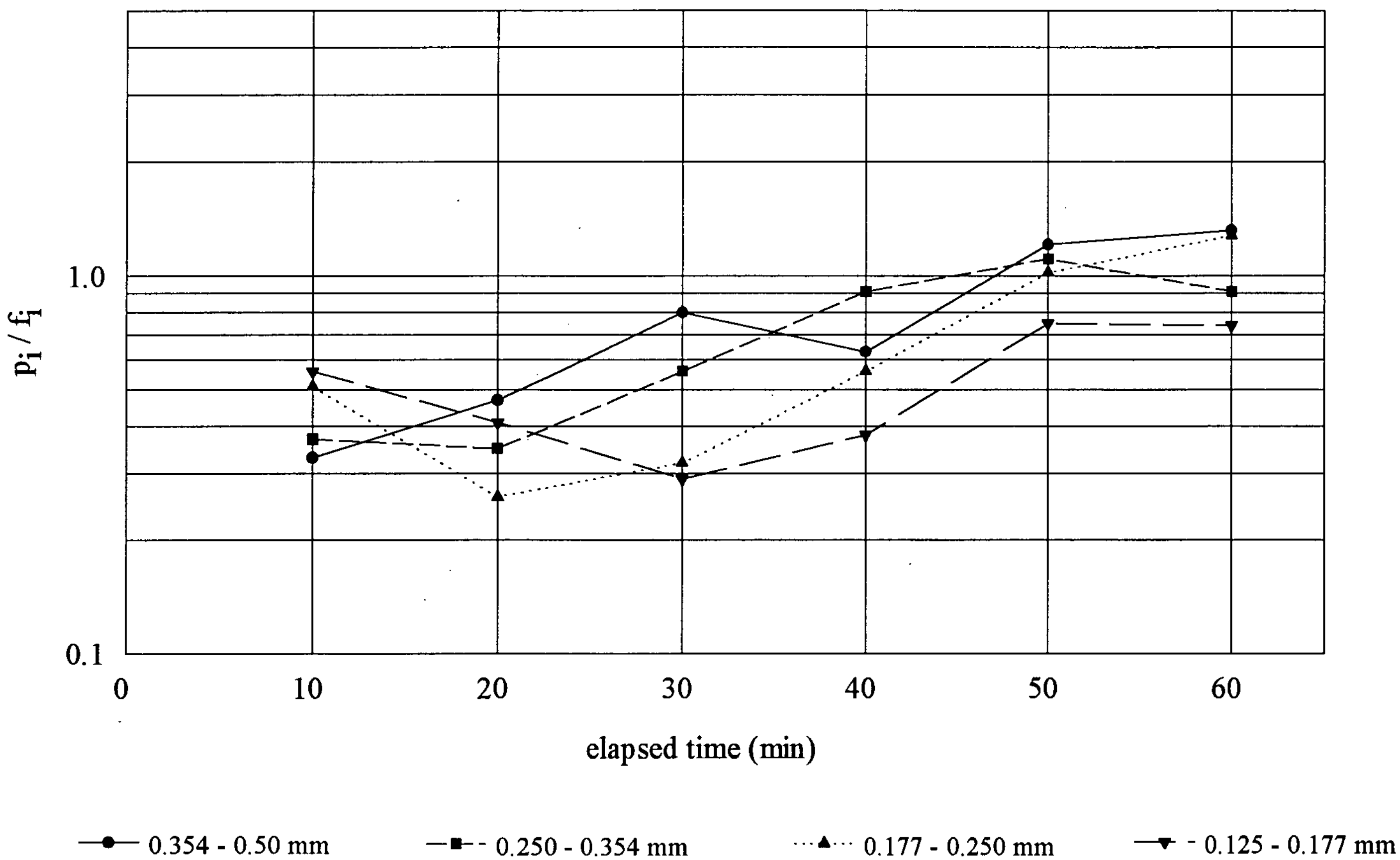

Figure 5-5. Fractional percentage of transported sediment relative to fractional percentage in bed versus time during flooding of Run 5 (fractions from 0.125 to 0.50 mm).

ii) Once mobilized, cassiterite was transported in close contact with the bed due to its high density, constantly testing the bed for a stable position.

iii) Frequent testing of the bed by cassiterite made transport distances greater than one or two meters extremely unlikely. The combined qualities of high density and fine grain size distribution relative to the bed created ample opportunities for cassiterite deposition, thus transport distances remained small. The ability of the bed to entrap mobilized cassiterite was demonstrated in Run 5 in which subsurface cassiterite concentrations between 5.1 and 5.3 m went from 0.0 % to 3.63 % after one hour of flooding . Cassiterite that was transported into the heavy mineral-free zone infiltrated into the subsurface and was not visible in significant surface concentrations.

5.3 Magnetite transport behaviour during pavement development

Magnetite, which was not present in the sediment mixture for Runs 1 - 3, was transported out of the flume by all imposed flows in Runs 4 - 6 (Table 4-11). During pavement development similar observations were made, even though the sediment mixture of Run 4 was coarser. The principal features are as follows:

i) Magnetite was not transported in proportion to its presence in the bed. Magnetite constituted 1.0 % of the bed by weight, but transport samples had significantly less magnetite (Table 4-11). Because significant surface concentrations of magnetite were not observed, grains were expected to be concentrating immediately below the pavement. Subsurface samples taken between 2 and 4 m, however, were not consistently enriched. Magnetite concentrations of 1.81 and 2.40 % were observed after 8 and 32 hours in Run 6, while subsurface samples of Runs 4 and 5 demonstrated a lack of enrichment (Tables 4-6 and 4-9). If magnetite was not enriched in the subsurface close to the channel entrance and was not being transported out of the channel in proportion to its presence in the bed, the implication is that the subsurface further downstream would have been more consistently enriched (Figure 5-1). Magnetite was therefore probably entrained at rates proportional to its presence in the bed close to the channel entrance where erosional rates were highest. The relatively high density of magnetite would have resulted in transport close to the bed with some grains becoming entrapped with downstream transport.

ii) Magnetite as a weight percentage of total sediment transported declined exponentially before levelling off after sixteen hours of flow (Table 4-11). Utilizing the concept of settling equivalence, magnetite grains should behave in a fashion similar to quartz grains 1.5 times greater in diameter (see section 2.2). The sand-sized light fractions, however, maintained constant weight percentages and were transported at rates proportional to their presence in the bed after the initial hour of intense transport (Figure 5-2, Appendix C). Shielding was therefore not a factor in reducing the mobility of the light fractions. It appears that the greater density and fine grain size of magnetite allowed individual grains to be more effectively shielded from the flow than their low density counterparts.

iii) The size distribution of transported magnetite became finer with pavement development (Figures 4-12, 4-13, and 4-14). The percentage of the coarsest fraction (0.250 - 0.354 mm) in transport relative to the two finer fractions declined over time while the finest fraction (0.125 - 0.177 m) exhibited the opposite behaviour. The median fraction (0.177 - 0.250 mm) maintained consistent percentage values relative to the coarsest and finest fractions. These results suggest either that i) the coarsest fraction was less effectively maintained in motion because it tested the bed more frequently or, ii) at the onset of pavement development coarse magnetite was being selectively entrained relative to the two finer magnetite fractions.

5.4 Magnetite transport behaviour during flooding

Size fractions of magnetite were also transported at disproportionate rates during flooding of Runs 4 - 6 despite the fact that all light fractions were in transport (Table 4-11, Appendix C). Magnetite as a percentage of total sediment transported had values consistently lower than 0.5 %, less than half its original proportion in the bed. Its lack of mobility was reflected in vertical sampling of the substrate after flooding in Runs 4 and 5 with high concentrations observed immediately below the pavement (Tables 4-8 and 4-10).

It is intuitively obvious that density played a key role in reduced transport rates but the size distribution of magnetite also appeared to be a factor, because light sediments finer than 0.50 mm were also transported at rates disproportionate to their presence in the bed (Table 5-2). In other words, magnetite appeared to be transported in a fashion similar to like-sized, low density particles. This similarity can be evaluated using the concept of transport equivalence introduced by Fletcher et al. (1992) (see section 2.4). Transport equivalent grains are defined as grains that are transported at proportionally similar rates in all flow conditions despite differences in physical properties. Fractions displaying the least variation in relative transport rates over a range of flow conditions are said to exhibit transport equivalence and are detected by comparing the relative transported weights of the magnetite fractions versus the light fractions (equation 2.3).

Fletcher et al. (1992) estimated transport equivalent sizes for magnetite based on 23 discharges from a gravel-bed stream. The same procedure could not be carried out in this experimental study due to time constraints simulating multiple floods of varying magnitudes. Transport equivalent sizes of magnetite were instead estimated from transport samples of a particular flood (the data from Runs 4 - 6 were not grouped because of different sediment mixtures and initial slopes). Variations in transport rates should provide equivalent information as varying discharge in estimating transport equivalent sizes.

The relative concentrations of each of the three magnetite fractions versus the nine low density sand-sized fractions were calculated at each sampling interval for the three runs. Coefficients of variation (CV = standard deviation / average) were calculated for each of the nine series of relative concentrations associated with a given magnetite size fraction. For a given magnetite fraction, the minimum CV value indicates the low density size fraction which is transported out of the flume at a proportionally similar rate. The resulting CV data for Runs 4 - 6 are summarized in Table 5-3. Values range from 0.06 to 0.84 and CV_{min} ranges from 0.06 to 0.36. Confidence limits could not be established because of the small sample size (n = 3, 6, and 4 for Runs 4, 5, and 6 respectively), but CV_{min} is consistently associated with similar-sized light fractions or plus/minus one size fraction The implication is that *grain size* is an important factor in inhibiting transport of magnetite during flooding. CV_{min} is not as clearly defined for Run 5 in comparison with Runs 4 and 6, which is not unexpected as the longer period of flooding resulted in less effective entrapment of fine sediment over time (Figure 5-5). For Runs 4 - 6 the following model is proposed for magnetite and light sediment transport during flooding.

i) A large portion of the bed surface was mobilized by flooding during pavement break-up. Coarse, light fractions had been concentrated on the surface during pavement development and these were transported at rates proportional to and greater than their presence in the bed (Appendix D). The size distribution of the transported sediment was therefore similar to that of the bed.

ii) Development of a highly mobile granular layer enabled the low and high density fine grains (< 0.50 mm) to fractionate from the coarser sediment and be transported in close contact with the bed,

Table 5-3. Coefficients of variation (CV) for relative concentrations of magnetite (Mag). For Runs 4 -6 n = 3, 6, and 4 respectively. CV_{min} is in bold and underlined. Similar fractions for light and heavy grains are italicized and underlined.

Size fraction (mm)	CV Run 4	CV Run 5	CV Run 6
Mag (0.250 - 0.354)			
1.41 - 2.00	0.24	0.63	0.22
1.00 - 1.41	0.27	0.61	0.32
0.71 - 1.00	0.30	0.60	0.35
0.50 - 0.71	0.36	0.68	0.32
0.354 - 0.50	0.34	0.73	0.17
<u>*0.250 - 0.354*</u>	0.22	0.61	0.21
0.177 - 0.250	<u>**0.12**</u>	0.32	<u>**0.13**</u>
0.125 - 0.177	0.17	<u>**0.31**</u>	0.31
0.090 - 0.125	0.32	0.54	0.44
Mag (0.177 - 0.250)			
1.41 - 2.00	0.35	0.83	0.35
1.00 - 1.41	0.41	0.84	0.45
0.71 - 1.00	0.44	0.77	0.49
0.50 - 0.71	0.52	0.71	0.47
0.354 - 0.50	0.50	0.64	0.31
0.250 - 0.354	0.38	0.67	0.32
<u>*0.177 - 0.250*</u>	0.18	<u>**0.36**</u>	<u>**0.06**</u>
0.125 - 0.177	<u>**0.17**</u>	0.58	0.29
0.090 - 0.125	0.27	0.75	0.41
Mag (0.125 - 0.177)			
1.41 - 2.00	0.31	0.69	0.29
1.00 - 1.41	0.37	0.69	0.42
0.71 - 1.00	0.41	0.66	0.47
0.50 - 0.71	0.49	0.72	0.44
0.354 - 0.50	0.46	0.74	0.29
0.250 - 0.354	0.34	0.64	0.27
0.177 - 0.250	<u>**0.13**</u>	0.37	<u>**0.15**</u>
<u>*0.125 - 0.177*</u>	<u>**0.13**</u>	<u>**0.36**</u>	0.25
0.090 - 0.125	0.24	0.56	0.36

thus being more prone to entrapment (Figure 5-6). The greater density of magnetite with respect to like-sized light fractions enhanced its propensity for entrapment. A concentration of fine sediment at the base of the mobile bed is consistent with shear sorting or kinetic sieving. Shear sorting refers to the vertical fractionation of grains due to dispersive pressures within a moving bed layer which push larger grains upward (Bagnold, 1954; Inman et al., 1966). Kinetic sieving was introduced by Middleton (1970) and refers to the downward movement of fine grains between the interstices of coarser sediment. In either case, light and heavy fine grains would concentrate at the base of the mobile granular layer.

In light of this interpretation results of the CV analysis can be expanded upon. The coarsest magnetite fraction (0.250 - 0.354 mm) was associated with finer light sediment, indicating that similar-sized light sediment did not fractionate from the mobile bed as effectively as magnetite and finer light sediment. Fractionation of the finer sediment was more effective as demonstrated by the fine magnetite fractions (0.125 - 0.250 mm) which were transported at rates proportionally similar to slightly coarser or similar-sized light sediment. While the CV analysis is not statistically significant, the results demonstrate the importance of grain size in controlling the transport behaviour of magnetite during flooding.

5.5 Overview of enrichment and transport processes

Sediment transport in gravel-bed streams is minimal for most of the year when discharge is relatively low and bedload consists primarily of sand-sized fractions. These conditions promote the development of a coarse surface pavement that requires high-energy flood events to break. Pavement break-up releases finer sediment in the subsurface and provides an opportunity for heavy mineral transport. From observations of gold and magnetite transport in Harris Creek, Fletcher

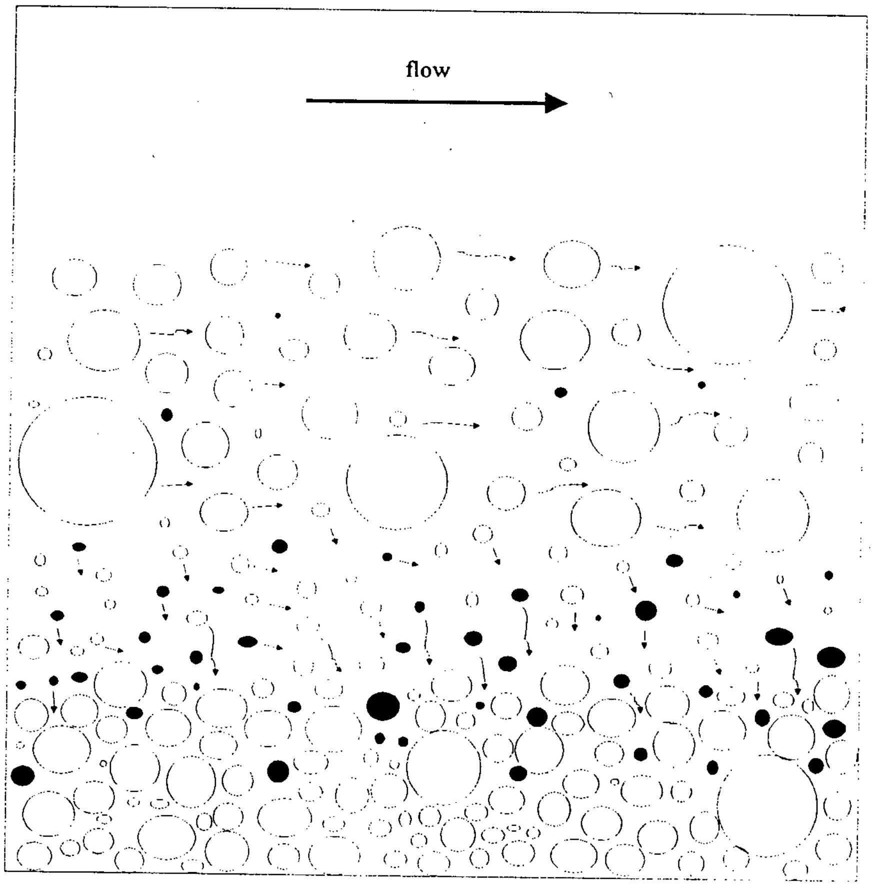

Figure 5-6. Schematic representation of vertical fractionation of the mobile bed during flooding. Finer grains are transported in frequent contact with the bed resulting in preferential entrapment. Magnetite is represented by the darker grains.

and Wolcott (1991) noted that pavement break-up and general mobilization of the light fractions was required for entrainment of the heavy fractions. These observations provided the basis for simulating sediment transport processes similar to Harris Creek..

Flume modelling, however, only approximated the behaviour of Harris Creek, because the falling limb of the flood was not replicated. This natural process is essential to pavement redevelopment and heavy mineral enrichment of the subsurface. Initial flow conditions in the flume were effective, however, in developing a pavement and creating high subsurface concentrations of cassiterite. Thus, while hydraulic conditions and temporal scale over which a pavement developed differed between the flume environment and natural system, bed conditions prior to flooding were similar. Pavement break-up during flooding could therefore be effectively simulated and heavy mineral transport behaviour within a mobile, granular bed could be observed.

While initial pavement development was not analogous to processes observed at Harris Creek, subsurface enrichment of cassiterite demonstrated the importance of selective entrainment as a concentrating mechanism. Initial flows were sufficient to transport sand-sized light fractions in proportion to their presence in the bed, leading to a progressive coarsening of the surface. Cassiterite was not entrained, however, due to its high density and fine grain size which enabled infiltration into the subsurface. Slingerland (1984) and Komar and Wang (1986) have emphasized the importance of selective entrainment as a concentrating mechanism for heavy minerals. Similar subsurface enrichments were observed by Kuhnle (1986) in his flume study of heavy mineral transport within a mixed size deposit. Under equilibrium and degrading conditions, lead and tungsten became concentrated in a thin layer beneath a surficial layer of lighter sediment. That is, the high density heavy minerals exhibited a tendency to resist entrainment and infiltrate into the subsurface in Kuhnle's (1986) experiments and in the present study. In contrast to cassiterite, magnetite was mobilized during initial flow conditions of pavement development. Although magnetite concentrations in transport samples were well below the bed percentage of 1.0 %, its greater mobility with respect to cassiterite indicates that heavy minerals of contrasting density will exhibit dissimilar transport behaviour under identical flow conditions. Flume experiments using magnetite as the heavy fraction therefore appear to be inappropriate when related to higher density minerals.

An important result of this study is that cassiterite was not mobilized until the pavement was broken and the majority of light fractions were in transport. Similar conditions for magnetite and gold transport in Harris Creek were noted by Fletcher and Wolcott (1991). In the present study, flooding of the pavement in Runs 2 - 6 led to the mobilization and transport of a wide range of particle sizes approximately in proportion to their presence in the bed (Figures 5-4 and 5-5, Appendix D). The same is true for Harris Creek where general mobilization of sediment occurred at flood discharges in excess of 10 m^3/s (Day and Fletcher, 1991). Because sediment transport in both the model and prototype indicate some limit of similarity, the approach of Parker et al. (1982) and Andrews (1983) (section 2.5) is applicable to this study for calculating critical shear stresses required for pavement break-up, hence cassiterite entrainment. Andrews' relation was applied in this study because it is more sensitive to selective entrainment at lower shear stresses (which was the case during pavement development).

Estimated critical shear stresses required for particle entrainment in Runs 2 - 4, based on Andrews, are listed in Table 5-4. While the median diameter was slightly lower for Runs 5 and 6 (1.33 vs 1.40 mm), this had little effect on calculated values and consequently, the values can be applied to all runs. The resulting critical values are close approximations of the shear stresses observed to initiate pavement break-up. For example, pavement was developed with a shear stress

Table 5-4. Estimated critical shear stresses for entrainment of sediment from developed pavements of Runs 2 - 4. Shear stresses were determined using the equation of Andrews (1983).

Size fraction (mm)	Geometric mean (D_i)	(D_i / D_{50})	θ_t	Shear stress (N/m^2)
22.6 - 32.0	26.9	19.1	0.020	8.71
16.0 - 22.6	19.0	13.5	0.020	6.16
11.3 - 16.0	13.4	9.5	0.020	4.35
8.0 - 11.3	9.5	6.7	0.020	3.08
5.66 - 8.0	6.73	4.8	0.021	2.32
4.0 - 5.66	4.76	3.4	0.029	2.22
2.83 - 4.0	3.36	2.4	0.039	2.13
2.0 - 2.83	2.38	1.7	0.053	2.04

of 2.87 N/m^2 in Run 5 while break-up and resulting cassiterite transport occurred when shear stress was increased to 3.28 N/m^2. This level of shear stress was necessary to mobilize the coarsest bed fractions (8.0 - 11.0 mm) and hence initiate pavement break-up. Andrews' (1983) equation predicted entrainment of this coarsest fraction when a shear stress of 3.08 N/m^2 is applied, closely approximating the actual value. Moreover, the equation predicted entrainment of the finer fractions at lower shear stresses which was the case during pavement development (Appendix C).

The same exercise can be performed with Runs 2 - 4 although pavement break-up did not depend on mobilization of the coarsest fractions (16.0 - 32.0 mm), which constituted less than 2.2 % of the bed by weight . The shear stress during flooding of Run 3 was 5.42 N/m^2 and the coarsest fraction transported in significant quantities was 11.3 - 16.0 mm. Andrews' relation predicted that this fraction would be mobilized by a shear stress of 4.35 N/m^2 and that a shear stress of 6.16 N/m^2 was required to mobilize the 16.0 - 22.6 mm fraction, thus accounting for why this fraction remained immobile during flooding. The applied shear stress of 5.42 N/m^2 appropriately falls between the two predicted numbers demonstrating that Andrews' relation is a useful approximation of shear stresses required to initiate pavement break-up and hence, entrain cassiterite.

Andrews' relation for estimating critical shear stress for pavement break-up and direct evidence of partial cassiterite transport in Run 5 have established the hydraulic conditions under which cassiterite should move. Cassiterite was notably absent, however, in transport samples leaving the channel. This indicates the effectiveness of entrapment in restricting cassiterite transport. Transport of cassiterite in close contact with the bed due to its high density and its fine grain size relative to the bed would have facilitated the entrapment process. Observations of sediment transport have also indicated that magnetite (< 0.354 mm) and fine light fractions (< 0.50 mm) were preferentially entrapped. Entrapment of these fractions was reflected by transport rates disproportionately less than their presence in the bed. The lower densities of these fractions, however, meant that entrapment was less effective in restricting bedload transport in comparison with cassiterite. The lack of transport equivalence between magnetite and cassiterite is more extreme than straight density criteria in Shields' relation would suggest. In a uniform deposit, the differences in critical shear stress for entrainment of equivalent grains of cassiterite and magnetite are not substantial (Figure 2-2). In this study, however, shielding and entrapment effects have had a greater impact on cassiterite's mobility than on magnetite.

An issue to be addressed still is the degree of similitude between the flume and Harris Creek. That is, are the processes observed in the flume representative of observations at Harris Creek. A variable experimental slope and high Froude numbers (section 5-1) are the principal deviations of similarity between model and prototype. Slope varied from 0.0060 to 0.0143 while the slope of Harris Creek was approximately 0.0130. Based on these values Run 4 is most similar to Harris Creek, but the slope in any natural gravel-bed river is variable. Of greater concern is the high experimental Froude numbers, which ranged from 1.85 to 2.68. Based on the hydraulic geometry at Harris Creek typical Froude values during flooding are 0.50 to 0.60. High Froude numbers, however, indicate that inertial forces dominated over gravitational forces, which should result in enhanced transport of all grain sizes and densities. Taking this factor into consideration the general immobility of cassiterite during flooding is a surprising result. Kuhnle (1986) was able to mobilize tungsten ($\rho = 19.3$ g/cm^3) and lead ($\rho = 11.4$ g/cm^3) within a mixed size deposit under nondegrading conditions (i.e. sediment feed). Transportation did not occur, however, until a heavy infralayer had developed. The immobility of cassiterite in this study is consistent with the tendency of heavy minerals to concentrate.

Despite the lack of strict similitude between the flume and Harris Creek, observations at peak discharges have identified grain size, density, and bed roughness as important factors which interact to control the enrichment of cassiterite and magnetite on the bed. Fletcher and Wolcott (1991) came to a similar conclusion from observations of magnetite and gold transport during flooding of Harris Creek. Theoretical models of heavy mineral transport are also commensurate with these findings (Slingerland, 1984; Reid and Frostick, 1984; Slingerland and Smith, 1986; Day and Fletcher, 1991). One can therefore conclude that flume models are effective in modelling heavy mineral transport behaviour typical of gravel-bed streams. The controlled environment of the flume reduces the natural variability of streams and enrichment processes are more clearly observed. This study provides a framework for further flume studies of the processes controlling heavy mineral entrainment, transportation, and deposition.

6.0 CONCLUSIONS

During pavement development cassiterite was not transported out of the flume. Selective entrainment of sand-sized light sediment produced lag deposits of concentrated cassiterite along the length of the flume. Samples taken to a depth of 1.25 cm in Runs 3, 4, and 5 detected concentrations of 1.46 to 2.45 % cassiterite by weight in the upper flume reach. Subsurface cassiterite concentrations in the lower reach were probably less enriched as rates of erosion decreased downstream due to a 6.0 cm board beneath the tailgate. There was no evidence of minor cassiterite transport within the channel based on results from Run 5. In this run, a section of the flume where the heavy minerals had been removed remained void of cassiterite after ninety-six hours of pavement development.

Magnetite was introduced to the flume sediment for Runs 4 - 6. In contrast to cassiterite, magnetite was transported out of the flume during pavement development, but in proportions considerably less than its original 1.0 % concentration in the bed. High rates of erosion in the upper reach prevented magnetite enrichment, while reduced downstream erosion and higher grain density caused entrapment with downstream transport. This is in contrast to the sand-sized light fractions that were transported out of the flume in proportions to their presence in the bed. The implication is that the greater density of magnetite allowed grains to be more effectively shielded from the flow than low density particles.

Flooding in Runs 2 - 6 induced pavement break-up and intense rates of light sediment transport, but cassiterite was not transported out of the channel. Transport within the channel did occur, however, based on the flume section in Run 5 where the heavy mineral fraction had been extracted. After sixty minutes of flooding a sample from the top centimeter of this region consisted of 3.63 % cassiterite by weight. It is believed that mobilized cassiterite was transported in close contact with the bed due to its high density. Transport distances remained minimal because of its density and fine grain size relative to the bed, which created numerous opportunities for entrapment. It is unresolved whether cassiterite transport demonstrated during Run 5 occurred in Runs 2 - 4 wherein a coarser sediment mixture was employed. Although applied shear stresses of Runs 2 - 4 were higher during flooding, the possibility exists that flow competence remained insufficient to override the shielding effect of larger grains.

The mobility of magnetite did not increase significantly during flooding. Magnetite as a percentage of total sediment transported had values consistently lower than 0.5 %, despite the fact that all light fractions were in transport. The size distribution of magnetite (0.125 - 0.354 mm) appeared to be the main factor in reduced transport rates, because light fractions finer than 0.354 mm were also transported at disproportionately lower rates. Development of a highly mobile granular layer during flooding is consistent with these results. A mobile bed would allow the low and high density fine sediment (< 0.354 mm) to fractionate from the coarser sediment and be transported in close contact with the bed, thus being more prone to entrapment. This process of fine sediment concentrating at the base of a mobile bed is referred to as shear sorting (Bagnold, 1954; Inmann et al., 1966) or kinetic sieving (Middleton, 1970).

The objective of this study was to simulate heavy mineral transport observed by Fletcher and Wolcott (1991) in Harris Creek, a gravel-bed river in the interior of British Columbia. They noted that pavement break-up during spring flooding was necessary for mobilization of the heavy mineral fraction. They inferred that a coarse surface framework redeveloped after peak discharge that preferentially entrapped heavy minerals being transported in close contact with the bed, leading to high subsurface concentrations. Consistent with observations of Fletcher and Wolcott, cassiterite was not mobilized in this study until the pavement was broken and the majority of light fractions were in transport. Once mobilized, transport was restricted by its high density and fine grain size which led to preferential entrapment. Hence, because of shielding, entrapment, and kinetic sieving effects, transport-equivalence between the light and heavy fractions is more extreme than straight density criteria in Shields' relation would suggest. When a wide range of grain sizes are present, as in this study, the effects of shielding and entrapment are particularly effective in restricting transport of fine heavy fractions. Overall, transport behaviour of heavy minerals in both Harris Creek and this study was a function of density, grain size, and bed roughness which interacted to control bed enrichment.

7.0 REFERENCES

Andrews, E.D. 1983. Entrainment of gravel from naturally sorted riverbed material. Geological Society of America Bulletin, **94**: 1225-1231.

Bagnold, R. A. 1956. The flow of cohesionless grains in fluid. Proceedings of the Royal Society of London Series A, **265**: 315-319.

Best, J. L., and Brayshaw, A. C. 1985. Flow separation - a physical process for the concentration of heavy minerals within alluvial channels. Geological Society of London Journal, **142**: 747-755.

Brady, L. L., and Jobson, H. E. 1973. An experimental study of heavy-mineral segragation under alluvial-flow conditions. United States Geological Survey, Professional Paper 562-K, 38 pp.

Day, S. J., and Fletcher, W. K. 1991. Formation of gold placers in a gravel-bed stream. Journal of Sedimentary Petrology, **61**: 871-883.

Dietrich, W. E. 1982. Settling velocities of natural particles. Water Resources Research, **18**: 1615-1626.

Egiazaroff, I. V. 1965. Calculation of nonuniform sediment concentrations. American Society of Civil Engineers, Journal of the Hydraulics Division, **91**: 225-247.

Einstein, H. A. 1942. Formulas for the Transportation of Bed Load. American Society of Civil Engineers Transactions, Vol. 107, Paper No. 2140, pp. 561-573.

Einstein, H. A. 1950. The bedload function for sediment transportation in open channel flows. US Department of Agriculture Technical Bulletin 1026, 78 pp.

Fletcher, W. K., and Wolcott, J. 1991. Transport of magnetite and gold in Harris Creek, British Columbia, and implications for exploration. Journal of Geochemical Exploration, **41**: 253-274

Fletcher, W. K., Church, M., and Wolcott, J. 1992. Fluvial-transport equivalence of heavy minerals in the sand size range. Canadian Journal of Earth Sciences, **29**: 2017-2021.

Gibbs, R. J., Matthews, M. D., and Link, D. A. 1971. The relationship between sphere size and settling velocity, **41**: 7-18.

Gomez, B., and Church, M. 1989. An assessment of bed load transport formulae for gravel bed rivers. Water Resources Research, **25**: 1161-1186.

Grigg, N. S., and Rathbun, R. E. 1969. Hydraulic equivalence of minerals with consideration of the reentrainment process. United States Geological Survey, Professional Paper 650-B, pp. B77-B80.

Hand, B. M. 1967. Differentiation of beach and sand dunes, using settling velocities of light and heavy minerals. Journal of Sedimentary Petrology, **37**: 514-520.

Hattingh, J., and Rust, I. C. 1993. Flood transport and deposition of tracer heavy minerals in a gravel-bed meander bend channel. Journal of Sedimentary Petrology, **63**: 828-834.

Inman, D. L., Ewing, G. C., and Corliss, J. B. 1966. Coastal sand dunes of Guerno Negro, Baja California, Mexico. Geological Society of America Bulletin, 77: 787-802.

Komar, P.D. 1987. Selective grain entraiment by a current from a bed of mixed sizes: a reanalysis. Journal of Sedimentary Petrology, **57**: 203-211.

Komar, P. D., and Wang, C. 1984. Processes of selective grain transport and the formation of placers on beaches. Journal of Geology, **92**: 637-655.

Kuhnle, R. A. 1986. Experimental studies of heavy-mineral transportation, segragation, and deposition in gravel-bed streams. Ph.D. Thesis, Massachusets Institute of Technology, 209 pp.

Kuhnle, R. A., and Southard, J. B. 1990. Flume experiments on the transport of heavy minerals in gravel-bed streams. Journal of Sedimentary Petrology, **60**: 687-696.

Ljungrenn, P., and Sundborg, A. 1968. Some aspects of fluvial sediments and fluvial morphology. II. A study of some heavy mineral deposits in the valley of the river Lule Alv. Geografiska Annaler, **50A**: 121-135.

Lowright, R., Williams, E. G., and Dachille, F. 1972. An analysis of factors controlling deviations in the hydraulic equivalence in some modern sands. Journal of Sedimentary Petrology, **42**: 635-645.

Middleton, G. V. 1970. Experimental studies related to problems of flysch sedimentation. *In* Flysch Sedimentology in North America. *Edited by* J. Lajoie, Geological Association of Canada Special Publication 7, pp. 253-272.

Milhous, R. I. 1973. Sediment transport in a gravel-bottomed stream. Ph.D. Thesis, Oregon State University, Corvallis, 232 pp.

Minter, W. E. L., and Toens, P. D. 1970. Experimental Simulation of gold deposition in gravel beds. Geological Society of South Africa Transactions, **73**: 89-98.

Parent, A. P. 1988. Scale Models of Gravel Bed Rivers. M.Sc. Thesis, University of British Columbia, Vancouver, 152 pp.

Parker, G., Klingeman, P., and McLean, D. G. 1982. Bedload and size distribution in paved gravel-bed streams. American Society of Civil Engineers, Journal of the Hydraulics Division, **108**: 544-571.

Rittenhouse, G. 1943. Transportation and deposition of heavy minerals. Geological Society of America Bulletin, **54**: 725-780.

Rouse, H. 1959. Elementary Mechanics of Fluids. Wiley, New York, 376 pp.

Rubey, W. W. 1933. The size distribution of heavy minerals within a water-laid sandstone. Journal of Sedimentary Petrology, **3**: 3-29.

Sallenger, A. H. 1979. Inverse grading and hydraulic equivalence in grain-flow deposits. Journal of Sedimentary Petrology, **49**: 553-562.

Sharp, J. J. 1981. Hydraulic Modelling. Butterworth and Co. Ltd., 242 pp.

Shields, A. 1936. Application of similarity principles and turbulence research to bedload movement. *Translation* W. P. Ott, J. C. Uchelen as Report No. 167, California Institute of Technology, Pasadena. 43 pp. (From German)

Slingerland, R. L. 1977. The effects of entrainment on the hydraulic equivalence relationships of light and heavy minerals in sands. Journal of Sedimentary Petrology, **47**: 753-770.

Slingerland, R. L. 1984. Role of hydraulic sorting in the origin of fluvial placers. Journal of Sedimentary petrology, **54**: 37-50.

Slingerland, R. L., and Smith, N. D. 1986. Occurrence and formation of water-laid placers. Annual Review of Earth and Planetary Sciences, **14**: 113-147.

Smith, N. D., and Minter, W. E. 1980. Sedimentological controls of gold and uranium in two Witwatersrand paleoplacers. Economic Geology, **75**: 1-14.

Steidmann, J. S. 1982. Size-density sorting of sand-size sphere during deposition from bedload transport and implications concerning hydraulic equivalence. Sedimentology, **29**: 877-883.

Toh, E. S. C. 1978. Comparison of exploration for alluvial tin and gold. *In* Proceedings of the 11th Commonwealth Mining and Metallurgy Congress, Hong Kong. *Edited by* M.J. Jones, Transcripts of the Institute of Mining and Metallurgy, pp. 269-278.

Vanoni, V. A. 1975. Sedimentation Engineering. American Society of Civil Engineers - Manuals and Reports on Engineering Practice - No. 54, 745 pp.

Vanoni, V. A., and Brooks, N. H. 1957. Laboratory studies of the roughness and suspended load of alluvial streams. Sedimentation Report No. E68, California Institute of Technology, Pasadena, California, 121 pp.

Wolcott, J. 1990. Flume studies of Gravel Bed Surface Response to Flowing Water. Ph.D. Thesis, University of British Columbia, Vancouver, 111 pp.

United States Inter-Agency Committee on Water Resources. 1958. A study of methods used in measurement and analysis of sediment loads in streams: Report K, operator's manual on the visual-accumulation-tube method for sedimentation analysis of sands. United States Inter-Agency Committee on Water Resources, Subcommittee on Sedimentation, St. Anthony Falls Hydraulic Laboratory, Minneapolis, Minnesota.

APPENDIX A

Summary of sediment transport rates for Runs 1 - 6.

Experiment # 1 - summary of sediment transport

Sample number	Flow (RPM)	Time (hr)	Sample duration (hr)	Weight (kg)	Transport rate (kg/hr)
HW1 (S) 1	1100	0.5	0.5	23.076	46.152
HW1 (S) 2	1100	1	0.5	11.009	22.018
HW1 (S) 3	1100	2	1	6.271	6.271
HW1 (S) 4	1100	4	2	4.360	2.180
HW1 (S) 5	1100	8	4	4.175	1.044
HW1 (S) 6	1100	16	8	3.064	0.383
HW1 (S) 7	1100	32	16	3.654	0.228
HW1 (S) 8	1100	48	16	1.972	0.123
HW1 (S) 9	1100	72	24	1.607	0.067
HW1 (S) 10	1100	96	24	1.277	0.053
HW1 (S) 11	1400	0.5	0.5	30.867	61.734
HW1 (S) 12	1400	1	0.5	18.247	36.494
HW1 (S) 13	1400	2	1	11.930	11.930
HW1 (S) 14	1400	4	2	9.110	4.555
HW1 (S) 15	1400	8	4	6.815	1.704
HW1 (S) 16	1400	16	8	7.546	0.943
HW1 (S) 17	1400	32	16	6.589	0.412
HW1 (S) 18	1400	48	16	4.313	0.270
HW1 (S) 19	1400	72	24	3.560	0.148
HW1 (S) 20	1400	96	24	1.891	0.079
HW1 (S) 21	1900	0.5	0.5	n/a	n/a
HW1 (S) 22	1900	1	0.5	20.787	41.574
HW1 (S) 23	1900	2	1	15.713	15.713
HW1 (S) 24	1900	4	2	10.803	5.402
HW1 (S) 25	1900	8	4	8.585	2.146
HW1 (S) 26	1900	16	8	9.925	1.241
HW1 (S) 27	1900	32	16	9.040	0.565
HW1 (S) 28	1900	48	16	7.246	0.453
HW1 (S) 29	1900	72	24	5.521	0.230
HW1 (S) 30	1900	96	24	2.967	0.124

Experiment # 2 - summary of sediment transport

Sample number	Flow (RPM)	Time (hr)	Sample duration (hr)	Weight (kg)	Transport rate (kg/hr)
HW2 (S) 1	1400	0.5	0.5	82.737	165.474
HW2 (S) 2	1400	1	0.5	22.407	44.814
HW2 (S) 3	1400	2	1	11.607	11.607
HW2 (S) 4	1400	4	2	10.799	5.400
HW2 (S) 5	1400	8	4	9.132	2.283
HW2 (S) 6	1400	16	8	8.358	1.045
HW2 (S) 7	1400	32	16	5.961	0.373
HW2 (S) 8	1400	48	16	4.473	0.280
HW2 (S) 9	1400	72	24	3.964	0.165
HW2 (S) 10	1400	96	24	2.471	0.103
HW1 (S) 1b	2400	10 min	10 min	10.997	65.982
HW1 (S) 2b	2400	20 min	10 min	29.420	176.520
HW1 (S) 3b	2400	30 min	10 min	22.566	135.396

Experiment # 3 - summary of sediment transport

Sample number	Flow (RPM)	Time (hr)	Sample duration (hr)	Weight (kg)	Transport rate (kg/hr)
HW3 (S) 1	1400	0.5	0.5	81.165	162.330
HW3 (S) 2	1400	1	0.5	21.654	43.308
HW3 (S) 3	1400	2	1	11.359	11.359
HW3 (S) 4	1400	4	2	7.547	3.774
HW3 (S) 5	1400	8	4	8.098	2.025
HW3 (S) 6	1400	16	8	8.241	1.030
HW3 (S) 7	1400	32	16	5.994	0.375
HW3 (S) 8	1400	48	16	4.480	0.280
HW3 (S) 9	1400	72	24	3.524	0.147
HW3 (S) 10	1400	96	24	2.173	0.091
HW3 (S) 1b	2400	10 min	10 min	13.453	80.718
HW3 (S) 2b	2400	20 min	10 min	25.372	152.232
HW3 (S) 3b	2400	30 min	10 min	29.232	175.392
HW3 (S) 4b	2400	40 min	10 min	12.663	75.978
HW3 (S) 5b	2400	50 min	10 min	13.418	80.508
HW3 (S) 6b	2400	60 min	10 min	8.328	49.968

Experiment # 4 - summary of sediment transport

Sample number	Flow (RPM)	Time (hr)	Sample duration (hr)	Weight (kg)	Transport rate (kg/hr)
HW4 (S) 1	1150	0.5	0.5	n/a	n/a
HW4 (S) 2	1150	1	0.5	38.318	76.636
HW4 (S) 3	1150	2	1	20.394	20.394
HW4 (S) 4	1150	4	2	9.470	4.735
HW4 (S) 5	1150	8	4	5.823	1.456
HW4 (S) 6	1150	16	8	5.041	0.630
HW4 (S) 7	1150	32	16	3.494	0.218
HW4 (S) 8	1150	48	16	2.754	0.172
HW4 (S) 9	1150	72	24	2.364	0.099
HW4 (S) 10	1150	96	24	1.373	0.057
HW4 (S) 1b	2200	5 min	5 min	45.125	541.500
HW4 (S) 2b	2200	10 min	5 min	67.893	814.716
HW4 (S) 3b	2200	15 min	5 min	47.640	571.680

Experiment # 5 - summary of sediment transport

Sample number	Flow (RPM)	Time (hr)	Sample duration (hr)	Weight (kg)	Transport rate (kg/hr)
HW5 (S) 1	1400	0.5	0.5	n/a	n/a
HW5 (S) 2	1400	1	0.5	50.410	100.820
HW5 (S) 3	1400	2	1	26.258	26.258
HW5 (S) 4	1400	4	2	10.112	5.056
HW5 (S) 5	1400	8	4	3.905	0.976
HW5 (S) 6	1400	16	8	8.686	1.086
HW5 (S) 7	1400	32	16	6.891	0.431
HW5 (S) 8	1400	48	16	4.951	0.309
HW5 (S) 9	1400	72	24	4.394	0.183
HW5 (S) 10	1400	96	24	1.758	0.073
HW5 (S) 1b	1700	15 min	15 min	0.422	1.688
HW5 (S) 1c	2000	10 min	10 min	4.068	24.408
HW5 (S) 2c	2000	20 min	10 min	10.251	61.506
HW5 (S) 3c	2000	30 min	10 min	16.444	98.664
HW5 (S) 4c	2000	40 min	10 min	9.760	58.560
HW5 (S) 5c	2000	50 min	10 min	7.756	46.536
HW5 (S) 6c	2000	60 min	10 min	6.071	36.426

Experiment # 6 - summary of sediment transport

Sample number	Flow (RPM)	Time (hr)	Sample duration (hr)	Weight (kg)	Transport rate (kg/hr)
HW6 (S) 1	1200	0.5	0.5	n/a	n/a
HW6 (S) 2	1200	1	0.5	28.854	57.708
HW6 (S) 3	1200	2	1	15.064	15.064
HW6 (S) 4	1200	4	2	12.531	6.266
HW6 (S) 5	1200	8	4	5.209	1.302
HW6 (S) 6	1200	16	8	1.993	0.249
HW6 (S) 7	1200	24	8	4.034	0.504
HW6 (S) 8	1200	30	6	2.385	0.398
HW6 (S) 9	1200	36	6	2.065	0.344
HW6 (S) 10	1200	48	12	1.939	0.162
HW6 (S) 11	1200	54	6	7.597	1.266
HW6 (S) 12	1200	60	6	2.722	0.454
HW6 (S) 13	1200	65.5	5.5	1.814	0.330
HW6 (S) 14	1200	72	6.5	1.878	0.289
HW6 (S) 15	1200	78	6	1.552	0.259
HW6 (S) 16	1200	84	6	1.492	0.249
HW6 (S) 17	1200	90	6	0.920	0.153
HW6 (S) 18	1200	97	7	1.354	0.193
HW6 (S) 19	1200	101	4	3.038	0.760
HW6 (S) 20	1200	110	9	1.814	0.202
HW6 (S) 21	1200	116	6	0.761	0.127
HW6 (S) 22	1200	139	23	1.075	0.047
HW6 (S) 23	1200	163	24	0.722	0.030
HW6 (S) 1b	1700	5 min	5 min	7.432	89.184
HW6 (S) 2b	1700	10 min	5 min	14.469	173.628
HW6 (S) 3b	1700	15 min	5 min	14.706	176.472
HW6 (S) 4b	1700	16 min	1 min	4.447	266.820
HW6 (S) 5b	1700	18 min	2min	7.122	213.660
HW6 (S) 1c	1900	5 min	5 min	0.157	1.884
HW6 (S) 2c	1900	10 min	5 min	0.313	3.756
HW6 (S) 3c	1900	15 min	5 min	0.401	4.812
HW6 (S) 4c	1900	20 min	5 min	0.271	3.252
HW6 (S) 5c	1900	25 min	5 min	0.244	2.928
HW6 (S) 6c	1900	30 min	5 min	0.211	2.532
HW6 (S) 7c	1900	35 min	5 min	0.143	1.716
HW6 (S) 8c	1900	40 min	5 min	0.182	2.184
HW6 (S) 9c	1900	45 min	5 min	0.102	1.224
HW6 (S) 10c	1900	55 min	10 min	0.205	1.230
HW6 (S) 11c	1900	65 min	10 min	0.137	0.822
HW6 (S) 12c	1900	80 min	15 min	0.168	0.672

N.B. c-series were trapped with scaled down Helley-Smith sampler

APPENDIX B

Velocity profile data for Runs 2 - 6. Data for Run 1 was not included as observations were not made of cassiterite distribution and a flood was not simulated.

N.B. Stations 1, 2, and 3 were taken at 5.6 m. Station 2 was situated on the centerline while Stations 1 and 3 were situated 15 cm to the left and right respectively looking downstream. Stations 4 and 5 were situated 5.2 and 6.0 m respectively along the centerline.

Experiment #2 - velocity profile data

Time : 4 hrs
Temp (oC) = 15.0

Station 1	*d = 5.2 cm*	*Station 2*	*d = 5.3 cm*	*Station 3*	*d = 5.3 cm*	*Station 4*	*d = 5.6 cm*	*Station5*	*d = 5.6 cm*
Height (cm)	Velocity (cm/s)	Height (cm)	Velocity (cm/s)	Height (cm)	Velocity (cm/s)	Height (cm)	Velocity (cm/s)	Height (cm)	Velocity (cm/s)
0.1	2.0	0.1	3.2	0.1	31.0	0.1	4.4	0.1	2.6
0.3	5.4	0.3	10.7	0.3	43.0	0.3	12.8	0.3	6.6
0.5	18.5	0.5	16.9	0.5	50.5	0.5	26.1	0.5	22.0
1.1	50.5	0.9	26.1	1.0	63.9	0.9	36.6	0.7	36.6
2.4	116.1	1.9	59.1	1.7	80.3	1.4	69.0	1.4	80.3
4.2	154.4	3.1	124.8	3.4	124.8	2.4	124.8	2.9	116.1
		4.5	165.6	4.4	143.9	4.0	154.4	4.4	134.1
Avg vel.	108.9	*Avg vel.*	105.6	*Avg vel.*	106.7	*Avg vel.*	113.7	*Avg vel.*	101.4

Time : 8 hrs
Temp (oC) = 15.0

Station 1	*d = 5.3 cm*	*Station 2*	*d = 5.2 cm*	*Station 3*	*d = 5.3 cm*	*Station 4*	*d = 5.1 cm*	*Station5*	*d = 5.6 cm*
Height (cm)	Velocity (cm/s)	Height (cm)	Velocity (cm/s)	Height (cm)	Velocity (cm/s)	Height (cm)	Velocity (cm/s)	Height (cm)	Velocity (cm/s)
0.1	8.8	0.1	1.3	0.1	18.5	0.1	22.0	0.1	1.8
0.3	12.8	0.3	5.9	0.3	33.7	0.3	36.6	0.3	6.6
0.5	20.2	0.5	16.9	0.5	46.6	0.5	50.5	0.5	16.9
0.8	43.0	0.9	31.0	0.9	59.1	1.1	74.4	1.1	46.6
1.6	80.3	1.6	43.0	1.6	74.4	1.9	93.2	1.6	74.4
2.6	100.4	3.3	108.0	3.4	108.0	2.9	108.0	2.7	100.4
4.5	124.8	4.7	143.9	4.8	134.1	3.9	124.8	4.3	124.8
Avg vel.	91.6	*Avg vel.*	89.9	*Avg vel.*	95.8	*Avg vel.*	98.1	*Avg vel.*	90.9

Experiment #2 - *velocity profile data*

Time : 32 hrs
Temp (oC) = 16.5

Station 1	*d = 5.6 cm*	*Station 2*	*d = 5.3 cm*	*Station 3*	*d = 5.8 cm*	*Station 4*	*d = 5.1 cm*	*Station5*	*d = 6.0 cm*
Height (cm)	Velocity (cm/s)	Height (cm)	Velocity (cm/s)	Height (cm)	Velocity (cm/s)	Height (cm)	Velocity (cm/s)	Height (cm)	Velocity (cm/s)
0.1	2.6	0.1	10.7	0.1	31.0	0.1	8.0	0.1	4.8
0.3	8.8	0.3	15.4	0.3	36.6	0.3	16.9	0.3	8.8
0.5	28.5	0.5	20.2	0.5	43.0	0.5	43.0	0.5	16.9
1.1	50.5	1.1	31.0	1.2	54.6	0.9	54.6	1.0	50.5
1.6	74.4	1.9	50.5	2.1	74.4	1.9	74.4	1.6	86.6
2.5	100.4	2.7	86.6	3.2	93.2	3.1	93.2	2.9	108.0
4.5	124.8	4.6	124.8	5.1	124.8	4.2	108.0	4.8	124.8
Avg vel.	91.8	*Avg vel.*	80.6	*Avg vel.*	89.7	*Avg vel.*	81.6	*Avg vel.*	97.2

Time : 48 hrs
Temp (oC) = 16.5

Station 1	*d = 5.4 cm*	*Station 2*	*d = 5.5 cm*	*Station 3*	*d = 5.3 cm*	*Station 4*	*d = 5.2 cm*	*Station5*	*d = 6.0 cm*
Height (cm)	Velocity (cm/s)	Height (cm)	Velocity (cm/s)	Height (cm)	Velocity (cm/s)	Height (cm)	Velocity (cm/s)	Height (cm)	Velocity (cm/s)
0.1	5.9	0.1	3.2	0.1	24.0	0.1	2.3	0.1	12.8
0.3	8.8	0.3	6.6	0.3	28.5	0.3	3.9	0.3	12.8
0.5	26.1	0.5	15.4	0.5	31.0	0.5	18.5	0.7	31.0
0.8	50.5	1.1	18.5	1.3	54.6	0.9	54.6	1.2	50.5
1.8	80.3	1.4	26.1	2.3	80.3	1.4	80.3	2.0	80.3
2.7	108.0	2.2	80.3	3.5	108.0	2.4	108.0	3.4	108.0
4.5	134.1	4.5	134.1	4.5	116.1	4.6	124.8	5.0	124.8
Avg vel.	96.8	*Avg vel.*	86.4	*Avg vel.*	87.0	*Avg vel.*	94.8	*Avg vel.*	91.5

Experiment #2 - velocity profile data

Time : 72 hrs
Temp (oC) = 17.0

Station 1	*d = 5.4 cm*	*Station 2*	*d = 5.4 cm*	*Station 3*	*d = 5.4 cm*	*Station 4*	*d = 5.4 cm*	*Station5*	*d = 5.9 cm*
Height (cm)	Velocity (cm/s)	Height (cm)	Velocity (cm/s)	Height (cm)	Velocity (cm/s)	Height (cm)	Velocity (cm/s)	Height (cm)	Velocity (cm/s)
0.1	9.7	0.1	2.8	0.1	26.1	0.1	3.9	0.1	7.2
0.3	16.9	0.3	7.2	0.3	28.5	0.3	7.2	0.3	12.8
0.5	36.6	0.5	15.4	0.5	28.5	0.5	12.8	0.5	22.0
0.9	63.9	0.9	18.5	0.7	36.6	0.8	36.6	0.8	39.7
1.4	74.4	1.3	33.7	1.2	63.9	1.4	93.2	1.6	74.4
2.7	100.4	2.3	93.2	2.6	100.4	2.9	124.8	2.8	108.0
4.6	143.9	4.5	143.9	4.7	134.1	4.4	134.1	4.8	134.1
Avg vel.	100.8	*Avg vel.*	94.0	*Avg vel.*	97.2	*Avg vel.*	105.0	*Avg vel.*	98.2

Time : 96 hrs
Temp (oC) = 17.0

Station 1	*d = 4.9 cm*	*Station 2*	*d = 5.3 cm*	*Station 3*	*d = 5.5 cm*	*Station 4*	*d = 5.1 cm*	*Station5*	*d = 5.6 cm*
Height (cm)	Velocity (cm/s)	Height (cm)	Velocity (cm/s)	Height (cm)	Velocity (cm/s)	Height (cm)	Velocity (cm/s)	Height (cm)	Velocity (cm/s)
0.1	16.9	0.1	4.8	0.1	18.5	0.1	50.5	0.1	8.8
0.3	36.6	0.3	7.2	0.3	24.0	0.4	54.6	0.3	14.1
0.5	50.5	0.5	11.7	0.5	28.5	0.6	63.9	0.5	26.1
1.0	74.4	1.0	18.5	1.2	69.0	1.4	93.2	0.9	50.5
2.5	108.0	1.7	59.1	1.9	93.2	2.6	108.0	1.2	59.1
4.2	143.9	2.8	93.2	2.2	124.8	4.6	143.9	2.9	93.2
		4.6	143.9	4.8	143.9			5.2	124.8
Avg vel.	106.1	*Avg vel.*	90.1	*Avg vel.*	109.9	*Avg vel.*	110.2	*Avg vel.*	87.3

Experiment #3 - velocity profile data

Time : 4 hrs
Temp (oC) = 15.0

Station 1	*d = 5.1 cm*	*Station 2*	*d = 5.0 cm*	*Station 3*	*d = 5.1 cm*	*Station 4*	*d = 5.3 cm*	*Station5*	*d = 5.0 cm*
Height (cm)	Velocity (cm/s)	Height (cm)	Velocity (cm/s)	Height (cm)	Velocity (cm/s)	Height (cm)	Velocity (cm/s)	Height (cm)	Velocity (cm/s)
0.1	2.3	0.1	2.6	0.1	15.4	0.1	1.0	0.1	14.1
0.3	12.8	0.3	5.4	0.3	26.1	0.3	3.9	0.3	26.1
0.5	31.0	0.5	18.5	0.5	31.0	0.5	7.2	0.5	36.6
1.0	50.5	0.9	43.0	1.1	43.0	1.4	43.0	1.0	59.1
1.8	69.0	1.8	80.3	1.8	69.0	1.8	63.9	1.6	80.3
2.6	93.2	3.0	108.0	3.1	93.2	2.6	86.6	2.2	93.2
4.4	134.1	4.2	124.8	4.2	116.1	4.3	108.0	4.1	124.8
Avg vel.	88.8	*Avg vel.*	88.7	*Avg vel.*	81.9	*Avg vel.*	75.3	*Avg vel.*	91.6

Time : 8 hrs
Temp (oC) = 15.0

Station 1	*d = 5.4 cm*	*Station 2*	*d = 4.9 cm*	*Station 3*	*d = 5.0 cm*	*Station 4*	*d = 5.2 cm*	*Station5*	*d = 5.2 cm*
Height (cm)	Velocity (cm/s)	Height (cm)	Velocity (cm/s)	Height (cm)	Velocity (cm/s)	Height (cm)	Velocity (cm/s)	Height (cm)	Velocity (cm/s)
0.1	8.0	0.1	3.2	0.1	3.9	0.1	2.0	0.1	7.2
0.3	18.5	0.3	9.7	0.3	15.4	0.3	4.8	0.3	18.5
0.5	24.0	0.5	16.9	0.5	31.0	0.5	12.8	0.5	33.7
0.9	36.6	0.8	36.6	1.1	54.6	1.0	31.0	0.9	50.5
1.7	59.1	1.4	59.1	1.8	74.4	1.8	50.5	1.5	74.4
2.6	86.6	2.3	86.6	3.1	108.0	3.2	80.3	2.8	108.0
4.3	124.8	4.1	116.1	4.2	116.1	4.4	108.0	4.7	134.1
Avg vel.	84.7	*Avg vel.*	80.3	*Avg vel.*	85.7	*Avg vel.*	69.6	*Avg vel.*	94.7

Experiment #3 - *velocity profile data cont.*

Time : 32 hrs
Temp (oC) = 15.5

Station 1	*d = 5.3 cm*	*Station 2*	*d = 5.4 cm*	*Station 3*	*d = 5.2 cm*	*Station 4*	*d = 5.2 cm*	*Station5*	*d = 5.3 cm*
Height (cm)	Velocity (cm/s)	Height (cm)	Velocity (cm/s)	Height (cm)	Velocity (cm/s)	Height (cm)	Velocity (cm/s)	Height (cm)	Velocity (cm/s)
0.1	22.0	0.1	2.0	0.1	39.7	0.1	8.8	0.1	3.2
0.3	31.0	0.3	3.5	0.3	43.0	0.3	10.7	0.3	9.7
0.5	39.7	0.5	5.9	0.6	50.5	0.5	18.5	0.5	31.0
1.1	59.1	0.7	12.8	0.8	63.9	1.1	36.6	1.3	59.1
1.8	80.3	1.0	33.7	1.5	80.3	2.1	54.6	2.1	80.3
3.4	100.4	2.4	80.3	2.9	93.2	3.1	80.3	2.9	93.2
4.5	124.8	4.5	108.0	4.2	116.1	4.5	116.1	4.7	116.1
Avg vel.	90.6	*Avg vel.*	75.2	*Avg vel.*	91.0	*Avg vel.*	73.6	*Avg vel.*	83.0

Time : 48 hrs
Temp (oC) = 16.0

Station 1	*d = 5.3 cm*	*Station 2*	*d = 4.9 cm*	*Station 3*	*d = 5.8 cm*	*Station 4*	*d = 5.5 cm*	*Station5*	*d = 5.6 cm*
Height (cm)	Velocity (cm/s)	Height (cm)	Velocity (cm/s)	Height (cm)	Velocity (cm/s)	Height (cm)	Velocity (cm/s)	Height (cm)	Velocity (cm/s)
0.1	7.2	0.1	3.9	0.1	4.8	0.1	3.9	0.1	10.7
0.3	15.4	0.3	8.8	0.3	15.4	0.3	8.8	0.3	18.5
0.5	31.0	0.5	20.2	0.5	28.5	0.5	22.0	0.6	26.1
1.3	63.9	1.0	50.5	1.2	63.9	1.1	43.0	1.2	50.5
2.0	80.3	1.3	69.0	1.8	80.3	1.9	54.6	1.8	80.3
2.9	108.0	2.6	93.2	3.0	108.0	3.1	80.3	3.4	108.0
4.6	124.8	4.3	116.1	5.2	134.1	4.3	108.0	4.9	134.1
Avg vel.	90.8	*Avg vel.*	82.9	*Avg vel.*	96.2	*Avg vel.*	73.4	*Avg vel.*	93.2

Experiment #3 - velocity profile data cont.

Time : 72 hrs
Temp (oC) = 16.5

Station 1	*d = 5.4 cm*	*Station 2*	*d = 5.1 cm*	*Station 3*	*d = 5.2 cm*	*Station 4*	*d = 5.2 cm*	*Station5*	*d = 5.5 cm*
Height (cm)	Velocity (cm/s)	Height (cm)	Velocity (cm/s)	Height (cm)	Velocity (cm/s)	Height (cm)	Velocity (cm/s)	Height (cm)	Velocity (cm/s)
0.1	2.6	0.1	9.7	0.1	18.5	0.1	6.6	0.1	15.4
0.3	5.9	0.3	12.8	0.3	31.0	0.3	10.7	0.3	22.0
0.5	31.0	0.5	22.0	0.5	46.6	0.5	26.1	0.5	28.5
1.0	59.1	0.6	36.6	0.8	59.1	0.7	36.6	0.8	43.0
1.5	80.3	1.1	63.9	1.5	80.3	1.4	59.1	1.6	69.0
3.0	108.0	3.4	93.2	2.8	108.0	2.2	80.3	3.0	100.4
4.7	134.1	4.4	124.8	4.7	124.8	4.1	108.0	4.9	124.8
Avg vel.	96.4	*Avg vel.*	86.3	*Avg vel.*	95.3	*Avg vel.*	78.7	*Avg vel.*	89.4

Time : 96 hrs
Temp (oC) = 16.5

Station 1	*d = 5.1 cm*	*Station 2*	*d = 4.8 cm*	*Station 3*	*d = 5.5 cm*	*Station 4*	*d = 5.2 cm*	*Station5*	*d = 5.6 cm*
Height (cm)	Velocity (cm/s)	Height (cm)	Velocity (cm/s)	Height (cm)	Velocity (cm/s)	Height (cm)	Velocity (cm/s)	Height (cm)	Velocity (cm/s)
0.1	18.5	0.1	15.4	0.1	26.1	0.1	3.9	0.1	12.8
0.3	26.1	0.3	22.0	0.4	46.6	0.3	8.8	0.3	18.5
0.5	36.6	0.5	33.7	0.6	59.1	0.5	26.1	0.6	31.0
0.9	54.6	0.8	43.0	1.2	74.4	0.9	54.6	1.0	50.5
1.9	80.3	1.6	69.0	2.0	86.6	1.8	69.0	1.6	63.9
3.4	116.1	2.9	100.4	2.8	108.0	3.0	108.0	3.0	93.2
4.7	134.1	4.2	116.1	4.2	116.1	4.3	143.9	4.9	124.8
Avg vel.	95.4	*Avg vel.*	84.0	*Avg vel.*	95.6	*Avg vel.*	96.5	*Avg vel.*	86.5

Experiment #4 - *velocity profile data*

Time : 4 hrs
Temp (oC) = 12.5

Station 1	*d = 4.5 cm*	*Station 2*	*d = 3.4 cm*	*Station 3*	*d = 3.2 cm*	*Station 4*	*d = 3.2 cm*	*Station5*	*d = 3.9 cm*
Height (cm)	Velocity (cm/s)	Height (cm)	Velocity (cm/s)	Height (cm)	Velocity (cm/s)	Height (cm)	Velocity (cm/s)	Height (cm)	Velocity (cm/s)
0.1	2.0	0.1	11.7	0.1	16.9	0.1	14.1	0.1	1.6
0.3	20.2	0.3	14.1	0.3	22.0	0.3	28.5	0.3	3.2
0.5	36.6	0.5	28.5	0.5	31.0	0.5	50.5	0.5	15.4
0.7	54.6	0.9	43.0	0.9	46.6	0.9	69.0	0.9	43.0
1.2	80.3	1.6	69.0	1.3	80.3	1.3	93.2	1.2	59.1
1.9	100.4	2.4	108.0	1.7	108.0	2.2	124.8	1.6	69.0
3.7	143.9	2.9	124.8	2.3	116.1	2.7	143.9	2.9	93.2
Avg vel.	102.0	*Avg vel.*	80.6	*Avg vel.*	86.4	*Avg vel.*	99.5	*Avg vel.*	67.7

Time : 8 hrs
Temp (oC) = 15.0

Station 1	*d = 4.7 cm*	*Station 2*	*d = 3.3 cm*	*Station 3*	*d = 3.1 cm*	*Station 4*	*d = 3.5 cm*	*Station5*	*d = 3.2 cm*
Height (cm)	Velocity (cm/s)	Height (cm)	Velocity (cm/s)	Height (cm)	Velocity (cm/s)	Height (cm)	Velocity (cm/s)	Height (cm)	Velocity (cm/s)
0.1	20.2	0.1	6.6	0.1	11.7	0.1	3.5	0.1	26.1
0.3	43.0	0.3	18.5	0.3	20.2	0.3	15.4	0.3	36.6
0.5	63.9	0.5	33.7	0.5	31.0	0.5	50.5	0.5	50.5
0.8	74.4	1.1	59.1	1.0	59.1	1.2	69.0	0.9	63.9
1.2	80.3	1.4	80.3	1.7	86.6	2.2	93.2	1.4	93.2
2.2	100.4	2.4	116.1	2.3	108.0	2.9	108.0	2.7	116.1
4.2	154.4								
Avg vel.	109.5	*Avg vel.*	81.0	*Avg vel.*	76.9	*Avg vel.*	79.7	*Avg vel.*	87.3

Experiment #4 - *velocity profile data cont.*

Time : 32 hrs
Temp (oC) = 16.0

Station 1	*d = 4.5 cm*	*Station 2*	*d = 3.2 cm*	*Station 3*	*d = 3.2 cm*	*Station 4*	*d = 3.5 cm*	*Station5*	*d = 3.6 cm*
Height (cm)	Velocity (cm/s)	Height (cm)	Velocity (cm/s)	Height (cm)	Velocity (cm/s)	Height (cm)	Velocity (cm/s)	Height (cm)	Velocity (cm/s)
0.1	18.5	0.1	12.8	0.1	22.0	0.1	6.6	0.1	11.7
0.3	36.6	0.3	22.0	0.3	31.0	0.3	15.4	0.3	18.5
0.5	43.0	0.6	28.5	0.5	39.7	0.5	31.0	0.5	28.5
0.8	54.6	1.0	43.0	0.9	54.6	0.9	50.5	0.9	50.5
1.4	63.9	1.2	59.1	1.5	63.9	1.3	63.9	1.3	59.1
2.7	93.2	2.0	86.6	2.2	74.4	1.9	80.3	2.2	80.3
3.7	108.0	2.6	100.4			2.8	93.2	2.8	93.2
Avg vel.	81.4	*Avg vel.*	68.3	*Avg vel.*	61.5	*Avg vel.*	68.4	*Avg vel.*	67.7

Time : 48 hrs
Temp (oC) = 16.0

Station 1	*d = 4.4 cm*	*Station 2*	*d = 3.3 cm*	*Station 3*	*d = 3.5 cm*	*Station 4*	*d = 3.4 cm*	*Station5*	*d = 3.4 cm*
Height (cm)	Velocity (cm/s)	Height (cm)	Velocity (cm/s)	Height (cm)	Velocity (cm/s)	Height (cm)	Velocity (cm/s)	Height (cm)	Velocity (cm/s)
0.1	31.0	0.1	4.8	0.1	8.8	0.1	6.6	0.1	24.0
0.3	36.6	0.3	14.1	0.3	22.0	0.3	18.5	0.3	36.6
0.5	39.7	0.5	22.0	0.5	28.5	0.5	26.1	0.6	50.5
1.0	59.1	1.0	50.5	0.8	39.7	0.9	43.0	0.9	59.1
1.6	80.3	1.7	80.3	1.8	63.9	1.5	63.9	1.5	69.0
2.3	93.2	2.6	100.4	2.6	86.6	2.2	86.6	2.0	86.6
3.6	124.8					2.7	93.2	2.8	93.2
Avg vel.	90.4	*Avg vel.*	70.2	*Avg vel.*	62.2	*Avg vel.*	66.6	*Avg vel.*	73.0

Experiment #4 - velocity profile data cont

Time : 72 hrs
Temp (oC) = 16.0

Station 1	*d = 4.6 cm*	*Station 2*	*d = 2.9 cm*	*Station 3*	*d = 3.2 cm*	*Station 4*	*d = 3.4 cm*	*Station5*	*d = 3.5 cm*
Height (cm)	Velocity (cm/s)	Height (cm)	Velocity (cm/s)	Height (cm)	Velocity (cm/s)	Height (cm)	Velocity (cm/s)	Height (cm)	Velocity (cm/s)
0.1	36.6	0.1	10.7	0.1	15.4	0.1	15.4	0.1	9.7
0.5	43.0	0.3	18.5	0.4	22.0	0.3	28.5	0.4	15.4
0.9	59.1	0.5	31.0	0.6	33.7	0.5	39.7	0.6	18.5
1.4	63.9	1.2	59.1	1.1	59.1	0.9	46.6	1.0	50.5
2.0	80.3	2.0	93.2	1.8	80.3	1.4	69.0	1.3	63.9
2.8	100.4	2.4	116.1	2.5	100.4	2.0	86.6	2.3	93.2
4.2	124.8					2.7	100.4	2.9	100.4
Avg vel.	88.3	*Avg vel.*	75.6	*Avg vel.*	70.8	*Avg vel.*	73.0	*Avg vel.*	70.4

Time : 96 hrs
Temp (oC) = 16.0

Station 1	*d = 4.6 cm*	*Station 2*	*d = 3.2 cm*	*Station 3*	*d = 3.0 cm*	*Station 4*	*d = 3.7 cm*	*Station5*	*d = 3.4 cm*
Height (cm)	Velocity (cm/s)	Height (cm)	Velocity (cm/s)	Height (cm)	Velocity (cm/s)	Height (cm)	Velocity (cm/s)	Height (cm)	Velocity (cm/s)
0.1	9.7	0.1	7.2	0.1	24.0	0.1	11.7	0.1	15.4
0.3	22.0	0.3	15.4	0.3	28.5	0.3	22.0	0.3	26.1
0.5	36.6	0.5	20.2	0.5	36.6	0.5	26.1	0.5	39.7
1.0	43.0	0.7	28.5	1.0	54.6	0.8	36.6	0.8	50.5
1.7	59.1	1.2	43.0	1.7	86.6	1.1	43.0	1.3	63.9
2.9	86.6	1.7	69.0	2.4	108.0	1.9	69.0	2.0	86.6
4.1	124.8	2.6	100.4			3.1	100.4	2.8	108.0
Avg vel.	80.1	*Avg vel.*	62.8	*Avg vel.*	76.9	*Avg vel.*	66.3	*Avg vel.*	75.4

Experiment #5 - velocity profile data

Time : 4 hrs
Temp (oC) = 16.5

Station 1	*d = 4.6 cm*	*Station 2*	*d = 4.7 cm*	*Station 3*	*d = 5.0 cm*	*Station 4*	*d = 4.7 cm*	*Station5*	*d = 4.9 cm*
Height (cm)	Velocity (cm/s)	Height (cm)	Velocity (cm/s)	Height (cm)	Velocity (cm/s)	Height (cm)	Velocity (cm/s)	Height (cm)	Velocity (cm/s)
0.1	16.9	0.1	7.2	0.1	7.2	0.1	4.8	0.1	8.8
0.3	24.0	0.3	36.6	0.3	20.2	0.3	8.8	0.3	18.5
0.5	36.6	0.5	50.5	0.5	46.6	0.5	31.0	0.5	36.6
1.1	69.0	1.1	69.0	1.2	69.0	1.0	59.1	0.7	50.5
1.9	93.2	1.5	80.3	2.0	93.2	2.1	93.2	1.3	69.0
2.7	108.0	2.8	108.0	2.6	100.4	3.7	124.8	2.3	93.2
4.0	124.8	3.9	124.8	4.1	116.1			4.2	124.8
Avg vel.	93.2	*Avg vel.*	94.1	*Avg vel.*	91.1	*Avg vel.*	91.2	*Avg vel.*	89.9

Time : 8 hrs
Temp (oC) = 16.5

Station 1	*d = 4.7 cm*	*Station 2*	*d = 5.0 cm*	*Station 3*	*d = 5.3 cm*	*Station 4*	*d = 4.9 cm*	*Station5*	*d = 5.2 cm*
Height (cm)	Velocity (cm/s)	Height (cm)	Velocity (cm/s)	Height (cm)	Velocity (cm/s)	Height (cm)	Velocity (cm/s)	Height (cm)	Velocity (cm/s)
0.1	10.7	0.1	2.8	0.1	7.2	0.1	3.9	0.1	7.2
0.3	18.5	0.3	7.2	0.3	15.4	0.3	10.7	0.3	12.8
0.5	39.7	0.5	20.2	0.5	26.1	0.5	16.9	0.5	24.0
1.1	63.9	0.8	59.1	1.0	59.1	0.7	46.6	0.7	39.7
1.5	74.4	1.7	86.6	2.0	93.2	1.0	63.9	1.5	80.3
2.6	108.0	3.1	116.1	3.1	108.0	2.1	108.0	2.9	108.0
4.1	124.8	4.1	124.8	4.6	124.8	3.9	124.8	4.3	124.8
Avg vel.	91.3	*Avg vel.*	95.1	*Avg vel.*	93.3	*Avg vel.*	96.3	*Avg vel.*	93.1

Experiment #5 - *velocity profile data*

Time : 32 hrs
Temp (oC) = 16.5

Station 1	*d = 4.9 cm*	*Station 2*	*d = 5.3 cm*	*Station 3*	*d = 5.1 cm*	*Station 4*	*d = 5.0 cm*	*Station5*	*d = 5.2 cm*
Height (cm)	Velocity (cm/s)	Height (cm)	Velocity (cm/s)	Height (cm)	Velocity (cm/s)	Height (cm)	Velocity (cm/s)	Height (cm)	Velocity (cm/s)
0.1	2.6	0.1	10.7	0.1	14.1	0.1	16.9	0.1	4.4
0.3	4.8	0.3	36.6	0.3	18.5	0.3	26.1	0.3	9.7
0.5	12.8	0.5	50.5	0.5	36.6	0.5	36.6	0.5	36.6
0.8	43.0	1.1	69.0	1.1	69.0	1.1	63.9	0.8	50.5
1.3	80.3	2.0	80.3	2.0	93.2	1.9	93.2	1.3	80.3
2.9	116.1	3.0	108.0	2.9	108.0	3.1	108.0	2.4	93.2
4.2	124.8	4.1	124.8	4.2	124.8	4.3	124.8	4.4	124.8
Avg vel.	93.8	*Avg vel.*	95.2	*Avg vel.*	95.1	*Avg vel.*	93.7	*Avg vel.*	92.6

Time : 48 hrs
Temp (oC) = 16.5

Station 1	*d = 4.7 cm*	*Station 2*	*d = 5.1 cm*	*Station 3*	*d = 5.2 cm*	*Station 4*	*d = 5.1 cm*	*Station5*	*d = 4.9 cm*
Height (cm)	Velocity (cm/s)	Height (cm)	Velocity (cm/s)	Height (cm)	Velocity (cm/s)	Height (cm)	Velocity (cm/s)	Height (cm)	Velocity (cm/s)
0.1	8.8	0.1	4.8	0.1	15.4	0.1	8.8	0.1	15.4
0.3	15.4	0.3	15.4	0.3	36.6	0.3	14.1	0.3	31.0
0.5	31.0	0.5	36.6	0.5	50.5	0.5	22.0	0.5	36.6
0.8	69.0	1.0	54.6	1.2	74.4	0.8	43.0	0.7	54.6
1.1	80.3	1.6	80.3	1.8	93.2	1.3	74.4	1.3	74.4
2.3	116.1	2.6	93.2	4.1	124.8	2.8	108.0	2.5	108.0
3.7	124.8	4.6	124.8			3.9	124.8	4.3	124.8
Avg vel.	101.3	*Avg vel.*	88.6	*Avg vel.*	98.1	*Avg vel.*	93.8	*Avg vel.*	94.7

Experiment #5 - velocity profile data

Time : 72 hrs
Temp (oC) = 16.5

Station 1	*d = 4.6 cm*	*Station 2*	*d = 5.1 cm*	*Station 3*	*d = 5.0 cm*	*Station 4*	*d = 5.2 cm*	*Station5*	*d = 4.8 cm*
Height (cm)	Velocity (cm/s)	Height (cm)	Velocity (cm/s)	Height (cm)	Velocity (cm/s)	Height (cm)	Velocity (cm/s)	Height (cm)	Velocity (cm/s)
0.1	10.7	0.1	24.0	0.1	22.0	0.1	8.8	0.1	22.0
0.3	18.5	0.3	33.7	0.3	26.1	0.3	26.1	0.3	26.1
0.5	31.0	0.5	43.0	0.5	39.7	0.5	43.0	0.5	59.1
0.9	69.0	0.8	54.6	1.0	59.1	1.2	80.3	1.5	93.2
1.9	93.2	1.5	80.3	1.7	100.4	2.9	124.8	2.8	116.1
2.7	108.0	2.5	93.2	3.7	124.8	4.4	134.1	4.1	134.1
4.2	124.8	4.3	124.8						
Avg vel.	93.1	*Avg vel.*	92.5	*Avg vel.*	99.8	*Avg vel.*	105.8	*Avg vel.*	104.7

Time : 96 hrs
Temp (oC) = 16.5

Station 1	*d = 4.8 cm*	*Station 2*	*d = 5.1 cm*	*Station 3*	*d = 5.1 cm*	*Station 4*	*d = 5.0 cm*	*Station5*	*d = 5.1 cm*
Height (cm)	Velocity (cm/s)	Height (cm)	Velocity (cm/s)	Height (cm)	Velocity (cm/s)	Height (cm)	Velocity (cm/s)	Height (cm)	Velocity (cm/s)
0.1	2.8	0.1	18.5	0.1	24.0	0.1	3.2	0.1	39.7
0.3	18.5	0.3	26.1	0.3	33.7	0.3	8.8	0.3	43.0
0.5	28.5	0.5	36.6	0.5	46.6	0.5	22.0	0.5	54.6
0.6	39.7	1.2	69.0	1.1	69.0	0.7	36.6	1.1	80.3
1.1	69.0	2.1	93.2	1.9	93.2	1.1	63.9	1.9	93.2
2.2	100.4	4.3	124.8	3.9	124.8	1.8	93.2	3.1	108.0
4.2	124.8					4.1	124.8	4.4	124.8
Avg vel.	91.6	*Avg vel.*	93.7	*Avg vel.*	97.3	*Avg vel.*	91.9	*Avg vel.*	98.8

Experiment #6 - velocity profile data

Time : 4 hrs
Temp (oC) = 15.5

Station 1	*d = 3.9 cm*	*Station 2*	*d = 3.8 cm*	*Station 3*	*d = 3.1 cm*	*Station 4*	*d = 4.3 cm*	*Station5*	*d = 4.4 cm*
Height (cm)	Velocity (cm/s)	Height (cm)	Velocity (cm/s)	Height (cm)	Velocity (cm/s)	Height (cm)	Velocity (cm/s)	Height (cm)	Velocity (cm/s)
0.1	2.3	0.1	12.8	0.1	3.2	0.1	50.5	0.1	3.9
0.3	8.0	0.3	36.6	0.3	6.6	0.3	59.1	0.3	16.9
0.5	18.5	0.5	50.5	0.6	22.0	0.8	93.2	0.6	39.7
0.8	36.6	0.8	59.1	0.9	54.6	1.5	116.1	1.0	50.5
1.3	59.1	1.4	93.2	1.9	80.3	2.3	134.1	1.6	93.2
2.4	100.4	2.4	134.1	2.8	93.2	3.0	143.9	2.2	108.0
3.2	124.8	3.2	143.9			3.5	143.9	4.0	143.9
Avg vel.	81.5	*Avg vel.*	105.8	*Avg vel.*	64.2	*Avg vel.*	122.9	*Avg vel.*	97.8

Time : 8 hrs
Temp (oC) = 15.5

Station 1	*d = 3.6 cm*	*Station 2*	*d = 4.0 cm*	*Station 3*	*d = 3.6 cm*	*Station 4*	*d = 4.3 cm*	*Station5*	*d = 4.1 cm*
Height (cm)	Velocity (cm/s)	Height (cm)	Velocity (cm/s)	Height (cm)	Velocity (cm/s)	Height (cm)	Velocity (cm/s)	Height (cm)	Velocity (cm/s)
0.1	3.2	0.1	7.2	0.1	3.9	0.1	2.3	0.1	12.8
0.3	12.8	0.3	18.5	0.3	5.4	0.3	50.5	0.3	28.5
0.5	18.5	0.5	26.1	0.5	6.6	0.5	59.1	0.5	43.0
0.9	43.0	0.9	59.1	0.9	7.2	1.2	80.3	0.9	59.1
1.2	69.0	1.3	86.6	1.1	43.0	2.0	116.1	1.3	93.2
1.7	93.2	1.6	108.0	2.0	93.2	3.7	165.6	2.5	124.8
3.4	143.9	3.1	165.6	3.0	124.8			3.2	143.9
Avg vel.	88.0	*Avg vel.*	111.3	*Avg vel.*	77.5	*Avg vel.*	117.5	*Avg vel.*	105.2

Experiment #6 - velocity profile data

Time : 24 hrs
Temp (oC) = 15.5

Station 1	*d = 3.5 cm*	*Station 2*	*d = 4.1 cm*	*Station 3*	*d = 3.4 cm*	*Station 4*	*d = 4.5 cm*	*Station5*	*d = 4.2 cm*
Height (cm)	Velocity (cm/s)	Height (cm)	Velocity (cm/s)	Height (cm)	Velocity (cm/s)	Height (cm)	Velocity (cm/s)	Height (cm)	Velocity (cm/s)
0.1	18.5	0.1	1.3	0.1	2.6	0.1	3.9	0.1	18.5
0.3	24.0	0.3	4.8	0.3	8.8	0.3	39.7	0.3	26.1
0.5	36.6	0.5	6.6	0.5	15.4	0.5	59.1	0.5	36.6
0.8	59.1	0.8	22.0	0.8	31.0	1.0	80.3	1.0	69.0
1.3	86.6	1.4	80.3	1.3	74.4	1.8	100.4	1.7	93.2
2.2	124.8	2.3	124.8	2.2	108.0	2.4	124.8	2.1	116.1
3.0	143.9	3.2	154.4	2.9	116.1	3.9	154.4	3.6	143.9
Avg vel.	100.1	*Avg vel.*	103.2	*Avg vel.*	79.2	*Avg vel.*	112.1	*Avg vel.*	102.6

Time : 48 hrs
Temp (oC) = 15.5

Station 1	*d = 4.6 cm*	*Station 2*	*d = 4.2 cm*	*Station 3*	*d = 3.8 cm*	*Station 4*	*d = 4.5 cm*	*Station5*	*d = 4.4 cm*
Height (cm)	Velocity (cm/s)	Height (cm)	Velocity (cm/s)	Height (cm)	Velocity (cm/s)	Height (cm)	Velocity (cm/s)	Height (cm)	Velocity (cm/s)
0.1	4.4	0.1	3.2	0.1	3.2	0.1	4.4	0.1	4.8
0.3	36.6	0.3	7.2	0.3	4.4	0.3	5.4	0.3	22.0
0.5	43.0	0.5	8.8	0.5	6.6	0.5	7.2	0.5	43.0
1.2	74.4	0.7	59.1	0.8	26.1	1.0	69.0	0.8	59.1
2.1	108.0	1.5	86.6	1.1	69.0	1.5	100.4	1.8	93.2
3.2	124.8	2.6	124.8	2.6	108.0	2.6	124.8	2.5	116.1
3.9	143.9	3.7	143.9	3.1	124.8	3.7	143.9	3.7	143.9
Avg vel.	104.2	*Avg vel.*	100.9	*Avg vel.*	84.0	*Avg vel.*	106.0	*Avg vel.*	101.4

Experiment #6 *- velocity profile data*

Time : 72 hrs
Temp (oC) = 15.5

Station 1	*d = 4.4 cm*	*Station 2*	*d = 4.2 cm*	*Station 3*	*d = 3.9 cm*	*Station 4*	*d = 4.4 cm*	*Station5*	*d = 4.2 cm*
Height (cm)	Velocity (cm/s)	Height (cm)	Velocity (cm/s)	Height (cm)	Velocity (cm/s)	Height (cm)	Velocity (cm/s)	Height (cm)	Velocity (cm/s)
0.1	3.5	0.1	31.0	0.1	3.2	0.1	22.0	0.1	22.0
0.3	10.7	0.3	36.6	0.3	10.7	0.3	36.6	0.3	31.0
0.5	36.6	0.5	50.5	0.5	15.4	0.5	46.6	0.5	36.6
0.8	59.1	1.2	69.0	1.1	50.5	1.0	69.0	1.0	59.1
1.5	93.2	1.9	108.0	1.8	80.3	1.9	108.0	1.4	80.3
2.2	124.8	2.5	124.8	2.3	93.2	2.9	124.8	2.1	108.0
3.8	165.6	3.8	154.4	3.4	108.0	3.8	143.9	3.7	143.9
Avg vel.	112.8	*Avg vel.*	108.8	*Avg vel.*	75.2	*Avg vel.*	105.9	*Avg vel.*	99.3

Time : 140 hrs
Temp (oC) = 17.0

Station 1	*d = 4.2 cm*	*Station 2*	*d = 3.4 cm*	*Station 3*	*d = 4.0 cm*	*Station 4*	*d = 3.2 cm*	*Station5*	*d = 3.7 cm*
Height (cm)	Velocity (cm/s)	Height (cm)	Velocity (cm/s)	Height (cm)	Velocity (cm/s)	Height (cm)	Velocity (cm/s)	Height (cm)	Velocity (cm/s)
0.1	46.6	0.1	43.0	0.1	15.4	0.1	24.0	0.1	24.0
0.3	54.6	0.3	46.6	0.3	18.5	0.3	50.5	0.3	39.7
0.5	59.1	0.5	50.5	0.5	36.6	0.5	63.9	0.5	50.5
1.1	80.3	1.2	80.3	1.0	69.0	0.9	93.2	1.3	80.3
2.3	116.1	1.9	108.0	2.0	124.8	1.7	124.8	2.3	108.0
3.7	124.8	2.8	134.1	3.0	143.9	2.7	143.9	3.2	134.1
Avg vel.	102.3	*Avg vel.*	100.1	*Avg vel.*	108.7	*Avg vel.*	110.8	*Avg vel.*	96.7

APPENDIX C

Size distribution of light fractions as a percentage of total sediment transported for Runs 1 - 6.

Experiment #1 *- fractional proportions of transported sediment*

size fracton (mm)	> 22.6	> 16.0	> 11.2	> 8.0	> 5.66	> 4.0	> 2.83	> 2.0	> 1.41	> 1.0	> 0.71	> 0.5	> 0.354	> 0.250	> 0.177	> 0.125	> 0.090
Sample #																	
HW1 (S) 1					0.46	3.16	5.62	8.26	19.73	21.45	15.70	11.63	9.12	3.43	0.80	0.42	0.22
HW1 (S) 2					0.34	1.50	3.23	5.91	14.12	17.59	11.64	11.37	13.08	10.77	4.52	4.65	1.29
HW1 (S) 3					0.09	0.43	1.24	3.24	10.38	15.71	12.71	12.83	14.00	12.40	9.09	6.47	1.41
HW1 (S) 4						0.23	1.01	2.72	11.41	17.74	12.97	13.60	14.67	11.95	5.29	6.53	1.88
HW1 (S) 5						0.17	0.61	2.79	11.89	16.99	12.82	11.81	13.14	11.26	10.14	7.04	1.35
HW1 (S) 6 *																	
HW1 (S) 7						0.16	0.57	3.26	13.62	18.85	13.72	10.93	11.57	10.78	8.51	6.65	1.40
HW1 (S) 8 *																	
HW1 (S) 9						0.16	0.62	3.83	16.08	20.06	12.37	11.47	12.07	9.98	4.93	6.65	1.77
HW1 (S) 10 *																	
HW1 (S) 11				0.44	1.60	7.97	10.76	10.43	17.39	16.14	9.45	6.66	6.03	4.84	2.32	4.38	1.60
HW1 (S) 12				0.21	1.43	5.06	6.29	8.18	15.71	15.30	10.66	8.66	9.29	8.05	6.39	3.84	0.94
HW1 (S) 13					0.27	1.95	3.79	6.08	16.27	17.74	11.07	9.92	10.59	9.76	5.23	5.81	1.53
HW1 (S) 14				0.30	0.43	1.75	3.44	7.27	15.02	17.94	11.11	9.85	10.60	9.54	4.48	5.99	2.18
HW1 (S) 15				0.23	0.74	1.68	3.94	7.74	15.34	16.21	11.19	9.55	10.79	8.91	7.25	4.92	1.51
HW1 (S) 16 *																	
HW1 (S) 17					0.36	1.70	3.91	7.31	15.81	17.55	11.18	10.29	11.27	9.50	4.40	5.20	1.52
HW1 (S) 18 *																	
HW1 (S) 19																	
HW1 (S) 20 *					0.48	2.57	5.36	8.56	15.91	17.70	11.10	9.77	10.26	8.67	2.74	5.16	1.72
HW1 (S) 21																	
HW 1 (S) 22			0.10	1.11	3.94	9.82	11.70	9.83	17.30	17.17	10.09	7.70	6.10	3.05	0.76	0.88	0.45
HW1 (S) 23			0.05	0.68	2.27	5.95	7.74	8.76	16.88	16.87	11.02	8.68	9.03	3.34	6.12	1.78	0.83
HW1 (S) 24			0.03	0.37	1.27	3.87	6.50	8.86	16.71	17.91	12.09	9.43	9.30	7.56	3.03	2.14	0.93
HW1 (S) 25			0.03	0.22	1.31	5.08	7.22	10.09	17.54	18.16	11.77	8.61	8.67	6.36	2.39	1.62	0.95
HW1 (S) 26 *																	
HW1 (S) 27			0.12	0.25	1.87	5.35	7.44	9.01	16.86	16.29	11.27	9.14	9.31	7.32	3.07	1.91	0.79
HW1 (S) 28 *																	
HW1 (S) 29 *																	
HW1 (S) 30				0.38	2.61	7.72	11.45	10.48	14.82	14.73	9.70	7.80	7.32	6.27	2.90	2.53	1.3

* = sample not sieved

Experiment #1 - *fractional proportions of surface samples*

size fraction (mm)	> 22.6	> 16.0	> 11.2	> 8.0	> 5.66	> 4.0	> 2.83	> 2.0	> 1.41	> 1.0	> 0.71	> 0.5	> 0.354	> 0.250	> 0.177	> 0.125	> 0.090
RPM & time																	
1100, 2hrs		3.73	14.79	10.40	12.40	16.46	14.20	8.20	7.84	5.55	2.46	1.18	0.96	0.71	0.42	0.27	0.44
1100, 8 hrs	17.50	2.08	6.75	6.96	10.36	15.39	14.22	8.64	7.60	5.29	2.18	1.00	0.87	0.50	0.21	0.14	0.31
1100, 32 hrs	15.78	1.67	9.94	8.87	9.47	17.80	14.36	7.72	6.59	3.99	1.47	0.78	0.62	0.41	0.04	0.24	0.25
1100, 96 hrs	11.48	3.96	6.20	9.52	11.15	16.13	13.93	7.82	7.44	5.30	2.47	1.40	1.20	0.80	0.62	0.24	0.34
1400, 2 hrs	18.71	4.87	8.44	9.39	13.92	18.07	11.26	5.03	4.21	2.90	1.15	0.64	0.55	0.41	0.03	0.15	0.26
1400, 8 hrs	10.04	12.09	10.28	14.81	14.35	14.78	10.50	4.80	3.52	2.39	0.95	0.48	0.31	0.30	0.10	0.08	0.23
1400, 32 hrs	11.31	6.76	7.47	14.82	14.26	16.30	13.61	5.54	3.94	2.73	1.15	0.66	0.50	0.41	0.15	0.10	0.27
1400, 96 hrs	15.50	8.46	10.84	12.65	14.02	17.59	11.28	3.97	2.59	1.52	0.56	0.24	0.20	0.13	0.00	0.11	0.33
1900, 2 hrs	22.39	4.11	10.41	10.72	12.64	15.59	10.97	3.89	3.47	2.63	1.19	0.65	0.50	0.24	0.22	0.10	0.29
1900, 8 hrs	11.94	8.53	12.26	15.18	12.29	17.72	11.64	3.74	2.56	1.77	0.76	0.47	0.39	0.24	0.11	0.08	0.33
1900, 32 hrs	19.84	6.56	14.48	12.72	12.60	14.55	9.78	3.09	2.51	1.70	0.76	0.39	0.27	0.29	0.08	0.08	0.29
1900, 96 hrs	16.27	7.98	11.99	14.11	12.97	16.63	9.36	3.40	2.80	2.04	0.94	0.47	0.32	0.32	0.10	0.09	0.22

Experiment #2 *- fractional proportions of transported and surface sediment*

size fraction (mm)	> 22.6	> 16.0	> 11.2	> 8.0	> 5.66	> 4.0	> 2.83	> 2.0	> 1.41	> 1.0	> 0.71	> 0.5	> 0.354	> 0.250	> 0.177	> 0.125	> 0.090
Sample #																	
HW2 (S) 1			0.27	1.07	2.74	8.32	11.53	10.19	18.18	16.56	10.34	6.67	5.98	4.46	1.76	1.39	0.53
HW2 (S) 2			0.01	0.14	1.08	3.00	4.89	7.22	14.53	17.11	11.95	9.78	10.55	8.47	5.24	4.60	1.42
HW2 (S) 3					0.51	1.54	3.00	5.73	15.75	19.74	14.01	11.39	10.89	8.73	4.39	3.22	1.09
HW2 (S) 4					0.17	1.19	3.48	7.16	16.98	18.96	13.34	10.47	10.51	8.52	4.62	3.40	1.19
HW2 (S) 5					0.19	0.92	2.97	6.42	16.14	18.08	12.37	9.78	10.12	9.72	6.30	5.31	1.69
HW2 (S) 6					0.15	1.41	3.81	8.19	18.27	19.38	12.83	9.44	9.35	8.14	4.51	3.54	0.98
HW2 (S) 7 *																	
HW2 (S) 8					0.36	1.21	3.99	8.10	15.85	18.35	13.07	10.55	10.63	8.88	4.57	3.58	0.86
HW2 (S) 9 *																	
HW2 (S) 10					0.16	2.07	5.57	9.29	17.80	17.97	12.04	9.15	9.52	7.06	4.78	3.69	0.90
HW2 (S) 1b			1.29	4.30	9.69	16.57	15.69	9.90	12.30	11.04	6.09	4.56	3.67	1.97	1.00	1.11	0.81
HW2 (S) 2b		0.03	0.40	2.91	6.94	14.01	13.46	9.03	14.20	13.74	8.80	5.96	4.81	2.88	1.35	1.04	0.43
HW2 (S) 3b			0.28	2.20	5.47	10.48	9.89	8.07	13.57	14.54	8.59	7.67	7.87	6.10	2.80	1.72	0.76
surf 2 hrs	4.91	7.48	6.62	16.41	15.53	18.47	12.44	5.43	4.74	3.47	1.55	0.94	0.73	0.56	0.15	0.17	0.40
surf 8 hrs	14.14	4.41	6.85	15.31	16.24	17.16	11.95	4.36	3.76	2.75	1.21	0.61	0.48	0.37	0.08	0.10	0.23
surf 32 hrs	13.27	5.46	12.28	12.27	14.44	20.33	10.45	3.79	3.07	2.11	0.85	0.43	0.29	0.34	0.14	0.18	0.31
surf 96 hrs	18.32	2.48	10.34	18.82	12.37	17.36	9.76	3.55	2.91	1.89	0.82	0.42	0.20	0.30	0.10	0.10	0.25
surf flood **	13.62	9.24	9.27	15.37	14.01	14.16	8.76	3.58	3.63	3.19	1.67	1.11	0.72	0.95	0.24	0.17	0.32

* = sample not sieved
** = surface sample taken at end of fifteen minute "flood"
surf = surface sample

Experiment #3 - *fractional proportions of transported, surface and subsurface sediment*

size fraction (mm)	> 22.6	> 16.0	> 11.2	> 8.0	> 5.66	> 4.0	> 2.83	> 2.0	> 1.41	> 1.0	> 0.71	> 0.5	> 0.354	> 0.250	> 0.177	> 0.125	> 0.090
Sample #																	
HW3 (S) 1			0.01	0.64	2.98	8.57	9.68	8.92	17.42	18.28	10.55	8.01	7.25	4.38	1.69	1.12	0.49
HW3 (S) 2			0.01	0.21	1.80	5.32	7.85	9.21	17.65	18.30	11.73	8.32	7.43	5.82	3.17	2.42	0.77
HW3 (S) 3				0.07	0.08	1.75	3.58	6.51	18.14	21.58	13.77	11.10	10.21	6.57	3.23	2.36	1.07
HW3 (S) 4				0.07	0.10	1.76	3.59	8.15	19.02	21.39	12.78	11.11	9.74	6.03	2.86	2.25	1.17
HW3 (S) 5					0.47	1.30	3.18	6.72	16.68	18.56	12.86	10.12	10.20	8.61	5.20	4.65	1.44
HW3 (S) 6					0.14	1.69	4.67	9.64	18.82	19.39	12.43	8.93	9.06	6.25	4.45	3.39	1.14
HW3 (S) 7 *																	
HW3 (S) 8					0.12	1.25	3.79	7.72	16.70	19.29	13.40	10.14	10.68	7.24	4.69	3.89	1.12
HW3 (S) 9 *																	
HW3 (S) 10					0.15	1.59	4.83	8.66	15.89	17.73	12.25	10.40	10.00	8.79	4.96	3.66	1.08
HW3 (S) 1b		0.23	1.13	4.38	9.59	17.97	14.73	9.07	10.41	10.08	6.23	4.11	3.50	3.24	2.02	2.21	1.08
HW3 (S) 2b		0.13	0.95	4.16	8.28	13.48	13.66	9.84	13.86	14.66	9.26	5.50	3.65	1.81	0.41	0.24	0.12
HW3 (S) 3b		0.02	0.47	2.41	4.83	8.51	9.99	8.46	15.26	16.03	9.51	8.26	7.87	4.89	1.83	1.10	0.55
HW3 (S) 4b			0.39	2.15	5.76	11.21	11.65	9.44	14.62	14.60	9.58	7.26	6.19	3.58	1.63	1.33	0.59
HW3 (S) 5b		0.05	0.31	1.37	4.22	7.04	8.44	7.60	12.88	15.50	9.66	8.66	9.29	7.25	3.70	2.68	1.34
HW3 (S) 6b			0.21	1.33	2.56	5.31	7.15	8.90	13.54	17.43	10.25	9.18	9.30	7.16	3.77	2.61	1.33
surf 2 hrs	12.78	5.88	9.76	11.85	14.19	18.03	10.80	4.81	4.32	3.34	1.42	0.96	0.84	0.43	0.14	0.13	0.32
surf 8 hrs	9.32	5.33	15.57	13.35	14.68	17.40	11.69	4.28	3.31	2.31	0.97	0.59	0.51	0.31	0.11	0.11	0.18
surf 32 hrs	14.30	7.39	18.92	12.87	13.50	16.07	9.87	2.70	1.85	1.15	0.41	0.25	0.21	0.12	0.15	0.06	0.18
surf 96 hrs	19.40	5.66	14.80	12.39	13.99	18.06	10.05	2.78	1.46	0.84	0.25	0.10	0.06	0.07	0.03	0.06	0.00
surf flood	5.11	5.43	16.87	19.75	15.46	15.44	9.80	3.61	3.00	2.36	1.08	0.62	0.40	0.36	0.16	0.16	0.40
sub 2 hrs			3.08	2.12	6.80	9.67	10.50	7.19	12.47	14.05	8.23	6.85	7.17	5.41	2.99	2.25	1.22
sub 8 hrs		2.51	1.23	2.55	5.14	10.49	8.96	7.90	12.67	13.02	8.60	6.78	7.10	5.59	3.65	2.87	0.95
sub 32 hrs			5.72	2.31	5.47	10.58	9.56	7.36	11.74	13.31	7.65	6.73	7.10	5.59	3.25	2.43	1.19
sub 96 hrs			1.63	3.76	6.54	10.10	9.86	8.12	13.05	12.02	9.22	6.60	6.83	5.39	3.32	2.46	1.14
sub flood			1.90	3.41	5.03	10.05	9.82	8.11	12.74	13.16	8.50	6.79	7.14	5.21	3.99	3.15	0.99

* = sample not sieved
surf = surface sample
sub = subsurface sample

Experiment #4 - *fractional proportions of transported, surface, and subsurface sediment*

size fraction (mm)	> 22.6	> 16.0	> 11.2	> 8.0	> 5.66	> 4.0	> 2.83	> 2.0	> 1.41	> 1.0	> 0.71	> 0.5	> 0.354	> 0.250	> 0.177	> 0.125	> 0.090
Sample #																	
HW4 (S) 1 *																	
HW4 (S) 2			0.09	0.40	1.47	2.88	6.20	6.93	13.70	19.98	11.96	9.90	10.18	7.93	3.90	3.45	1.02
HW4 (S) 3		0.03	0.00	0.11	0.51	2.67	4.49	7.06	15.35	21.39	12.68	10.64	10.59	7.33	3.39	2.94	0.82
HW4 (S) 4					0.23	1.05	2.70	7.13	17.15	23.15	13.90	10.70	10.52	6.41	3.61	2.77	0.69
HW4 (S) 5					0.12	0.91	2.23	6.58	15.32	21.87	12.73	10.80	11.68	8.96	4.36	3.61	0.83
HW4 (S) 6					0.15	0.74	2.44	6.38	15.91	22.09	12.96	11.35	11.48	8.62	4.13	3.03	0.72
HW4 (S) 7				0.08	0.13	1.12	2.43	6.20	11.72	23.31	13.20	11.38	12.18	9.60	4.69	3.35	0.61
HW4 (S) 8					0.13	1.28	2.77	7.31	16.07	22.22	13.03	10.69	10.87	7.99	3.73	3.04	0.87
HW4 (S) 9					0.26	1.42	3.03	6.88	15.81	20.90	12.39	10.82	11.59	8.63	3.92	4.36	0.88
HW4 (S) 10					0.44	1.54	3.33	7.24	16.31	21.68	12.34	9.98	10.74	8.20	4.03	3.33	0.79
HW4 (S) 1b	0.16	1.21	3.88	7.30	10.47	14.90	12.13	8.85	10.30	10.83	5.65	4.02	3.99	2.92	1.40	1.37	0.61
HW4 (S) 2b	0.75	0.82	2.31	4.36	7.16	10.12	10.14	8.77	12.54	15.03	8.49	6.87	6.43	3.70	1.13	1.01	0.38
HW4 (S) 3b	0.46	1.17	2.42	4.02	6.33	10.83	10.40	8.27	12.18	14.74	8.05	6.99	6.79	4.19	1.46	1.28	0.42
surf 2 hrs	25.10	3.74	7.21	13.33	15.52	15.81	10.57	3.46	2.02	1.82	0.48	0.27	0.21	0.16	0.10	0.11	0.10
surf 8 hrs	18.53	6.47	9.93	13.40	15.57	14.89	10.43	3.77	2.45	2.38	0.76	0.55	0.43	0.23	0.09	0.07	0.05
surf 32 hrs	34.41	6.98	12.48	13.28	9.12	11.56	7.36	2.18	1.20	0.87	0.20	0.08	0.09	0.05	0.04	0.05	0.06
surf 96 hrs	12.18	9.05	14.57	15.19	16.90	15.19	9.95	3.12	1.59	1.29	0.30	0.13	0.10	0.11	0.06	0.08	0.18
sub 2 hrs		2.42	2.15	4.49	5.70	9.81	9.30	8.01	9.59	16.45	7.91	7.23	6.49	5.14	2.70	2.03	0.57
sub 8 hrs		1.74	0.64	3.32	6.05	10.31	10.58	8.86	10.09	16.85	7.65	6.77	6.15	5.04	2.99	2.32	0.64
sub 32 hrs			2.28	2.74	6.35	12.66	9.84	8.99	10.27	16.52	7.56	6.06	6.08	4.81	2.97	2.24	0.64
sub 96 hrs			1.66	1.82	3.79	11.37	11.57	8.96	10.38	17.73	7.78	6.32	6.42	5.33	3.36	2.76	0.77

* = sample not sieved
surf = surface sample
sub = subsurface sample

Experiment #5 - *fractional proportions of transported, surface, and subsurface sediment*

size fraction (mm)	> 22.6	> 16.0	> 11.2	> 8.0	> 5.66	> 4.0	> 2.83	> 2.0	> 1.41	> 1.0	> 0.71	> 0.5	> 0.354	> 0.250	> 0.177	> 0.125	> 0.090
Sample #																	
HW5 (S) 1 *																	
HW5 (S) 2				0.55	1.84	6.17	6.61	6.90	13.64	17.80	10.82	9.35	8.66	8.17	5.13	3.32	1.05
HW5 (S) 3				0.09	0.76	2.58	4.63	6.34	13.69	19.64	12.10	10.74	9.84	8.67	5.93	3.85	1.14
HW5 (S) 4					0.20	1.40	3.36	5.71	15.98	22.63	13.47	11.50	10.32	8.04	4.27	2.38	0.72
HW5 (S) 5					0.33	1.65	4.67	8.69	20.41	24.23	12.33	9.62	6.69	6.75	2.54	1.45	0.63
HW5 (S) 6					0.32	1.04	3.16	6.83	16.30	21.69	12.87	10.56	9.46	8.23	5.00	3.43	1.12
HW5 (S) 7					0.12	1.09	3.43	7.66	16.78	21.99	13.01	10.23	8.71	8.07	4.80	3.16	0.97
HW5 (S) 8					0.27	2.12	5.18	8.51	15.96	20.17	11.49	9.78	8.81	8.31	5.15	3.34	0.91
HW5 (S) 9					0.07	1.80	4.46	8.15	16.51	21.46	12.59	10.20	9.82	6.26	4.56	3.13	1.02
HW5 (S) 10					0.20	2.24	4.46	7.74	14.14	17.98	11.11	10.72	11.95	8.45	5.86	4.04	1.11
HW5 (S) 1b				0.62	2.19	6.90	8.99	9.56	11.47	12.46	7.28	6.66	7.23	7.83	7.14	7.64	4.04
HW5 (S) 1c				2.08	8.16	16.68	17.29	12.14	12.39	12.37	6.07	3.22	2.47	2.16	1.92	1.80	1.24
HW5 (S) 2c				1.54	6.25	14.27	14.22	10.69	14.34	16.38	8.70	5.13	3.47	2.09	1.00	1.31	0.63
HW5 (S) 3c				1.82	4.86	11.63	12.30	10.00	14.07	16.94	9.10	7.44	5.91	3.33	1.20	0.94	0.46
HW5 (S) 4c				1.40	3.98	11.21	10.61	9.57	15.30	16.50	10.07	7.22	4.67	5.34	2.11	1.20	0.82
HW5 (S) 5c				1.45	4.50	7.83	9.01	8.48	12.14	16.25	9.71	8.13	8.95	6.52	3.88	2.41	0.72
HW5 (S) 6c																	
surf 2 hrs				21.64	20.99	22.54	16.71	6.70	4.61	3.44	1.19	0.62	0.52	0.35	0.16	0.16	0.35
surf 8 hrs				23.94	24.24	25.83	15.19	4.95	2.78	1.59	0.46	0.23	0.13	0.18	0.10	0.13	0.25
surf 32 hrs				20.59	20.85	24.92	17.75	6.15	4.17	2.69	0.94	0.51	0.24	0.56	0.22	0.15	0.27
surf 96 hrs				18.92	21.67	27.84	17.55	5.86	3.57	2.41	0.74	0.36	0.25	0.25	0.19	0.11	0.27
sub 2 hrs				2.50	5.07	9.46	9.04	8.74	13.45	16.08	8.92	7.21	6.38	5.72	3.97	2.56	0.93
sub 8 hrs				4.44	4.83	8.06	9.60	8.56	13.25	15.61	8.62	6.93	6.51	5.69	4.35	2.62	0.92
sub 32 hrs				2.37	6.92	11.05	9.68	8.74	12.55	14.02	7.57	6.39	6.24	6.45	4.32	2.68	1.02
sub 96 hrs				3.01	6.46	9.20	9.34	8.77	12.80	14.87	7.92	6.64	6.87	5.65	4.46	2.88	1.13

* = sample not sieved
surf = surface sample
sub = subsurface sample

Experiment #6 *- fractional proportions of transported sediment*

size fraction (mm)	> 22.6	> 16.0	> 11.2	> 8.0	> 5.66	> 4.0	> 2.83	> 2.0	> 1.41	> 1.0	> 0.71	> 0.5	> 0.354	> 0.250	> 0.177	> 0.125	> 0.090
Sample #																	
HW6 (S) 1 *																	
HW6 (S) 2				0.18	1.13	4.07	4.91	7.16	15.62	18.55	12.59	9.95	10.50	6.17	5.47	2.94	0.77
HW6 (S) 3				0.06	0.84	1.82	4.74	8.16	15.97	18.88	12.34	9.43	10.23	6.36	6.21	3.90	1.07
HW6 (S) 4					0.22	2.13	3.35	6.23	15.50	19.73	13.48	10.69	11.35	6.78	6.25	3.56	0.75
HW6 (S) 5					0.05	0.84	1.62	5.04	14.88	19.51	13.10	10.54	12.21	8.22	8.06	4.74	1.21
HW6 (S) 6					0.04	0.27	0.98	6.24	9.91	23.47	14.15	12.13	11.02	11.56	5.85	3.60	0.79
HW6 (S) 7					0.40	1.28	2.47	6.44	17.37	20.72	12.98	9.70	10.53	6.61	6.78	3.84	0.87
HW6 (S) 8					0.24	1.40	3.18	6.52	16.33	19.75	12.99	10.22	11.38	7.13	6.46	3.54	0.84
HW6 (S) 9						1.23	2.98	6.55	16.16	19.71	13.16	10.24	11.32	7.35	6.63	3.80	0.86
HW6 (S) 10					0.29	1.08	2.63	6.41	16.69	20.09	13.18	10.38	11.38	7.10	6.48	3.52	0.75
HW6 (S) 11				0.09	0.65	6.63	9.29	11.68	17.66	19.58	11.95	6.58	6.53	3.58	3.08	2.04	0.65
HW6 (S) 12				0.10	0.62	2.75	4.97	7.49	16.16	18.98	11.67	9.48	10.61	6.61	6.31	3.41	0.83
HW6 (S) 13				0.16	0.77	3.03	5.46	8.08	17.53	20.12	11.89	8.43	9.16	5.82	5.47	3.28	0.80
HW6 (S) 14				0.09	0.61	2.88	5.33	9.65	20.54	20.86	11.27	7.12	8.56	5.07	4.57	2.71	0.74
HW6 (S) 15				0.12	0.79	3.43	5.41	7.93	17.06	20.29	12.89	8.84	9.31	5.56	4.83	2.85	0.69
HW6 (S) 16					0.40	3.13	5.14	10.37	18.39	20.44	12.37	8.07	8.73	5.20	4.43	2.60	0.71
HW6 (S) 17				0.09	0.72	2.35	4.76	8.67	17.50	19.59	11.22	8.32	9.90	6.68	5.91	3.43	0.86
HW6 (S) 18					0.61	3.58	5.49	8.66	17.18	19.66	12.98	8.88	9.12	5.58	4.36	3.19	0.71
HW6 (S) 19					0.44	2.33	4.80	7.77	17.53	20.41	13.36	9.97	9.81	5.41	4.49	2.96	0.71
HW6 (S) 20					0.42	2.14	3.58	6.36	13.91	17.16	11.46	10.86	13.31	8.32	7.18	4.23	1.06
HW6 (S) 21					0.85	2.53	4.02	6.75	13.35	15.04	10.25	10.61	13.63	8.72	8.16	4.91	1.18
HW6 (S) 22				0.19	0.42	2.44	4.55	8.28	16.64	18.56	11.65	9.81	10.65	6.46	5.95	3.64	0.78
HW6 (S) 23				0.07	1.15	4.71	6.06	13.34	26.03	25.33	11.06	4.31	3.60	1.69	1.32	0.99	0.34
HW6 (S) 1b				4.93	9.95	16.13	14.74	9.38	9.91	8.08	4.41	3.44	4.49	3.72	4.72	4.39	1.72
HW6 (S) 2b				4.21	9.57	14.67	13.12	8.83	10.76	11.16	6.72	5.20	5.86	3.69	3.29	2.15	0.78
HW6 (S) 3b *																	
HW6 (S) 4b				2.80	8.34	17.84	15.03	9.67	11.14	11.88	7.12	4.51	3.51	3.91	1.91	1.68	0.66
HW6 (S) 5b				3.44	8.20	14.20	12.78	8.98	11.82	11.44	6.72	5.77	6.61	4.21	3.47	1.81	0.53

* = sample not sieved

Experiment #6 - *fractional proportions of transported, surface, and subsurface sediment*

size fraction (mm)	> 22.6	> 16.0	> 11.2	> 8.0	> 5.66	> 4.0	> 2.83	> 2.0	> 1.41	> 1.0	> 0.71	> 0.5	> 0.354	> 0.250	> 0.177	> 0.125	> 0.090
Sample #																	
HW6 (S) 1c				5.45	2.85	6.40	7.23	7.86	12.37	14.77	8.75	5.20	5.64	3.87	6.91	8.81	3.87
HW6 (S) 2c				1.28	4.69	6.68	8.73	7.09	10.56	12.65	8.80	7.54	10.82	9.12	5.87	4.30	1.86
HW6 (S) 3c				1.23	3.08	7.16	8.24	8.11	13.22	15.39	10.14	8.46	10.14	6.78	4.96	2.15	0.95
HW6 (S) 4c				1.26	2.03	4.77	5.88	6.88	11.02	14.12	9.72	8.02	11.98	10.35	6.88	4.99	2.11
HW6 (S) 5c				4.57	4.12	7.58	6.92	6.51	10.13	11.70	8.07	7.58	10.75	8.94	7.08	4.24	1.81
HW6 (S) 6c				2.49	3.95	7.52	5.97	6.20	9.26	11.56	7.61	7.42	10.15	11.28	7.85	6.39	2.35
HW6 (S) 7c				2.79	5.23	8.78	6.41	5.09	8.22	9.48	6.76	6.69	9.41	9.06	11.29	8.22	2.58
HW6 (S) 8c				4.73	6.82	6.55	6.88	5.67	7.82	9.74	6.49	5.67	8.20	9.36	9.96	9.85	2.26
HW6 (S) 9c				10.27	8.88	10.07	7.31	5.13	7.80	8.09	5.13	3.85	5.23	5.73	9.97	9.58	2.96
HW6 (S) 10c				1.42	3.91	7.57	8.16	8.50	12.21	14.02	8.84	6.94	7.38	6.45	6.79	5.91	1.91
HW6 (S) 11c				2.64	4.77	8.95	9.68	8.00	11.30	11.89	7.41	6.09	7.70	5.87	6.60	5.94	3.15
HW6 (S) 12c				4.34	6.78	10.23	9.34	6.72	9.40	10.89	6.78	6.07	7.85	6.31	6.31	6.42	2.56
surf 2 hrs				14.79	18.51	23.82	15.71	8.33	6.19	6.31	2.17	1.19	1.10	0.73	0.46	0.34	0.37
surf 8 hrs				20.52	20.05	24.54	14.94	7.36	4.30	4.43	1.29	0.63	0.63	0.49	0.33	0.22	0.27
surf 32 hrs				17.14	24.59	26.20	16.98	7.15	3.15	2.63	0.71	0.30	0.14	0.49	0.16	0.16	0.19
surf 96 hrs #																	
surf flood **				26.28	27.33	20.94	13.05	4.25	3.05	2.16	0.85	0.45	0.37	0.33	0.49	0.45	0.00
sub 2 hrs				2.48	4.84	9.09	9.55	8.90	13.98	14.71	9.16	6.65	7.09	4.66	4.99	2.96	0.94
sub 8 hrs				2.39	5.21	9.87	9.19	8.55	13.77	14.01	8.51	6.51	7.34	5.28	5.38	2.97	1.01
sub 32 hrs				2.76	4.40	8.39	9.99	9.46	10.64	16.37	7.97	6.58	7.16	6.95	4.81	3.46	1.07
sub 96 hrs #																	
sub flood **				4.93	8.02	13.56	11.33	8.00	10.44	9.92	5.61	4.83	5.70	4.86	6.99	4.74	1.08

surf = surface sample
sub = subsurface sample
** = surface / subsurface sample taken at 4.5 m at close of second flood
# = surface/subsurface samples not taken

APPENDIX D

Fractional percentage of transported sediment relative to presence in bed (p_i / f_i).

Experiment #1 *- fractional proportion of transported sediment relative to presence in bed*

size fracton (mm)	> 22.6	> 16.0	> 11.2	> 8.0	> 5.66	> 4.0	> 2.83	> 2.0	> 1.41	> 1.0	> 0.71	> 0.5	> 0.354	> 0.250	> 0.177	> 0.125	> 0.090
Sample #																	
HW1 (S) 1					0.10	0.34	0.63	1.05	1.73	1.53	1.94	1.71	1.23	0.58	0.21	0.13	0.18
HW1 (S) 2					0.07	0.16	0.36	0.75	1.24	1.26	1.44	1.67	1.77	1.83	1.19	1.45	1.08
HW1 (S) 3					0.02	0.05	0.14	0.41	0.91	1.12	1.57	1.89	1.89	2.10	2.39	2.02	1.18
HW1 (S) 4						0.02	0.11	0.34	1.00	1.27	1.60	2.00	1.98	2.03	1.39	2.04	1.57
HW1 (S) 5						0.02	0.07	0.35	1.04	1.21	1.58	1.74	1.78	1.91	2.67	2.20	1.13
HW1 (S) 6 *																	
HW1 (S) 7						0.02	0.06	0.41	1.19	1.35	1.69	1.61	1.56	1.83	2.24	2.08	1.17
HW1 (S) 8 *																	
HW1 (S) 9						0.02	0.07	0.48	1.41	1.43	1.53	1.69	1.63	1.69	1.30	2.08	1.48
HW1 (S) 10 *																	
HW1 (S) 11				0.14	0.35	0.86	1.21	1.32	1.53	1.15	1.17	0.98	0.81	0.82	0.61	1.37	1.33
HW1 (S) 12				0.07	0.31	0.54	0.71	1.04	1.38	1.09	1.32	1.27	1.26	1.36	1.68	1.20	0.78
HW1 (S) 13					0.06	0.21	0.43	0.77	1.43	1.27	1.37	1.46	1.43	1.65	1.38	1.82	1.28
HW1 (S) 14				0.09	0.09	0.19	0.39	0.92	1.32	1.28	1.37	1.45	1.43	1.62	1.18	1.87	1.82
HW1 (S) 15				0.07	0.16	0.18	0.44	0.98	1.35	1.16	1.38	1.40	1.46	1.51	1.91	1.54	1.26
HW1 (S) 16 *																	
HW1 (S) 17					0.08	0.18	0.44	0.93	1.39	1.25	1.38	1.51	1.52	1.61	1.16	1.63	1.27
HW1 (S) 18 *																	
HW1 (S) 19					0.10	0.28	0.60	1.08	1.40	1.26	1.37	1.44	1.39	1.47	0.72	1.61	1.43
HW1 (S) 20 *																	
HW1 (S) 21																	
HW 1 (S) 22			0.05	0.35	0.86	1.06	1.31	1.24	1.52	1.23	1.25	1.13	0.82	0.52	0.20	0.28	0.38
HW1 (S) 23			0.02	0.21	0.49	0.64	0.87	1.11	1.48	1.21	1.36	1.28	1.22	0.57	1.61	0.56	0.69
HW1 (S) 24			0.01	0.12	0.28	0.42	0.73	1.12	1.47	1.28	1.49	1.39	1.26	1.28	0.80	0.67	0.78
HW1 (S) 25			0.01	0.07	0.28	0.55	0.81	1.28	1.54	1.30	1.45	1.27	1.17	1.08	0.63	0.51	0.79
HW1 (S) 26 *																	
HW1 (S) 27			0.06	0.08	0.41	0.58	0.84	1.14	1.48	1.16	1.39	1.34	1.26	1.24	0.81	0.60	0.66
HW1 (S) 28 *																	
HW1 (S) 29 *																	
HW1 (S) 30				0.12	0.57	0.83	1.29	1.33	1.30	1.05	1.20	1.15	0.99	1.06	0.76	0.79	1.08

* = sample not sieved

Experiment #2 - *fractional proportion of transported sediment relative to presence in bed*

size fraction (mm)	> 22.6	> 16.0	> 11.2	> 8.0	> 5.66	> 4.0	> 2.83	> 2.0	> 1.41	> 1.0	> 0.71	> 0.5	> 0.354	> 0.250	> 0.177	> 0.125	> 0.090
Sample #																	
HW2 (S) 1			0.13	0.33	0.60	0.89	1.30	1.29	1.59	1.18	1.28	0.98	0.81	0.76	0.46	0.43	0.44
HW2 (S) 2				0.04	0.23	0.32	0.55	0.91	1.27	1.22	1.48	1.44	1.43	1.44	1.38	1.44	1.18
HW2 (S) 3					0.11	0.17	0.34	0.73	1.38	1.41	1.73	1.68	1.47	1.48	1.16	1.01	0.91
HW2 (S) 4					0.04	0.13	0.39	0.91	1.49	1.35	1.65	1.54	1.42	1.44	1.22	1.06	0.99
HW2 (S) 5					0.04	0.10	0.33	0.81	1.42	1.29	1.53	1.44	1.37	1.65	1.66	1.66	1.41
HW2 (S) 6					0.03	0.15	0.43	1.04	1.60	1.38	1.58	1.39	1.26	1.38	1.19	1.11	0.82
HW2 (S) 7 *																	
HW2 (S) 8					0.08	0.13	0.45	1.03	1.39	1.31	1.61	1.55	1.44	1.51	1.20	1.12	0.72
HW2 (S) 9 *																	
HW2 (S) 10					0.03	0.22	0.63	1.18	1.56	1.28	1.49	1.35	1.29	1.20	1.26	1.15	0.75
HW2 (S) 1b			0.61	1.34	2.11	1.78	1.76	1.25	1.08	0.79	0.75	0.67	0.50	0.33	0.26	0.35	0.68
HW2 (S) 2b		0.03	0.19	0.91	1.51	1.51	1.51	1.14	1.25	0.98	1.09	0.88	0.65	0.49	0.36	0.33	0.36
HW2 (S) 3b			0.13	0.69	1.19	1.13	1.11	1.02	1.19	1.04	1.06	1.13	1.06	1.03	0.74	0.54	0.63

* = sample not sieved

Experiment #3 - *fractional proportion of transported sediment relative to proportion in bed*

size fraction (mm)	> 22.6	> 16.0	> 11.2	> 8.0	> 5.66	> 4.0	> 2.83	> 2.0	> 1.41	> 1.0	> 0.71	> 0.5	> 0.354	> 0.250	> 0.177	> 0.125	> 0.090
Sample #																	
HW3 (S) 1				0.20	0.65	0.92	1.09	1.13	1.53	1.31	1.30	1.18	0.98	0.74	0.44	0.35	0.41
HW3 (S) 2				0.07	0.39	0.57	0.88	1.17	1.55	1.31	1.45	1.22	1.00	0.99	0.83	0.76	0.64
HW3 (S) 3				0.02	0.02	0.19	0.40	0.82	1.59	1.54	1.70	1.63	1.38	1.11	0.85	0.74	0.89
HW3 (S) 4				0.02	0.02	0.19	0.40	1.03	1.67	1.53	1.58	1.63	1.32	1.02	0.75	0.70	0.98
HW3 (S) 5					0.10	0.14	0.36	0.85	1.46	1.33	1.59	1.49	1.38	1.46	1.37	1.45	1.20
HW3 (S) 6					0.03	0.18	0.52	1.22	1.65	1.39	1.53	1.31	1.22	1.06	1.17	1.06	0.95
HW3 (S) 7 *																	
HW3 (S) 8					0.03	0.13	0.43	0.98	1.46	1.38	1.65	1.49	1.44	1.23	1.23	1.22	0.93
HW3 (S) 9 *																	
HW3 (S) 10					0.03	0.17	0.54	1.10	1.39	1.27	1.51	1.53	1.35	1.49	1.31	1.14	0.90
HW3 (S) 1b		0.21	0.54	1.37	2.08	1.93	1.66	1.15	0.91	0.72	0.77	0.60	0.47	0.55	0.53	0.69	0.90
HW3 (S) 2b		0.12	0.45	1.30	1.80	1.45	1.53	1.25	1.22	1.05	1.14	0.81	0.49	0.31	0.11	0.08	0.10
HW3 (S) 3b		0.02	0.22	0.75	1.05	0.92	1.12	1.07	1.34	1.15	1.17	1.21	1.06	0.83	0.48	0.34	0.46
HW3 (S) 4b			0.19	0.67	1.25	1.21	1.31	1.19	1.28	1.04	1.18	1.07	0.84	0.61	0.43	0.42	0.49
HW3 (S) 5b		0.05	0.15	0.43	0.92	0.76	0.95	0.96	1.13	1.11	1.19	1.27	1.26	1.23	0.97	0.84	1.12
HW3 (S) 6b			0.10	0.42	0.56	0.57	0.80	1.13	1.19	1.25	1.27	1.35	1.26	1.21	0.99	0.82	1.11

* = sample not sieved

Experiment #4 - *fractional proportion of transported sediment relative to presence in bed*

size fraction (mm)	> 22.6	> 16.0	> 11.2	> 8.0	> 5.66	> 4.0	> 2.83	> 2.0	> 1.41	> 1.0	> 0.71	> 0.5	> 0.354	> 0.250	> 0.177	> 0.125	> 0.090
Sample #																	
HW4 (S) 1 *																	
HW4 (S) 2			0.04	0.13	0.32	0.31	0.70	0.88	1.20	1.43	1.48	1.46	1.38	1.34	1.03	1.08	0.85
HW4 (S) 3		0.03		0.03	0.11	0.29	0.50	0.89	1.35	1.53	1.57	1.56	1.43	1.24	0.89	0.92	0.68
HW4 (S) 4					0.05	0.11	0.30	0.90	1.50	1.65	1.72	1.57	1.42	1.09	0.95	0.87	0.58
HW4 (S) 5					0.03	0.10	0.25	0.83	1.34	1.56	1.57	1.59	1.58	1.52	1.15	1.13	0.69
HW4 (S) 6					0.03	0.08	0.27	0.81	1.40	1.58	1.60	1.67	1.55	1.46	1.09	0.95	0.60
HW4 (S) 7				0.03	0.03	0.12	0.27	0.78	1.03	1.67	1.63	1.67	1.65	1.63	1.23	1.05	0.51
HW4 (S) 8					0.03	0.14	0.31	0.93	1.41	1.59	1.61	1.57	1.47	1.35	0.98	0.95	0.73
HW4 (S) 9					0.06	0.15	0.34	0.87	1.39	1.49	1.53	1.59	1.57	1.46	1.03	1.36	0.73
HW4 (S) 10					0.10	0.17	0.37	0.92	1.43	1.55	1.52	1.47	1.45	1.39	1.06	1.04	0.66
HW4 (S) 1b	0.15	1.10	1.85	2.28	2.28	1.60	1.36	1.12	0.90	0.77	0.70	0.59	0.54	0.49	0.37	0.43	0.51
HW4 (S) 2b	0.68	0.75	1.10	1.36	1.56	1.09	1.14	1.11	1.10	1.07	1.05	1.01	0.87	0.63	0.30	0.32	0.32
HW4 (S) 3b	0.42	1.06	1.15	1.26	1.38	1.16	1.17	1.05	1.07	1.05	0.99	1.03	0.92	0.71	0.38	0.40	0.35

* = sample not sieved

Experiment #5 - *fractional proportion of transported sediment relative to presence in bed*

size fraction (mm)	> 22.6	> 16.0	> 11.2	> 8.0	> 5.66	> 4.0	> 2.83	> 2.0	> 1.41	> 1.0	> 0.71	> 0.5	> 0.354	> 0.250	> 0.177	> 0.125	> 0.090
Sample #																	
HW5 (S) 1 *																	
HW5 (S) 2				0.17	0.40	0.66	0.74	0.87	1.20	1.27	1.34	1.38	1.17	1.38	1.35	1.04	0.88
HW5 (S) 3				0.03	0.17	0.28	0.52	0.80	1.20	1.40	1.49	1.58	1.33	1.47	1.56	1.20	0.95
HW5 (S) 4					0.04	0.15	0.38	0.72	1.40	1.62	1.66	1.69	1.39	1.36	1.12	0.74	0.60
HW5 (S) 5					0.07	0.18	0.52	1.10	1.79	1.73	1.52	1.41	0.90	1.14	0.67	0.45	0.53
HW5 (S) 6					0.07	0.11	0.36	0.86	1.43	1.55	1.59	1.55	1.28	1.39	1.32	1.07	0.93
HW5 (S) 7					0.03	0.12	0.39	0.97	1.47	1.57	1.61	1.50	1.18	1.37	1.26	0.99	0.81
HW5 (S) 8					0.06	0.23	0.58	1.08	1.40	1.44	1.42	1.44	1.19	1.41	1.36	1.04	0.76
HW5 (S) 9					0.02	0.19	0.50	1.03	1.45	1.53	1.55	1.50	1.33	1.06	1.20	0.98	0.85
HW5 (S) 10					0.04	0.24	0.50	0.98	1.24	1.28	1.37	1.58	1.61	1.43	1.54	1.26	0.93
HW5 (S) 1b				0.19	0.48	0.74	1.01	1.21	1.01	0.89	0.90	0.98	0.98	1.33	1.88	2.39	3.37
HW5 (S) 1c				0.65	1.77	1.79	1.94	1.54	1.09	0.88	0.75	0.47	0.33	0.37	0.51	0.56	1.03
HW5 (S) 2c				0.48	1.36	1.53	1.60	1.35	1.26	1.17	1.07	0.75	0.47	0.35	0.26	0.41	0.53
HW5 (S) 3c				0.57	1.06	1.25	1.38	1.27	1.23	1.21	1.12	1.09	0.80	0.56	0.32	0.29	0.38
HW5 (S) 4c				0.44	0.87	1.21	1.19	1.21	1.34	1.18	1.24	1.06	0.63	0.91	0.56	0.38	0.68
HW5 (S) 5c				0.45	0.98	0.84	1.01	1.07	1.06	1.16	1.20	1.20	1.21	1.11	1.02	0.75	0.60
HW5 (S) 6c				0.42	0.86	0.78	0.92	1.09	1.22	1.09	1.20	1.23	1.32	0.91	1.28	0.74	0.80

* = sample not sieved

Experiment #6 - *fractional proportions of transported sediment*

size fraction (mm)	> 22.6	> 16.0	> 11.2	> 8.0	> 5.66	> 4.0	> 2.83	> 2.0	> 1.41	> 1.0	> 0.71	> 0.5	> 0.354	> 0.250	> 0.177	> 0.125	> 0.090
Sample #																	
HW6 (S) 1 *																	
HW6 (S) 2				0.06	0.25	0.44	0.55	0.91	1.37	1.33	1.55	1.46	1.42	1.05	1.44	0.92	0.64
HW6 (S) 3				0.02	0.18	0.20	0.53	1.03	1.40	1.35	1.52	1.39	1.38	1.08	1.63	1.22	0.89
HW6 (S) 4					0.05	0.23	0.38	0.79	1.36	1.41	1.66	1.57	1.53	1.15	1.64	1.11	0.63
HW6 (S) 5					0.01	0.09	0.18	0.64	1.31	1.39	1.62	1.55	1.65	1.39	2.12	1.48	1.01
HW6 (S) 6					0.01	0.03	0.11	0.79	0.87	1.68	1.75	1.78	1.49	1.96	1.54	1.13	0.66
HW6 (S) 7					0.09	0.14	0.28	0.82	1.52	1.48	1.60	1.43	1.42	1.12	1.78	1.20	0.73
HW6 (S) 8					0.05	0.15	0.36	0.83	1.43	1.41	1.60	1.50	1.54	1.21	1.70	1.11	0.70
HW6 (S) 9						0.13	0.33	0.83	1.42	1.41	1.62	1.51	1.53	1.25	1.74	1.19	0.72
HW6 (S) 10					0.06	0.12	0.30	0.81	1.46	1.44	1.63	1.53	1.54	1.20	1.71	1.10	0.63
HW6 (S) 11				0.03	0.14	0.71	1.04	1.48	1.55	1.40	1.48	0.97	0.88	0.61	0.81	0.64	0.54
HW6 (S) 12				0.03	0.13	0.30	0.56	0.95	1.42	1.36	1.44	1.39	1.43	1.12	1.66	1.07	0.69
HW6 (S) 13				0.05	0.17	0.33	0.61	1.02	1.54	1.44	1.47	1.24	1.24	0.99	1.44	1.03	0.67
HW6 (S) 14				0.03	0.13	0.31	0.60	1.22	1.80	1.49	1.39	1.05	1.16	0.86	1.20	0.85	0.62
HW6 (S) 15				0.04	0.17	0.37	0.61	1.00	1.50	1.45	1.59	1.30	1.26	0.94	1.27	0.89	0.58
HW6 (S) 16					0.09	0.34	0.58	1.31	1.61	1.46	1.53	1.19	1.18	0.88	1.17	0.81	0.59
HW6 (S) 17				0.03	0.16	0.25	0.53	1.10	1.54	1.40	1.39	1.22	1.34	1.13	1.56	1.07	0.72
HW6 (S) 18					0.13	0.38	0.62	1.10	1.51	1.40	1.60	1.31	1.23	0.95	1.15	1.00	0.59
HW6 (S) 19					0.10	0.25	0.54	0.98	1.54	1.46	1.65	1.47	1.33	0.92	1.18	0.93	0.59
HW6 (S) 20					0.09	0.23	0.40	0.81	1.22	1.23	1.41	1.60	1.80	1.41	1.89	1.32	0.88
HW6 (S) 21					0.18	0.27	0.45	0.85	1.17	1.07	1.27	1.56	1.84	1.48	2.15	1.53	0.98
HW6 (S) 22				0.06	0.09	0.26	0.51	1.05	1.46	1.33	1.44	1.44	1.44	1.09	1.57	1.14	0.65
HW6 (S) 23				0.02	0.25	0.51	0.68	1.69	2.28	1.81	1.37	0.63	0.49	0.29	0.35	0.31	0.28
HW6 (S) 1b				1.54	2.16	1.73	1.66	1.19	0.87	0.58	0.54	0.51	0.61	0.63	1.24	1.37	1.43
HW6 (S) 2b				1.32	2.08	1.58	1.47	1.12	0.94	0.80	0.83	0.76	0.79	0.63	0.87	0.67	0.65
HW6 (S) 3b *																	
HW6 (S) 4b				0.88	1.81	1.92	1.69	1.22	0.98	0.85	0.88	0.66	0.47	0.66	0.50	0.53	0.55
HW6 (S) 5b				1.08	1.78	1.53	1.44	1.14	1.04	0.82	0.83	0.85	0.89	0.71	0.91	0.57	0.44

* = sample not sieved

APPENDIX E

Water surface slope and average depth for Runs 2 - 6.

Appendix E **-** *slope data and average depth for Runs 2 - 6*

Distance downstream	3.0 m	4.0 m	5.0 m	6.0 m	7.0 m	8.0 m	Slope	Avg. depth (cm)
Run 2								
8 hrs	40 .4	41.0	42.1	43.0	44.0	44.3	0.84	4.6
32 hrs	40.6	41.3	42.2	43.1	43.9	44.5	0.81	4.6
72 hrs	40.5	41.5	42.3	43.3	44.1	44.4	0.81	4.5
96 hrs	40.3	41.3	42.2	43.2	43.9	44.2	0.81	4.6
Run 3								
8 hrs	40.1	41.0	42.3	42.8	43.6	44.1	0.81	4.4
32 hrs	39.4	41.0	42.1	42.6	43.7	44.0	0.90	4.5
72 hrs	40.1	41.1	42.1	42.8	43.6	43.9	0.78	4.6
96 hrs	39.9	41.2	42.2	42.7	43.7	43.9	0.80	4.5
Run 4								
8 hrs	42.2	43.7	45.4	47.0	47.9	49.5	1.45	2.7
32 hrs	42.2	43.5	45.4	46.7	48.1	49.5	1.47	2.9
96 hrs	42.3	43.6	45.4	46.8	48.1	49.3	1.43	2.8
Run 5								
8 hrs	41.5	41.9	42.7	43.4	44.0	44.5	0.63	4.8
32 hrs	41.4	41.8	42.7	43.3	43.9	44.2	0.60	4.7
72 hrs	41.4	42.1	42.5	43.2	43.8	44.2	0.57	4.8
96 hrs	41.2	42.0	42.6	43.3	43.9	44.1	0.60	5.3
Run 6								
8 hrs	42.6	43.9	44.8	45.7	46.9	48.1	1.07	2.9
32 hrs	42.5	44.0	45.0	45.9	46.9	48.1	1.07	2.9
72 hrs	42.7	43.6	45.2	45.7	46.4	47.6	0.95	3.2
96 hrs	42.8	43.9	45.2	45.9	46.7	47.7	0.96	3.1